



VIGILADA MINEDUCACIÓN

Master Thesis

DEVELOPMENT OF CONTROL STRATEGIES FOR A  
VARIABLE STIFFNESS ANKLE EXOSKELETON FOR  
GAIT REHABILITATION

Daniel Alejandro Gómez Vargas

Supervisor:

Prof. Dr. Carlos Andrés Cifuentes García

Co-supervisor:

Prof. Dr. Marcela Múnica Ramírez

A thesis submitted in fulfillment of the requirements for the degree of  
Master in Electronic Engineering

November 2020

*"Knowledge is an unending adventure  
at the edge of uncertainty."*

*Jacob Bronowski*

*"Scientific research  
is one of the most exciting  
and rewarding of occupations."*

*Frederick Sanger*

*"What matters in life is not what happens to you  
but what you remember  
and how you remember it."*

*Gabriel García Márquez*

## Acknowledgements

This thesis was partially supported by the project "Development of an adaptable robotic platform for rehabilitation and gait assistance" funded by *Ministerio de Ciencia Tecnología* (MinCiencias grant 801-2017), the research network REASISTE (CYTED grant 216RT0504), and internal fundings from the Colombian School of Engineering Julio Garavito. Likewise, I would like to thank the international cooperation network created since this project's conception. Especially to Prof. Dr. Carlos Rodríguez Guerrero, who is part of the Robotics and MultiBody Mechanics research group at Vrije Universiteit Brussel in Belgium, and Kinesiologist Patricio Barría Aburto, who is a lead researcher at Club de Leones, Cruz del Sur Rehabilitation Center in Chile. Additionally, I would like to thank all the researchers, students, and patients who contributed to the development, implementation, and evaluation of this project.

On the other hand, I want to emphasize that I dedicate this project to my guardian angel, who always accompanies me, guides me, and in some way, has allowed me to become the person I am today. Of course, I also want to thank my mother, Maria, my sisters, Angelica and Ana, and my brother, David, who have given me their support and strength during difficult times, as well as their unconditional love to always keep going. I wish to give very special thanks to Germán, Martha, and Laura, who believed in me and allowed me to fulfill my dreams. Likewise, I would like to express my enormous gratitude to my thesis directors, Carlos and Marcela, in the first place, for their trust and friendship, as well as their accompaniment, support, and guidance throughout this formative process. Also, I wish to thank the members of the Center for Biomechatronics, colleagues, and friends who always gave me their support and knowledge. Thanks to Sergio, Felipe, Diego, Majo, Nathalia, Miguel, Orion, Jonathan, Alejo, Andrés, Pips, Margarita, Juan and Luis.

*Esta tesis fue posible gracias al proyecto "Desarrollo de una plataforma robótica adaptable para rehabilitación y asistencia de la marcha" financiado por el Ministerio de Ciencia y Tecnología (MinCiencias grant 801-2017), la red de investigación REASISTE financiada por el CYTED (subvención 216RT0504) y proyectos de rubros internos de la Escuela Colombiana de Ingeniería Julio Garavito. De igual forma, quiero agradecer a la red de cooperación internacional que se ha creado desde la concepción de este proyecto, especialmente, al Prof. Dr. Carlos Rodríguez Guerrero, quien hace parte del grupo de investigación de Robótica y Mecánica Multicuerpo de la Universidad de Vrije en Bélgica, y al Kinesiólogo Patricio Barría Aburto, investigador principal del Centro de Rehabilitación Club de Leones Cruz del Sur en Chile. Adicionalmente, quiero agradecer a todos los investigadores, estudiantes y pacientes que de alguna forma contribuyeron al desarrollo, implementación y evaluación de este proyecto.*

*Por otra parte, quiero recalcar que dedico este proyecto a mi ángel protector quien siempre me acompaña, me guía y de alguna forma me ha permitido convertirme en la persona que soy hoy en día. Por supuesto, quiero también agradecer a mi madre María, a mis hermanas Angélica y Ana y a mi hermano David quienes me han brindado su apoyo y fortaleza durante momentos tan difíciles, además de su amor incondicional para siempre seguir adelante. Quiero dar un agradecimiento muy especial a Germán, Martha y Laura quienes creyeron en mí y me brindaron la oportunidad de cumplir mis sueños. De igual forma, quiero expresar un enorme agradecimiento a mis directores de tesis, Carlos y Marcela, en primer lugar, por su confianza y amistad, además de su acompañamiento, apoyo y orientación durante todo este proceso formativo. Asimismo, a todo el equipo del Center for Biomechatronics, compañeros y amigos que siempre me brindaron su apoyo y conocimiento. Gracias a Sergio, Felipe, Diego, Majo, Nathalia, Miguel, Orion, Jonathan, Andrés, Margarita, Juan y Luis.*

## Abstract

Currently, designing robotic devices to assist and rehabilitate the ankle is challenging due to the joint's complexity and its fundamental role in walking. This research field has been motivated by the disability's high incidence of neurological disorders and their effects in Activities of Daily Living's (ADL) execution that reduces people's life quality. This way, powered ankle-foot orthoses (PAFOs) or ankle exoskeletons are being developed to counteract the gait limitation and to improve motor recovery. In this context, this master's dissertation presents the design, development, and implementation of a novel wearable and portable ankle exoskeleton, called T-FLEX, based on Variable Stiffness Actuators (VSAs). Thus, different high-level control strategies were developed and implemented to support gait rehabilitation with T-FLEX. Likewise, an experimental characterization determined the T-FLEX's applicability in assistive scenarios and measured the device's capabilities during this task. Lastly, two experimental validations with people who exhibited ankle dysfunctions were carried out to assess the device's effectiveness during gait rehabilitation. In general terms, this dissertation determined that T-FLEX is capable of assisting gait patterns with gait cycle duration greater than 0.74 seconds. Moreover, this work assessed the T-FLEX's actuation system in a passive orthotic structure during a first-use trial and evaluated T-FLEX in a rehabilitation program with a chronic stroke patient. The gait assistance assessment showed improvements in foot clearance and lower limb's kinematics. However, the users exhibited reductions in Spatio-temporal parameters related mainly to the orthotic structure used in this study. For the validation in therapy mode, T-FLEX evidenced positive effects: (1) increasing cadence, (2) reducing the plantarflexion movement during swing phase, (3) decreasing the spasticity level and increasing the passive lower limb joints' range of motion (ROM) after 18 sessions. T-FLEX can assist human gait and support rehabilitation processes of neurological patients with ankle dysfunctions. Future works will address improvements in the device synchronization, the assessment in a larger sample population, the interactive feedback strategies' development, and the dynamic experimental characterization' execution.

**Keywords:** Ankle Exoskeleton, PAFO, Control Strategies, Ankle Rehabilitation, Variable Stiffness Actuator, Gait Rehabilitation, Wearable Robot.

# Glossary

**6MT** 6-Meter Test.

**ADL** Activities of Daily Living.

**Ag-PMc** Adaptive Gain Proportional Myoelectric Controller.

**AGoRA** In Spanish *Desarrollo de una plataforma robótica adaptable para rehabilitación y asistencia de la marcha.*

**BPnA** Bidirectional Rotary Pneumatic Actuator.

**CDA** Cable-Driven Actuator.

**CNS** Central Nervous System.

**CP** Cerebral Palsy.

**ECIJG** In Spanish *Escuela Colombiana de Ingeniería Julio Garavito.*

**EMG** Electromyography.

**FF** Foot-Flat.

**FSR** Force Sensitive Resistor.

**GDI** Gait Deviation Index.

**GPS** Gait Profile Score.

**HMM** Hidden Markov Model.

**HO** Heel-Off.

**HS** Heel Strike.

**HyA** Hydraulic Actuator.

**IMU** Inertial Measurement Unit.

**MAP** Movement Analysis Profile.

**MinCiencias** In Spanish *Ministerio de Ciencia y Tecnología*.

**MRA** Magnetorheological Actuator.

**PAFO** Powered Ankle-Foot orthosis.

**PAM** Pneumatic Artificial Muscle.

**PID** Proportional-Integral-Derivative.

**PLA** Polylactic Acid.

**PMc** Proportional Myoelectric Controller.

**PnA** Pneumatic Actuator.

**PWM** Pulse-Width Modulation.

**QUEST** Quebec User Evaluation of Satisfaction with assistive Technology.

**REASISTE** In Spanish *Red Iberoamericana de Rehabilitación y Asistencia de Pacientes con Daño Neurológico mediante Exoesqueletos Robóticos de Bajo Coste*.

**RMS** Root Mean Square.

**ROM** Ranges of Motion.

**ROS** Robotic Operating System.

**SCI** Spinal Cord Injury.

**SEA** Serial Elastic Actuator.

**SOM** Spring Over Muscle.

**StA** Stiff Actuator.

**SW** Swing.

**TTL** Transistor-Transistor Logic.

**USB** Universal Serial Bus.

**VSA** Variable Stiffness Actuator.

**WHO** World Health Organization.



# List of Tables

2.1	Comparison of the actuation systems implemented on PAFOs . . . . .	24
4.1	T-FLEX's temporal parameters for the step response . . . . .	51
4.2	Variation percentages for comparing force levels . . . . .	54
4.3	P-values for comparing both configurations . . . . .	57
4.4	T-FLEX's capabilities for gait applications . . . . .	62
5.1	Subjects anthropometric measurements and clinical information. . . . .	70
5.2	Range of motion on the participants' lower limb joints in the proposed scenarios	76
5.3	Gait Deviation Index for each subject in Baseline and T-FLEX scenarios . .	79
5.4	Percentage of variation of spatial-temporal parameters . . . . .	80
5.5	Spatial-temporal parameters and GDI for the baseline and assisted gait . . .	81
5.6	Probability value (p-value) of each subject for stance and swing phases . . .	82
6.1	Subject's ROM on lower limb joints for the pre and post functional assessments	93
6.2	QUEST survey responses for the T-FLEX after the therapy sessions . . . . .	97

# List of Figures

1.1	Robotic devices and systems that include the AGoRA project. . . . .	7
3.1	Wearable and portable ankle exoskeleton T-FLEX . . . . .	29
3.2	Electronic system and communication protocols implemented on T-FLEX .	31
3.3	T-FLEX's control architecture . . . . .	32
3.4	Visual interface to control and configure T-FLEX from any smart device . .	33
3.5	T-FLEX's goal applications and their principal characteristics . . . . .	34
3.6	Control scheme for stationary rehabilitation using T-FLEX . . . . .	36
3.7	T-FLEX's control signals during a stationary therapy . . . . .	38
3.8	T-FLEX's control scheme for gait applications . . . . .	40
3.9	T-FLEX's control signals during an assistive application . . . . .	41
3.10	Mechanical configurations and elements involved in the T-FLEX exoskeleton during a gait cycle . . . . .	42
4.1	Mechanical structure and electronic system of the test bench based on the T-FLEX exoskeleton . . . . .	46

---

4.2	Step response of the system for the movements assessed . . . . .	50
4.3	System responses for the chirp signal in the tendons-alone configuration under a force level of 10 N . . . . .	58
4.4	Bandwidth values of the T-FLEX's actuators for different configurations, amplitudes, movements, and force levels on the tendons . . . . .	60
4.5	Maximum torque values on the ankle for the different analyzed setups. . . . .	61
5.1	T-FLEX exoskeleton's actuation system implemented on the passive orthotic structure . . . . .	71
5.2	Biomechanical setup model used in the study for each participant . . . . .	71
5.3	Volunteers' ankle kinematic during the gait cycle . . . . .	75
5.4	T-FLEX's effect on the joints range of motion . . . . .	78
5.5	Movement Analysis Profile . . . . .	79
5.6	Results of the usability assessment through the QUEST test . . . . .	82
6.1	Experimental setup postures proposed for assessment in therapy . . . . .	90
6.2	Percentage of variation for the kinematic and Spatio-temporal parameters in walking over the treadmill . . . . .	94
6.3	Mean RMS values per session during the study for the tibialis anterior and gastrocnemius . . . . .	95
6.4	Muscular activity behavior throughout the session in terms of mean and standard deviation between sessions . . . . .	96

# Contents

Acknowledgements	ii
Glossary	iv
List of Tables	vii
List of Figures	viii
<b>1 Introduction</b>	<b>2</b>
1.1 Motivation . . . . .	2
1.2 Background . . . . .	5
1.3 Objectives . . . . .	7
1.3.1 General Objective . . . . .	7
1.3.2 Specific Objectives . . . . .	8
1.4 Contributions . . . . .	8
1.5 Publications . . . . .	9
1.6 Document Organization . . . . .	10

---

<b>2</b>	<b>Human Ankle in Mobility</b>	<b>12</b>
2.1	Ankle-Foot Complex and its Role in Human Gait . . . . .	12
2.2	Neurological Conditions Affecting the Ankle . . . . .	14
2.2.1	Foot Drop . . . . .	15
2.2.2	Equinovarus Foot . . . . .	15
2.2.3	Ankle Spasticity . . . . .	16
2.3	Ankle Rehabilitation and Assistance . . . . .	16
2.3.1	Conventional Techniques and Devices . . . . .	17
2.3.2	Robotic Solutions . . . . .	18
2.4	Conclusions . . . . .	25
<b>3</b>	<b>T-FLEX Ankle Exoskeleton</b>	<b>26</b>
3.1	Mechanical Design . . . . .	26
3.1.1	Design Premises . . . . .	27
3.1.2	Mechanical Principles . . . . .	28
3.1.3	Mechanical Structure . . . . .	28
3.2	Electronic System . . . . .	29
3.2.1	Hardware . . . . .	29
3.2.2	Software . . . . .	30
3.2.3	Control Architecture . . . . .	31

3.2.4	Visual Interface . . . . .	32
3.3	Operational Modes . . . . .	34
3.3.1	Therapy Mode . . . . .	34
3.3.2	Assistance Mode . . . . .	37
3.4	Conclusions . . . . .	43
<b>4</b>	<b>Experimental Characterization of T-FLEX</b>	<b>44</b>
4.1	Test Bench's Mechatronic Design . . . . .	45
4.2	Experimental Design . . . . .	46
4.2.1	Experimental Procedure . . . . .	47
4.2.2	Data Acquisition and Processing Equipment . . . . .	48
4.2.3	Statistical Analysis . . . . .	48
4.3	Results . . . . .	49
4.3.1	Step Response . . . . .	49
4.3.2	Chirp Response . . . . .	57
4.3.3	T-FLEX in gait applications . . . . .	62
4.4	Discussion . . . . .	63
4.5	Conclusions . . . . .	67
<b>5</b>	<b>Validation in Gait Assistance</b>	<b>68</b>
5.1	Experimental Design . . . . .	69

---

5.1.1	Participants . . . . .	69
5.1.2	Experimental Setup . . . . .	70
5.1.3	Biomechanical Analysis . . . . .	72
5.1.4	Experimental Procedure . . . . .	72
5.1.5	Usability Assessment . . . . .	73
5.1.6	Statistical Analysis . . . . .	73
5.2	Results . . . . .	74
5.2.1	Kinematics . . . . .	74
5.2.2	Spatio-temporal Parameters . . . . .	80
5.2.3	Usability Assessment . . . . .	81
5.2.4	Statistical Analysis . . . . .	81
5.3	Discussion . . . . .	83
5.4	Conclusions . . . . .	86
<b>6</b>	<b>Validation in Gait Rehabilitation</b>	<b>87</b>
6.1	Experimental Design . . . . .	88
6.1.1	Participant . . . . .	88
6.1.2	Pre and Post Functional Assessment . . . . .	88
6.1.3	Experimental Procedure . . . . .	89
6.1.4	T-FLEX's Parameters . . . . .	90

6.1.5	Data processing and acquisition . . . . .	91
6.1.6	Usability Assessment . . . . .	91
6.1.7	Statistical Analysis . . . . .	91
6.2	Results . . . . .	92
6.2.1	Pre and Post functional Assessment . . . . .	92
6.2.2	Muscular Activity . . . . .	94
6.2.3	Usability Assessment . . . . .	96
6.3	Discussion . . . . .	96
6.4	Conclusions . . . . .	99
<b>7</b>	<b>Conclusions and Future Works</b>	<b>100</b>
	<b>References</b>	<b>104</b>



# Chapter 1

## Introduction

The work presented in this dissertation focuses on the development and validation of control strategies applied to the T-FLEX ankle exoskeleton, which is part of the AGoRA project [1]. The device's experimental characterization, intended to provide the maximum capabilities and the most appropriate configuration for assistive applications, is described. Moreover, experimental validation with stroke patients for both assistance and rehabilitation to assess T-FLEX in real applications is outlined. This chapter introduces the main motivations and research objectives that lead to the development of this dissertation. Finally, the main contributions, publications, and the document's reminder are also described.

### 1.1 Motivation

Mobility is a fundamental human capacity defined as moving throughout an environment and efficiently performing daily tasks [2]. Within this capacity, the ankle-foot complex plays a primary role in ensuring a proper execution [3]. Specifically, in the gait cycle, the ankle provides to the human the capabilities of (1) propelling the leg, (2) ensuring clean contact between the foot and the ground, (3) absorbing shock and impacts, and (4) avoiding foot-

drag in the swing phase [3]. However, some pathologies, such as Stroke, Spinal Cord Injury (SCI), and Cerebral Palsy (CP), can affect those functions [2,4], inducing abnormal motions because of compensatory reactions in the affected limb [3].

In global terms, people with disabilities reach 15% of the world's population (i.e., 1 billion people approximately) [5], being stroke the main cause [6]. Specifically, this pathology reports 15 million new cases every year [7,8], wherein 5 million people die and others 5 million remain permanently disabled [8]. Moreover, studies indicate that from the 10 million stroke survivors, 90 % of them exhibit motor impairments related to after-effects such as severe or complete loss of motor functions (hemiplegia) or weakness (hemiparesis) in a body's side [9,10]. On the other hand, SCI reaches from 250.000 to 500.000 new cases annually [11], where 30 % of affected people present deterioration in the health status (i.e., loss of motor and sensory functions, resulting in spasticity and pain syndromes) [10,12]. Finally, CP reports a prevalence rate from 1.5 to 4 cases per 1.000 births [13]. This condition causes limitations such as abnormal posture, altered movement, and reduced muscle tone [14],

To overcome the impairments in the locomotor system, conventional physical therapy is commonly implemented to improve patients' health conditions and provide a certain degree of independence in activities of daily living (ADL) [15,16]. Traditional physical therapy comprehends exercises such as repetitive movements and task-oriented training, aiming to provide the patient the maximum independence as possible for executing ADL [17]. Nevertheless, this process requires more time, effort, and several therapists focused on a single patient [18].

Consequently, technology is being used in rehabilitation as an efficient solution to improve conventional therapy [19–21]. Those devices employ concepts such as neuroplasticity and adaptable abilities of the central nervous system (CNS), showing promising results [21–23]. On the other hand, the ankle dysfunctions can remain in the patients after therapy [24]. Thus, to provide stability and prevent injuries due to the lack of ankle control, passive orthotic devices are prescribed [25]. A passive orthosis is a mechanical structure that only allows the

dorsi-plantarflexion movements and restricts other motion planes. However, although passive devices help the patient execute ADL [26], the user does not improve the gait pattern, and conversely, the locomotion is affected by both the dysfunction and the ankle restriction [27].

Therefore, robotic devices are being developed to support the rehabilitation processes and assist user gait [18, 28]. Specifically, the powered ankle-foot orthoses (PAFOs) or ankle exoskeletons integrate the principles applied in passive orthotic structures, although they incorporate the advantages of robotics (i.e., energy supply using actuators, user monitoring through sensors, programmed functionality profiles, among others) [28]. Those devices have been divided by the state-of-art according to their purpose, and the system actuation implemented [29,30]. In terms of the actuation system, the most common actuators used in PAFOs are (1) stiff, (2) pneumatic, and (3) series elastic [29,31]. However, other actuation principles are based on the previous actuators, such as the variable stiffness actuation (VSA) [31].

VSA uses the same concept as series elastic (i.e., an elastic element with a spring between the actuator and the load), although this principle includes a variable stiffness spring instead of a constant value [31–33]. The core feature of actuators based on VSA is changing the system output stiffness in different interaction cases with the environment (e.g., constant load and constant position) [32]. Moreover, this principle also presents advantages in shock loads and backdrivability, like the series elastic actuators [31,33]. Considering the mentioned advantages, for robotic applications where the robot interacts intensively with humans, this type of actuation is widely recommended [34,35]. Specifically, a study found reductions in user’s metabolic cost concerning the actuators’ stiffness level [35].

Within this context, T-FLEX was developed in the scope of the AGoRA project, constituting a wearable and portable ankle exoskeleton based on VSA to assist the dorsi-plantarflexion movements without restricting other ankle motions. T-FLEX applies novel concepts derived from the human body’s functioning, looking for providing a potential tool in rehabilitation and assistance scenarios. Thus, the stakeholders (e.g., patients and their social environment,

therapist, clinical staff, and researchers) could benefit from the outcomes presented in this dissertation, and overall, from the AGoRA project.

## 1.2 Background

This dissertation is developed in the context of the research project "Development of an Adaptable Robotic Platform for Gait Rehabilitation and Assistance" (AGoRA project) supported by *Ministerio de Ciencia y Tecnología* (MinCiencias grant 801-2017) and internal funding from the Colombian School of Engineering Julio Garavito (ECIJG). Moreover, this thesis is also supported by the Ibero-American Network for the Rehabilitation and Assistance of Patients with Neurological Impairments through Low-Cost Robotic Exoskeletons REASISTE (Grant 216RT0504).

The AGoRA project is primarily led by Prof. Dr. Carlos A. Cifuentes (professor at the Department of Biomedical Engineering and head of the *Center for Biomechanics* at ECIJG). The project's research team is formed by a cooperation network comprising both national and international research groups and institutions. In the clinical context, the trauma and rehabilitation group of *La Sabana* University Clinic (led by Dr. Catalina Gómez) constitutes the project's medical partner. On the other hand, for the technical and research development, the project team integrates three international research groups: (1) the Neural and Cognitive Engineering group of the Center for Automation and Robotics at the Spanish National Research Council headed by Dr. Eduardo Rocon (Spain), (2) the Institute of Automation at the University of San Juan led by Dr. Ricardo Carelli (Argentina), and (3) the Robotics and Industrial Automation Group at the Federal University of Espírito Santo headed by Dr. Anselmo Frizzera-Neto (Brazil).

The AGoRA project's primary goal consists of deploying and validating a robotic platform for gait rehabilitation and assistance. This objective demands the establishment of appropriate

interaction techniques between the user and the robotic platform. Thus, different sensors and actuators can estimate the interaction and respond appropriately to it. Within the project development, two interfaces are conceived: (1) a cognitive interface, where the user controls the robot while receiving feedback, and (2) a physical interface for the forces exchange between the user and the platform.

Therefore, to achieve the AGoRA project's purpose, a robotic platform composed of two rehabilitation devices will be addressed. Specifically, an active lower limb exoskeleton and a smart walker will constitute the final AGoRA project's robotic platform. Likewise, the exoskeleton will be divided into two devices: (1) a stiff exoskeleton to support the knee and hip joints, and (2) a soft exoskeleton to assist the ankle. The robotic platform will be controlled by an interface serving as a communication channel between the patient and the rehabilitation therapy, equipped with a processing unit to support the implemented software architecture.

Figure 1.1 illustrates the main elements of the AGoRA project and its multimodal interface. The platform uses several sensors and actuators to provide: (1) an electro-mechanical actuation (i.e., using the motor-encoder-gearbox kit for the stiff exoskeleton, the servomotors and tendons for the soft exoskeleton, and the motor-encoder kit on the robotic walker ), (2) a user's physical estimation (i.e., through triaxial force sensors and strain gauges), (3) a user's state estimation (i.e., employing inertial sensors, electromyography, and laser), and (4) an environment interaction (i.e., using the camera and a laser range finder sensor).

From the AGoRA project's scope mentioned above, this master dissertation intends to develop and validate control strategies in the ankle exoskeleton T-FLEX for assistance and rehabilitation of gait. This way, this work intends to answer the following research question: Does the implementation of control strategies in the T-FLEX exoskeleton promote recovering in motor functions in a rehabilitation scenario?

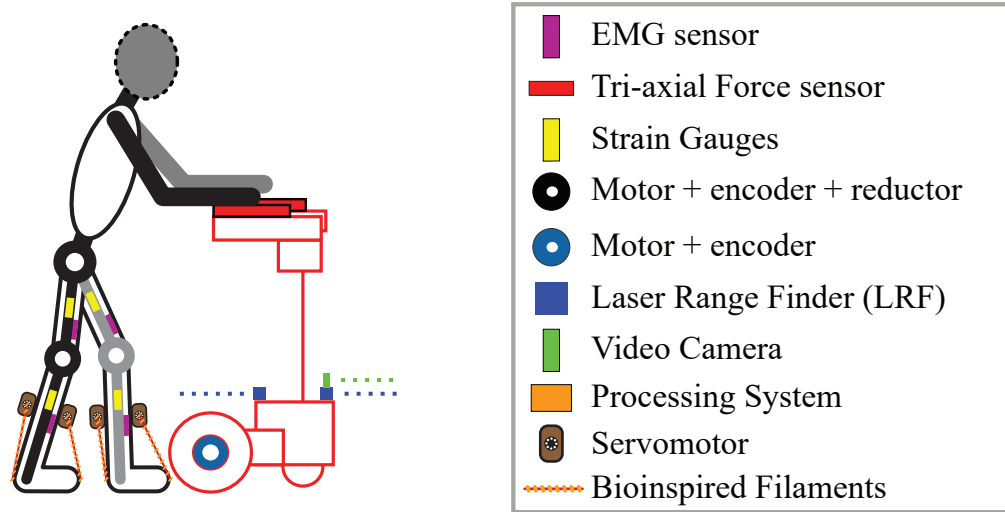


Figure 1.1: Robotic devices and systems that include the AGoRA project.

Finally, later stages of the AGoRA project will extend the robotic platform’s capabilities, integrating and joining the functionalities of both exoskeletons and the smart walker in clinical scenarios. Thus, the development of novel rehabilitation techniques involving the devices and the design of shared high-level control strategies will be addressed.

## 1.3 Objectives

This work proposes developing and validating control strategies applied in the ankle exoskeleton T-FLEX for gait rehabilitation and assistance. Thus, this dissertation exhibits the first understanding of T-FLEX as well as the feasibility of application in patients who suffer neurological impairments. For that, this work defines the following objectives.

### 1.3.1 General Objective

Develop control strategies for a variable stiffness ankle-foot orthosis for gait rehabilitation of patients with ankle impairments.

### 1.3.2 Specific Objectives

- Conduct a systematic review of the literature in ankle rehabilitation employing exoskeletons.
- Develop a control system architecture for T-FLEX considering both, kinematics and detection of user's gait phases.
- Model and characterize the actuation system proposed in T-FLEX.
- Propose therapies using the T-FLEX exoskeleton in a rehabilitation program.
- Assess the short-term effects in a group of stroke patients with ankle impairments using T-FLEX.

## 1.4 Contributions

The dissertation's primary contributions presented in this document are framed in the main activities of the AGoRA project, which are focused on the development of an ankle exoskeleton for rehabilitation and assistance. The fulfillment of this work covers a series of technical and scientific contributions presented as follows:

1. The hardware and software developments related to the T-FLEX exoskeleton. The visual feedback developments and the mechanical structure were performed in cooperation with the master and undergraduate students of the AGoRA project.
2. The T-FLEX's characterization's design and execution using a test bench structure to verify the application in assistive tasks and measure the device capabilities.
3. The design and development of the control system and the software architecture for T-FLEX are based on the Robotic Operating System (ROS). This architecture was designed under the premise of being modular and easily reproducible.

4. The design and execution of experimental protocols for the assessment of T-FLEX in patients with ankle dysfunctions. The international cooperation network of the project allowed support in the validation of the device in walking.

## 1.5 Publications

The dissertation presented in this document has been reported to the scientific community through the following publications:

1. (**Conference Proceedings**) **D. Gomez-Vargas**, M. J. Pinto-Bernal, F. Ballén, M. Múniera and C. A. Cifuentes, "Therapy with T-FLEX Ankle Exoskeleton for Motor Recovery: A Case Study with a Stroke Survivor," 2020 8th IEEE RAS/EMBS International Conference for Biomedical Robotics and Biomechatronics (BioRob), New York City, NY, USA, 2020, pp. 491-496, DOI: 10.1109/BioRob49111.2020.9224277.
2. (**Conference Proceedings**) A. Pino, **D. Gomez-Vargas**, M. Munera, and C.A. Cifuentes, "Visual Feedback Strategy based on Serious Games for Therapy with T-FLEX Ankle Exoskeleton" The International Symposium on Wearable Robotics (WeRob2020) and WearRAcon Europe, 2020
3. (**Book Chapter**) Sierra S., Arciniegas L., Ballen-Moreno F., **Gomez-Vargas D.**, Munera M., Cifuentes C.A. "Adaptable Robotic Platform for Gait Rehabilitation and Assistance: Design Concepts and Applications" 2020 In: Exoskeleton Robots for Rehabilitation and Healthcare Devices. SpringerBriefs in Applied Sciences and Technology. Springer, Singapore, DOI: 10.1007/978-981-15-4732-4\_5
4. (**Conference Proceedings**) M. Sánchez-Manchola, **D. Gómez-Vargas**, D. Casas-Bocanegra, M. Múniera and C. A. Cifuentes, "Development of a Robotic LowerLimb Exoskeleton for Gait Rehabilitation: AGoRA Exoskeleton" 2018 IEEE ANDESCON, 2018, pp. 1-6, DOI: 10.1109/ANDESCON.2018.8564692.



5. (**Conference Proceedings**) M. Manchola, D. Serrano, **D. Gómez**, F. Ballen, D. Casas, M. Munera, and C.A. Cifuentes, "T-FLEX: Variable stiffness ankle-foot orthosis for gait assistance" *The International Symposium on Wearable Robotics*, 2018, (pp. 160-164). Springer, Cham, DOI: 10.1007/978-3-030-01887-0\_31.
6. (**Journal [Submitted]**) **D. Gomez-Vargas**, F. Ballén-Moreno, D. Casas-Bocanegra, M. Múniera and C. A. Cifuentes, "T-FLEX: A novel Ankle Exoskeleton based on Variable Stiffness Actuators for Rehabilitation and Assistance" *Actuators*.
7. (**Journal [Submitted]**) **D. Gomez-Vargas**, F. Ballén-Moreno, C. Rodriguez-Guerrero, M. Múniera and C. A. Cifuentes, "Experimental Characterization of the T-FLEX Ankle Exoskeleton for Gait Assistance" *Control Engineering Practice*
8. (**Journal [Submitted]**) **D. Gomez-Vargas**, F. Ballén-Moreno, P. Barria, R. Aguilar, J. M. Azorín, M. Múniera and C. A. Cifuentes, "Actuation system of the ankle exoskeleton T-FLEX: first use experimental validation in people with stroke." *Frontiers in Neuroscience*.

## 1.6 Document Organization

This dissertation presents the electronic and software design of the ankle exoskeleton T-FLEX belonging to the AGoRA project. Moreover, this document includes the design and implementation of several high-level control strategies for rehabilitation and assistance scenarios and the experimental characterization of the device. Finally, this work reports preliminary validations with pathological users in walking assistance and a short rehabilitation program. Thus, the document is structured as follows:

- **Chapter 1** presents the primary motivations and research goals of this work. Additionally, this chapter describes the research project that frames this dissertation, and the key contributions of this thesis.

- **Chapter 2** introduces the human gait, focusing on the ankle-foot complex's role. Likewise, this chapter explains the principal ankle dysfunctions and the different gait rehabilitation alternatives and techniques. Lastly, this chapter presents the literature review regarding the robotic devices, control strategies, and actuation principles applied to the PAFOs.
- **Chapter 3** describes the ankle exoskeleton T-FLEX in terms of the mechanical structure, electronic system, and the implemented visual interface. Moreover this chapter also presents the control architecture implemented in T-FLEX and the high-level strategies proposed for both assistance and rehabilitation applications.
- **Chapter 4** describes the T-FLEX's experimental characterization from the test bench's design to the outcomes regarding the device performance, the influence of the involved elements, T-FLEX capabilities, and the applicability in assistive scenarios.
- **Chapter 5** reports the experimental validation in T-FLEX's first-use with stroke patients for an assistive task overground. This way, this chapter analyzes the effect of T-FLEX on the user's kinematics and the influence on spatiotemporal parameters
- **Chapter 6** details the preliminary validation of T-FLEX in a rehabilitation program with a stroke patient who exhibited spasticity. This chapter presents the electromyography (EMG) behavior and the changes in the ranges of motions (ROMs) and spatiotemporal parameters.
- **Chapter 7** summarizes and highlights the main conclusions and remarks of this dissertation. Moreover, this chapter proposes the future works to be addressed, focusing on the execution of a long-term validation study and the integration with the AGoRA project's robotic platform.

# Chapter 2

## Human Ankle in Mobility

The ankle plays a fundamental role in human mobility, being a primary capacity that influences aspects such as health condition, social interaction, execution of ADL, and people's quality of life. In conceptual terms, this faculty is defined as the ability to move and interact within an environment. Nevertheless, different neurological conditions can affect locomotor functions, affecting mobility performance. This way, from the ankle's importance and the need for mobility, rehabilitation through conventional and robotics solutions is commonly used to recover the loss functions. Thus, this chapter describes the ankle-complex role in human mobility and the principal dysfunctions in these joints. Likewise, this chapter summarizes current conventional and robotic solutions applied to the ankle-foot complex for rehabilitation and assistance.

### 2.1 Ankle-Foot Complex and its Role in Human Gait

The ankle-foot complex consists of 28 bones divided into the distal tibia and distal fibula, seven tarsals, five metatarsals, and 14 phalangeal bones [36]. These joints, formed by the bones, work synchronously to accomplish distinctive functions in ADL's execution [36]. In

contrast to other lower joints, the ankle-foot complex movements involve several planes of motion [36, 37]. For instance, supination requires plantarflexion, inversion, and adduction movements, while pronation includes dorsiflexion, eversion, and abduction [37].

In terms of the range of motion (ROM), the ankle has variations concerning the geographical and cultural differences [37]. Specifically, for the main movements on the ankle, studies estimate standardized ranges between 65 and 75 degrees in the sagittal plane (i.e., 10 to 20 degrees covers the dorsiflexion and 40 to 55 the plantarflexion) and 35 degrees in the frontal plane (i.e., 23 degrees during eversion and 12 degrees in inversion) [3, 37]. However, ADL's execution requires reduced ROM values. For instance, the dorsi-plantarflexion movements need 30 degrees for walking and 37 and 56 degrees for ascending and descending stairs, respectively [36, 37].

In the kinetic context, the ankle-foot complex works as a power dissipator, bearing approximately five times body weight during stance in normal walking and up to thirteen times body weight during other ADLs (e.g., running) [37, 38]. Nevertheless, the ankle also can work as a generator, providing enough torque to execute propulsion tasks. This way, to accomplish ADLs properly (e.g., walking), this complex joint needs to generate a torque per kilogram of 1.6 Nm/kg approximately [3, 37].

From the characteristics presented above, the ankle-foot complex has several functions during the gait cycle. Thus, the ankle roles are mainly related to the proper transition between phases, shock absorption in the heel strike, body center of mass's transference, torque's supply to initiate the swing, and control to avoid toe drag [29, 39]. In the muscular context, three muscles' groups intervene in these functions: (1) invertor muscles (i.e., tibialis posterior-anterior and flexor hallucis longus-soleus), (2) evertor muscles (i.e., peroneus longus-brevis and extensor digitorum-hallucis longus), and (3) triceps surae muscles (i.e., gastrocnemius and the soleus) [3, 37].

## 2.2 Neurological Conditions Affecting the Ankle

Different pathologies can affect human mobility resulting in alterations of stability, cadence, gait speed, proper joints control, and gait balance [3, 40]. This way, the motor impairments' effects can lead to a limited ADL's execution, reducing people's quality of life [2, 4]. In neurological terms, cerebrovascular accident (stroke), Spinal Cord Injury (SCI), and Cerebral Palsy (CP) are the principal causes of those alterations [2, 4].

According to the World Health Organization (WHO), around 1 billion people (i.e., 15% of the world population) exhibit any disability type [41]. Moreover, studies report an increase in this number of nearly double by 2050 [42]. Within the current statistics, low- and middle-income countries register the higher rates compared to the high-income countries [43], leading to a relevant impact because of accessibility issues and the lack of health care services [41].

Specifically, stroke is the principal cause of disability and the second leading cause of death worldwide [6]. This pathology reports 15 million new cases annually, of which more than 60% exhibit partial or chronic motor dysfunctions [44]. Conceptually, stroke is defined as a neurological injury that can be presented in two cases: (1) ischemic, where a blood clot blocks a blood vessel in the brain, and (2) hemorrhagic, when a ruptured blood vessel bleeds into the brain [45]. For both situations, the brain functions suffer affectations causing motor and cognitive failures in the survivor [46].

On the other hand, SCI also registers a significant number of impaired people. Studies report statistics of up to half a million people who suffered SCI with an incidence of 18.000 new cases every year [11]. This condition refers to the spinal's traumatic damages, causing fractures on the vertebrae [47]. SCI leads to neurological dysfunctions whose affectation level depends on the region affected by the spinal contusion [47, 48].

Lastly, Cerebral Palsy groups around 800.000 people worldwide [49]. This neurological dis-

order occurs before birth generally, although there are cases during life's first years [50]. Statistically, the CP's prevalence rate registers cases from 1.5 to 4 per 1000 children [51], related to abnormal development or neurological damage in the brain [52].

Considering the neurological conditions that affect mobility, the ankle-foot complex can evidence several after-effects, altering its normal functions described previously [53, 54]. This way, patients commonly generate compensatory movements to supply the affected ankle functions [27]. For instance, in gait applications, people perform a steppage gait, bending the hip and knee excessively to lift the foot higher [55]. However, altered patterns such as circumduction gait (i.e., when the leg remains straight and swings to the side in a semicircle to move forward) are also used [55]. In this sense, the principal ankle dysfunctions are detailed below.

### **2.2.1 Foot Drop**

Foot drop is a locomotor dysfunction caused by different neurological impairments. People who suffer from this condition cannot raise the front foot part because of weakness or muscle paralysis [55]. Thus, this pathology exhibits difficulty to clear the foot while walking, often dragging or scuffing along the ground, resulting in a characteristic slapping gait [55, 56]. Likewise, the foot drop produces poor positioning and unsteadiness of the ankle and knee during standing states, causing limitations in balance and stability during ADLs [55].

### **2.2.2 Equinovarus Foot**

Equinovarus foot is a motor disorder present in hemiplegic patients, characterized by the reduction in ankle dorsiflexion and alteration in the forefoot inversion [57]. This condition affects the swing phase, causing the forefoot to strike the ground first instead of the heel [57]. Thus, equinovarus foot produces inadequate support, which has negative consequences for

both balance and gait [58]. Likewise, the gait pattern alteration caused by this pathology leads to changes in the muscle morphology and ankle's force production capacity [57].

### 2.2.3 Ankle Spasticity

Spasticity is a motor disorder characterized by increased muscle tone with excessive tendons jerks [59]. This complication can involve single or multiple muscle groups, causing pain and discomfort in ADL's execution [60]. Specifically, this condition includes muscle hypertonia, hyperactive deep-tendon reflex, clonus, and velocity-dependent resistance to passive stretch [61]. In functional terms, the ankle spasticity leads to diminished power generation, decreased joints' ROM, reduced stability for the stance phase, and is consequently considered a relevant risk factor for falls [62].

## 2.3 Ankle Rehabilitation and Assistance

Physical therapy in a rehabilitation scenario has been widely used to counteract motor dysfunctions because of neurological conditions [15]. Specifically, this process helps to improve the motor and neurological recovery in affected people [63]. For that, the rehabilitation includes training in both task-specific and context-specific, particularly in the early stages after injury [64]. Those tasks intend to promote the patients' capacities for completing multiple activities such as bed mobility, body motions to execute ADL, and patient-environment interaction [16].

Nevertheless, the ankle dysfunctions can remain in the patients after therapy [24]. Thus, to provide stability and prevent injuries due to the lack of ankle control, passive orthotic devices [25], and robotic tools [18, 28] are used. In this sense, the principal conventional techniques and the robotic solutions to assist and rehabilitate the ankle are detailed below.

### **2.3.1 Conventional Techniques and Devices**

Conventional physical therapy involves rehabilitation processes' execution by health professionals without being supported by a robotic tool [18]. Different techniques to recover the patients' motor capacities are widely applied within this methodology, exhibiting positive outcomes [15]. On the other hand, in the assistive context, passive structures mainly counteract the motor limitations and guarantee certain independence level performing ADL [25].

#### **2.3.1.1 Exercises Programmes**

Physical exercises prevent immobilization's complications and improve patient's skills to achieve proper ADL's execution. On the one hand, this activity covers passive exercises wherein the therapist moves the body part passively through the total joint's ROM. This way, passive training prevents possible contractures and abnormal postures [65]. On the other hand, active exercises (i.e., the patient actively moves the joint) are also applied. For this type, the patient attempts simple movements during the first stages until achieving complex tasks. These exercises usually are combined with multiple repetitions to induce motor re-learning [65].

#### **2.3.1.2 Neuro-physiological Techniques**

In this case, the developed techniques use neurophysiological principles for motor control and recovery [65]. Thus, this methodology includes mainly (1) sensory stimuli's application to facilitate or inhibit an activity, (2) treatment plans based on achievements, (3) motor re-learning induced by repetitions, and (4) close therapist-patient interaction [65].

From the neurophysiological principles, different strategies such as Bobath (i.e., movement pattern and postural control's corrections by handling the major joints in the affected body



part), proprioceptive neuromuscular facilitation for stimulating proprioceptors in the affected limbs, and Brunnstrom (i.e., involving a reflex or a synergistic movement to attain appropriate movement control and functional performance), can be found [65,66]. These strategies can integrate verbal, visual, and tactile feedback to facilitate their proper application [66].

### **2.3.1.3 Passive Orthotic Devices**

Considering the ankle dysfunctions that can remain after therapy, passive orthotic devices are commonly prescribed [25,26]. Those devices comprehend mechanical structures, based on customized molded plastic designs, that only allow the dorsi-plantarflexion movements and restrict the other planes of motion [25]. Thus, passive orthoses provide stability counteracting the ankle's weakness, prevent injuries related to the lack of ankle control, and improve foot clearance in gait activities [25,26].

## **2.3.2 Robotic Solutions**

Robotic tools are being applied to support the rehabilitation processes and assist the user gait, showing promising results [21–23,28]. Developing those devices derives from the need to overcome the drawbacks exhibited by traditional therapy and passive devices.

In the therapy context, conventional procedures are intensive tasks that require more time, effort, and several therapists focused on a single patient [18]. Moreover, in assistive terms, although the passive structure helps in ADL's execution, the user does not improve the gait pattern, and conversely, the locomotion is affected by both the dysfunction and the ankle restriction [27].

Currently, there are mainly two robot's kinds for ankle rehabilitation and assistance: (1) wearable devices that aim at improving ankle performance during gait, and (2) platform-based robots that intend solely on the improvement of ankle functions [24]. Therefore,

wearable devices, also called Powered Ankle-Foot Orthoses PAFOs or ankle exoskeletons, exhibit advantages concerning platform-based systems in aspects such as multimodality and applicability [24].

PAFOs integrate the principles applied in passive orthotic structures, although incorporating the robotics' benefits (i.e., energy supply using actuators, user monitoring through sensors, programmed functionality profiles, among others) [28]. In functionality terms, those devices mainly aim at improving the patients' gait pattern or decrease the biological effort during walking [29]. In this sense, the following sections present the standard actuation systems and the control strategies implemented on wearable devices.

### **2.3.2.1 Actuation Systems implemented on PAFOs**

The state-of-art classifies into three main categories the actuation principles applied in PAFOs: (1) Stiff Actuators (StAs), (2) Serial Elastic Actuators (SEAs), and (3) Pneumatic Actuators (PnAs) [29]. However, some works also include other less common principles used as actuation mechanisms, such as (4) Hydraulic Actuators (HyAs), and (5) Magnetorheological Actuators (MRAs) [30]. Likewise, other actuation systems widely implemented nowadays can be categorized as (6) Variable Stiffness Actuators (VSAs), and (7) Cable-Driven Actuators (CDAs).

1. **Stiff Actuators:** PAFOs with StAs are composed of motors coupled with gear transmissions. They are generally supported by rigid structures, allowing the torque transmission directly to the joint axis. The main advantages in StAs are the high torque supplied and the bandwidth concerning other mechanisms [67]. Notwithstanding, StAs exhibit drawbacks for the ankle's applications regarding the impact's absorption, misalignments, backdrivable capability, and physical interaction.
2. **Series Elastic Actuators:** SEAs are being applied in PAFOs to counteract the limitations of StAs. In this sense, the system includes an elastic element with a constant

spring between the actuator and the load. SEAs actuate as a low pass filter to shock loads, where the amount of elasticity increases or decreases the absorption tolerance [67]. Moreover, systems based on SEA have backdrivable capabilities because the load is uncoupled from the actuator. This way, the user-device physical interaction improves in wearable applications. Nevertheless, SEA technology exhibits a dependency on amplitude and phase related to the elastic element's force, resulting in system bandwidth's variations [67].

3. **Pneumatic Actuators:** These actuators are based on bioinspired actuation. In essence, PnAs are contractile and linear motion engines operated by gas pressure. The most common PnA's type is Pneumatic Artificial Muscle (PAM). PAMs are composed of flexible membranes, that once they are inflated exert a pulling force on the end-effector [68]. Other configurations are using PnA technology such as double-acting Spring Over Muscle actuators (SOM), and Bidirectional rotary Pneumatic Actuators (BPnAs) [29]. The main advantages of PnAs are high flexibility and softness in the actuation, which is comparable with a natural muscle [69]. Nonetheless, this actuator generally needs external air supplies, precluding the portable solutions' implementation. Additionally, PAMs present low bandwidth and modeling challenges for interaction scenarios [69].
4. **Hydraulic Actuators:** HyAs use pressurized fluids to transmit torque to the joint. To this end, flexible hoses transport the fluid to the actuator, and thus they can be snaked over the joint in locations that are impractical for the other actuation mechanism [70]. This actuation type can provide high torque, but this feature also comes with a disadvantage given by the required equipment's heavyweight and complexity [71]. On the other hand, HyAs exhibit backdrivability within the limits of fluid drag forces [70], improving the physical interaction concerning StAs.
5. **Magnetorheological Actuators:** MRAs integrate controllable fluid with variable viscosity. This viscosity varies through the exposition to magnetic fields [72]. The

main MRA's advantage is related to the inherent stabilization capability when providing torque [73]. Additionally, this actuator can provide a quiet, simple, and faster response compared to other mechanisms. The drawbacks include the complex and heavyweight equipment implemented to achieve this actuation and the high energy consumption [72].

6. **Variable Stiffness Actuators:** VSAs use the same concept as SEAs, although instead of coupling an elastic material with a constant spring, an element with a variable spring is included. The core VSA's feature is the capability for changing the output stiffness in two interactions cases with the environment: (1) constant load and (2) constant position [32]. This actuation type is recommended in rehabilitation fields using robotic devices to interact intensively with the human [34]. In terms of disadvantages, VSAs share the same limitations as SEAs. However, the complexity of controlling and modeling systems with this actuation system is increased.

7. **Cable-Driven Actuators:** This actuator consists of a moving platform connected to a fixed base through a certain amount of cables. Thus, the cables' length changes individually using a motor with a spool, which results in reeling in and out [74]. The principal drawbacks in CDAs are related to the inability to allow passive backdrivability because of the high friction and the low capacity to transmit torque in portable devices.

### 2.3.2.2 Control Strategies for PAFOs

From the actuation system principles mentioned above, PAFOs have implemented different control strategies to guarantee proper physical interaction in terms of overall safety, transparency, and level of patient participation [75]. Additionally, these strategies mainly aim at regulating the force levels and motions applied to the joint under rehabilitation processes [34]. For this purpose, the literature classifies the control strategies into two groups: (1) low-level and (2) high-level [76].

**Low-level strategies:** Low-level refers to basic implemented strategies for controlling actuators such as position, force, admittance, and impedance controllers [76]. These strategies support more elaborate control architectures focused on real applications with human interaction named as high-level. The low-level strategy selection will depend on the actuator type and the sensors' feedback in an interaction scenario. Moreover, the control law could be given by different techniques applied to linear and non-linear systems such as fuzzy logic, PID and its variations, adaptive control, controllers based on neural networks, and others [77].

**High-level strategies:** High-level control strategies are algorithms designed explicitly to promote ankle plasticity [78]. These strategies are classified depending on the user-device interaction's level and the effort performed by the user. Within this group, different methods can be found: (1) passive controllers, (2) active controllers, (3) active-assistive controllers, and (4) active-resistive controllers.

1. **Passive Controllers:** In this control type, the device performs motions on the ankle joint, and the user requires no effort [78].
2. **Active Controllers:** This strategy requires the user to voluntarily move to a pre-specified target while the device records kinematic and kinetic parameters. In other words, the robot works as an assessor [29, 78].
3. **Active-assistive Controllers:** For this controller type, there is user-device cooperation for executing a specific task. Initially, the system has the same function as an active controller, but if the user fails in the motion, the device will provide the assistance needed to achieve the goal [29, 78].
4. **Active-resistive Controllers:** This controller is intended to be a trainer. To this end, the device generates an opposing force that resists the user's movement [78].

On the other hand, the sensors' inclusion in ankle devices can in turn divide the control strategies into the following categories: (1) proportional myoelectric controller (PMc), (2) adaptive gain proportional myoelectric controller (Ag-PMc), (3) phase-based controller, and (4) push-button controller [29].

The proportional and adaptive myoelectric controllers are related to muscle activity's acquisition and processing [29]. In both cases, the device starts the actuation when the muscle exceeds the electrical activity in a determined range [29]. The difference consists in the control action executed by the device. Specifically, PMc generates an output proportional to the user activity, but Ag-PMc adjusts the gain to have the maximal peak actuation [29].

Conversely, the phase-based controller is the most common strategy used in rehabilitation and assistance scenarios [29]. In this controller type, the control action depends on the gait events detection. For this purpose, wearable sensors such as Inertial Measurement Unit (IMU) and Force Sensitive Resistor (FSR) are implemented. Finally, in the push-button controller, the actuation is proportional to the push-button's displacement [29]. This strategy leads to controlled teleoperation by the user.

From the strategies and actuation principles presented above, Table 2.1 presents a comparison between the different types of actuator systems implemented in PAFOs. It considers relevant aspects such as the type of backdrivability, level of torque provided for ankle rehabilitation, portability, bandwidth, ease of implementation, common low-level control strategies employed, and some examples of real applications.

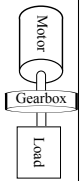
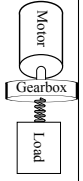
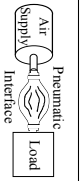
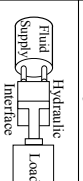

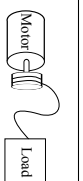
Characteristics	Type of Actuators						
	StA	SEA	PnA	Hya	MRA	VSA	CDA
<b>Schematic</b>							
<b>Back-drivability</b>	Active	Passive: Dependency on the spring constant	Passive	Passive within the limits of fluid drag forces.	Active	Passive: Dependency on the initial spring constant	Active
<b>Torque Provided</b>	High Torque	Torque reduced by the elastic element	High and medium	High Torque	High Torque	Torque reduced by elastic element	Medium torque partial assistance level
<b>Portability</b>	Portable	Portable	Portable for low assistance levels	Portable	Non-portable	Portable	Portable
<b>Bandwidth</b>	High bandwidth	Dependency on the spring constant	Medium bandwidth	High bandwidth	High response times	Dependency on the spring constant	Dependency on the coiling and uncoiling
<b>Integration</b>	Simple	Simple	Complex	Complex	Complex	Simple	Simple
<b>Common Low-level controllers</b>	Position, Admittance, Impedance	Position - inherent torque Impedance	Force, Torque	Force, Torque	Force	Position - inherent torque or stiffness Impedance	Position Impedance
<b>PAFOs</b>	[79], [80]	[81], [82], [83]	[84], [85], [86]	[87], [88]	[89]	[90], [91], [33]	[92], [93]

Table 2.1: Comparison of the actuation systems implemented on PAFOs

## 2.4 Conclusions

Considering the ankle role in gait and hence the relevance in the execution of ADL, the development of robotic devices has been motivated to counteract the after-effects caused by neurological disorders. Likewise, these devices have been applied in rehabilitation scenarios to support the therapists and optimize the sessions. This way, the health professionals can be focused on the users' progress and performance without having to spend time and effort on physical tasks with the patient.

The inclusion of robotics aims at improving the motor recovery results compared to conventional therapy. However, despite the robotics advantages and the promising results in rehabilitation, the ankle remains a challenging research area because of the movement complexity, involved joints, and the ankle's functions. In this context, this chapter summarized the main robotic solutions applied to the ankle's recovery and assistance focused on wearable devices (i.e., PAFOs). Moreover, the principal actuation systems and control strategies implemented in this application were also described.



# Chapter 3

## T-FLEX ankle exoskeleton: Design and Operation

Considering motivations and current developments for ankle rehabilitation and assistance showed previously, this chapter introduces the design and development of the T-FLEX ankle exoskeleton, which is part of the AGoRA platform and wherein this dissertation is focused. This device integrates a compliant actuation system and a soft structure ideal for neurological patients. Moreover, the proposed T-FLEX's design responds to the human body's biological functioning, incorporating the robotics' advantages in assistive and rehabilitation scenarios.

### 3.1 Mechanical Design

T-FLEX is a wearable and portable ankle exoskeleton intended for patients with ankle limitations resulting from neurological disorders. The implemented actuation system and designed structure integrate the device into a small exoskeleton's group called fully compliant exoskeletons [31]. The following sections describe the design premises, mechanical principles, and the mechanical structure that comprehend T-FLEX.

### 3.1.1 Design Premises

From the ankle functions and their affectations related to the pathologies presented in Chapter 2, the T-FLEX's design mainly intends to (1) provide stability to the user, (2) correct the pathological ankle posture, (3) assist the dorsi-plantarflexion movements, and (4) allow the ankle motions in other planes. First and second premises are kept within the minimum requirements, which are provided by both robotic devices and passive orthotic structures prescribed to the ankle treatment [25, 26]. Specifically, stability allows independence during ADL's execution, blocking the ankle's weakness and providing firmly foot-ground support [25]. Likewise, corrections in pathological ankle postures limit the falls and injuries' risks [26, 94].

For dorsi-plantarflexion assistance, the principal interest lies in improving the gait pattern. This way, other joints' compensatory movements (e.g., in the hip and knee joints), during ADL's execution [27], can be reduced. Likewise, the changes in the user's kinematics lead to improve the metabolic costs and decrease permanent damage's risk to the locomotor system [27]. On the other hand, in rehabilitation terms, assisted movements on the ankle allow designing intensive therapies. Thus, the health professional can focus on the patient's progress and performance instead of executing the exercises. Furthermore, considering the robotics' advantages explained in chapter 2, interactive sessions can be carried out, recording and displaying session data, and interconnecting with other robotic systems.

Lastly, the non-restriction in ankle motions represent one of the fundamental pillars in the T-FLEX's development. In this aspect, the device evidences a relevant change concerning other ankle exoskeletons [31]. Generally, PAFOs integrate rigid structures to support the actuator and transmit the torque directly to the joint [29, 31]. However, those designs present drawbacks related to misalignments when the torque is directly transmitted [75] and restrictions when the rigid elements surround the ankle. Moreover, complete blocking on the ankle affects the user's balance and alters the gait pattern during gait applications [95, 96].

### 3.1.2 Mechanical Principles

T-FLEX integrates two main mechanical principles to achieve the design premises mentioned above: (1) variable stiffness actuation and (2) bidirectional movement (i.e., agonist and antagonist configuration). The first principle intends to modify the stiffness level of the system according to the gait phases. For this purpose, the device includes a novel composite tendon whose mechanical behavior, tested in stress trials, is similar to the human Achilles tendon (i.e., Young's modulus between 500-1800 Mpa) [97]. The tendon braid flexible materials (i.e., thermoplastic elastomer and fibers of polyethylene) and stiff filaments (i.e., polytetrafluoroethylene) to achieve an exponential stress-strain curve. The volumetric proportion between both materials is 15% being the stiff filaments the minimum volume value to guarantee this function.

The second principle is the bidirectional actuation emulating the muscles' agonist and antagonist configuration [98]. T-FLEX uses stiff filaments combined with the tendons to assist the user's dorsi-plantarflexion movements. The composite tendons attach the frontal and posterior actuators to the foot-tip and the heel, respectively. Likewise, T-FLEX includes stiff filaments to integrate both motors in the ankle movements' execution. Those elements attach the opposite actuator with the corresponding foot part (i.e., the posterior motor to the foot-tip and frontal motor to the heel), Thus, the posterior actuator aids the dorsiflexion, and the frontal actuator contributes to the plantarflexion.

### 3.1.3 Mechanical Structure

T-FLEX incorporates 3D printed pieces of polylactic acid (PLA) to support the actuators. Besides, interfaces composed of flexible polyurethane-coated and coated with silicone fixes the actuators to the user's shank (see Figure 3.1). This design allows portable applications, avoids slipping, and reduces pressure points on the limb related to reaction forces when the device actuates. Conversely, to transmit torque on the ankle, T-FLEX uses an insole

adapted with printed pieces for attaching the composite tendons to the foot (i.e., heel for plantarflexion and metatarsals for dorsiflexion).

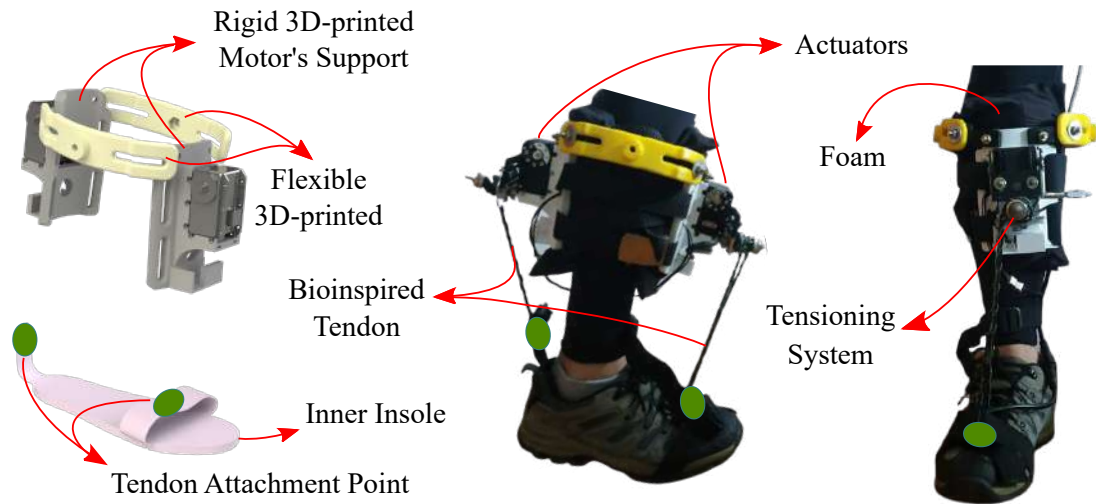


Figure 3.1: Wearable and portable ankle exoskeleton T-FLEX. The remarked elements refer to the main parts of the device.

## 3.2 Electronic System

From the premises and goal applications exhibited above, T-FLEX integrates two smart servomotors, an inertial sensor, and a processing unit within the open-source robotic meta-operating system. Likewise, considering the target population, a visual interface was designed and implemented to control and configure the device. The principal elements and developments, which T-FLEX contains, are illustrated in Figure 3.2 and detailed below.

### 3.2.1 Hardware

T-FLEX has two servomotors Dynamixel MX106-T (Robotis, Korea) placed on the posterior and anterior part of the user's affected shank. Each actuator has a stall torque of 10 Nm with a maximum no-load speed of 55 rpm. Moreover, the servomotor includes a microcontroller ARM CORTEX-M3 (72 MHz, 32Bit) to control, configure, and connect the actuator with

an external device. The actuators work under the transistor-transistor logic protocol (TTL). Thereby the device includes a Universal Serial Bus (USB) converter.

On the other hand, the sensing system comprises an inertial measurement unit (IMU) BNO055 (Bosch, Germany) placed on the foot tip, running at 100 Hz. For assistive and rehabilitation scenarios, the IMU information (i.e., angular velocity and acceleration) is used to trigger the device. Specifically, for gait applications, an algorithm based on machine learning estimates the user's gait phases in real-time [99]. In contrast, for the therapy, a statistical algorithm determines the user's movement intention.

For the processing, T-FLEX uses a Raspberry Pi 3 Board running in Debian operating system. Thus, the computer acquires sensor information, runs the control algorithms, and sends the control commands to the actuators. Finally, in the power supply context, the device has a LiPo battery of 4000mah 4S 14.8V 30C, which allows an autonomy close to 4 hours in non-extreme conditions (i.e., high level of spasticity and excessive strain on the tendons or stiff filaments).

### 3.2.2 Software

The software implemented on the T-FLEX exoskeleton is based on the Robot Operative System (ROS) architecture, a Linux-based meta-operative system widely used in the robotics field. This system provides relevant advantages such as modularity to incorporate sensors and actuators already supported, operability to communicate with multiple processes, robustness against unexpected events, and quickly developed modules' replicability [100].

Within this framework, the controllers, algorithms, and sensor acquisitions were deployed and implemented. The libraries for actuators' communication and control are based on the Dynamixel Workbench package supported by Robotis (Seoul, Korea). This way, T-FLEX has a public repository with the device's functionalities and controllers available at [https://github.com/GummiExo/t\\_flex](https://github.com/GummiExo/t_flex). This repository details the procedures to configure

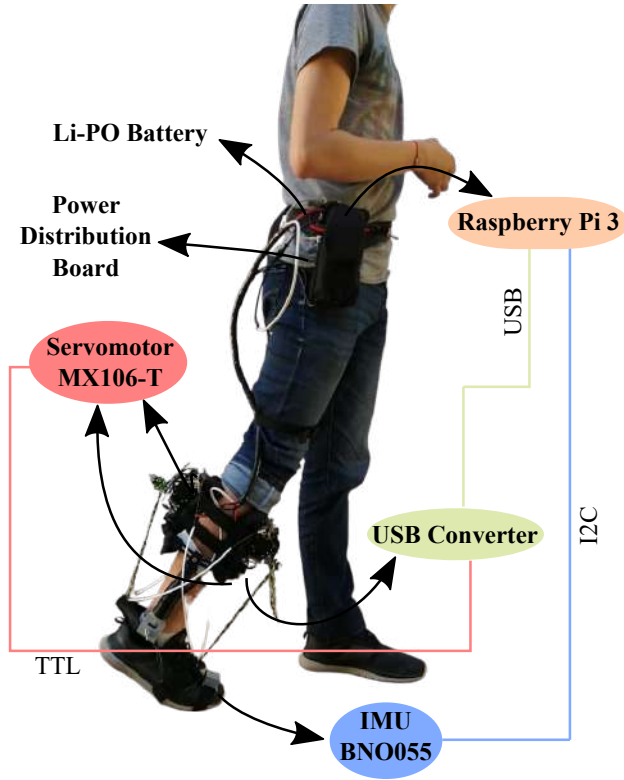


Figure 3.2: Electronic system and communication protocols implemented on T-FLEX

the actuators and the device’s computer, install required libraries for proper operation, and connect the device for using it. Likewise, it contains the mechanical structure’s files, which could be openly replicated under a non-commercial license.

### 3.2.3 Control Architecture

T-FLEX has a control architecture divided into two main parts: (1) actuators controller and (2) mechanical design’s effect. The first part refers to the internal PID controller implemented on each motor as Figure 3.3 shows. This controller has as input a goal motor position (i.e.,  $\theta_1$  for the anterior actuator and  $\theta_2$  for the posterior servomotor) converted to profiles of velocity and acceleration (i.e.,  $v_{1,2}$  and  $a_{1,2}$ ). The PID controller calculates the PWM output based on those profiles. Finally, an inverter supplies the PWM value to the actuator (i.e.,  $\overline{V_{m1}}$  and  $\overline{V_{m2}}$ ), and an encoder closes the control loop.

The second part covers effects due to the tendons' inclusion in T-FLEX (see Figure 3.3). Actuation systems based on VSA have a dependency on the spring behavior in terms of provided torque and system's bandwidth, as chapter 2 shows. This way, the composite tendon included in T-FLEX leads to limited bandwidth and actuators' torque reduction (i.e.,  $\tau_{T1}$  and  $\tau_{T2}$ ), where its effect depends on the configured initial force level.

Nevertheless, considering the T-FLEX's mechanical design presented above, the torque on the ankle (i.e.,  $\tau_{A1}$  and  $\tau_{A2}$ ) increases proportionally concerning the user's foot length (see Figure 3.3). Moreover, regarding the assisted movements, the torque in dorsiflexion is greater than plantarflexion. This characteristic is because the distance between the ankle and the foot part, where the torque is transmitted (i.e., heel for plantarflexion and metatarsal for dorsiflexion), is different.

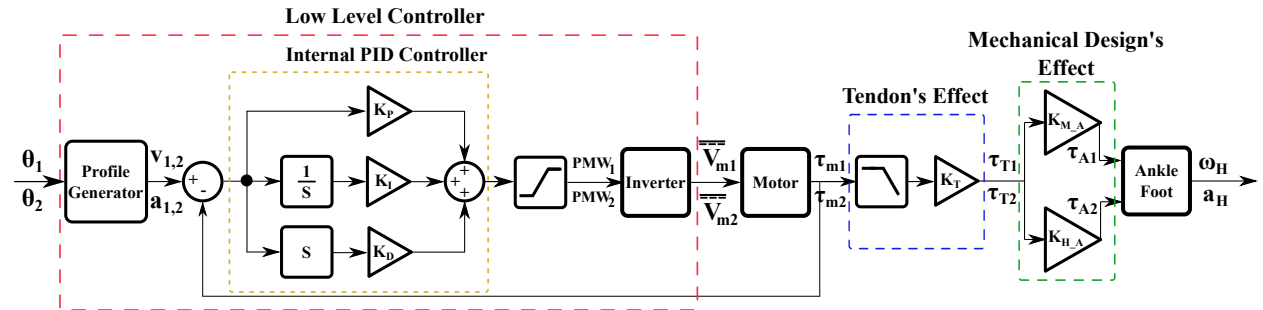


Figure 3.3: T-FLEX's control architecture. The red box refers to the low-level controller composed of the internal PID controller and the PWM. The blue box represents the tendon's effect in terms of limited bandwidth and reduced provided torque. The green box denotes the mechanical design's effects related to the distance between the tendon attachment point and the ankle.

### 3.2.4 Visual Interface

T-FLEX is a robotic tool aimed at rehabilitation and assistance scenarios. For this reason, Figure 3.4 shows a friendly visual interface to control and configure the device by the target users (i.e., health professionals and patients). Thus, this web interface incorporates functionalities such as (1) calibration of the device's ROM, (2) operation modes' selection, and (3) parameters configuration for those modes.

The first functionality (i.e., calibration stage) is a manual procedure, where the system records the actuators' maximum values to replicate the motion during the selected modality. Thus, the user can define the actuation ROM up to the limit value, avoiding injuries or pain related to the spasticity events. Likewise, the interaction forces can be modified concerning the patient's health conditions, varying the intensity whether the user exhibits the ankle's weakness or spasticity.

For the second and third functionalities, the user can choose the desired application with the device. Therefore, T-FLEX implements two operational modes detailed in the next section: (1) therapy through the assisted dorsi-plantarflexion repetitions and (2) gait assistance in portable applications. Within these modes, different parameters can modify the device's performance and the therapy's intensity (e.g., session duration, actuators' velocity, and repetition frequency).

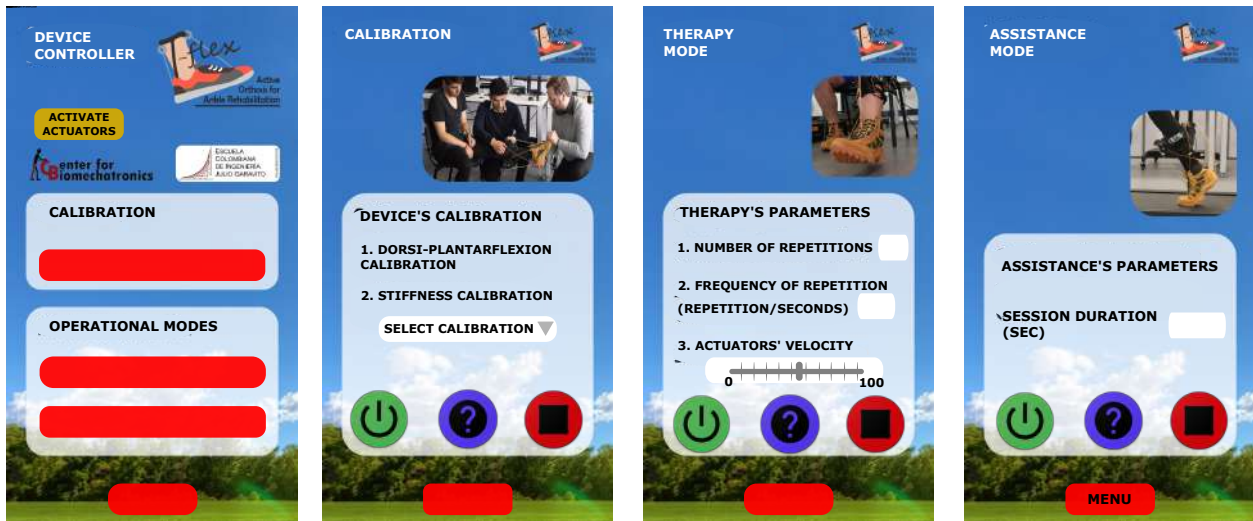


Figure 3.4: Visual interface to control and configure T-FLEX from any smart device

The visual interface is based on HTML language, where the functionalities and interactivity run under a JavaScript programming language. This way, the user can control and configure the device from any smart device. Likewise, the system integrates a server process to connect the interface with the T-FLEX's functionalities executed in ROS. The visual interface codes,



the installation procedures, and the users' guide are contained in a public repository available at [https://github.com/GummiExo/t\\_flex](https://github.com/GummiExo/t_flex)

### 3.3 Operational Modes

From the T-FLEX's goal applications, two modalities were implemented on the device. The first modality, i.e., Therapy Mode (see Figure 3.5A), refers to a rehabilitation scenario with T-FLEX, where the device executes repetitions, assisting the user's dorsi-plantarflexion movements. The second modality, i.e., Assistance Mode (see Figure 3.5B), intends to apply T-FLEX in assistive scenarios during ADL's execution as walking. As mentioned above, for both modalities, each patient's calibration stage is necessary to record the ROM and adjust the T-FLEX's performance.

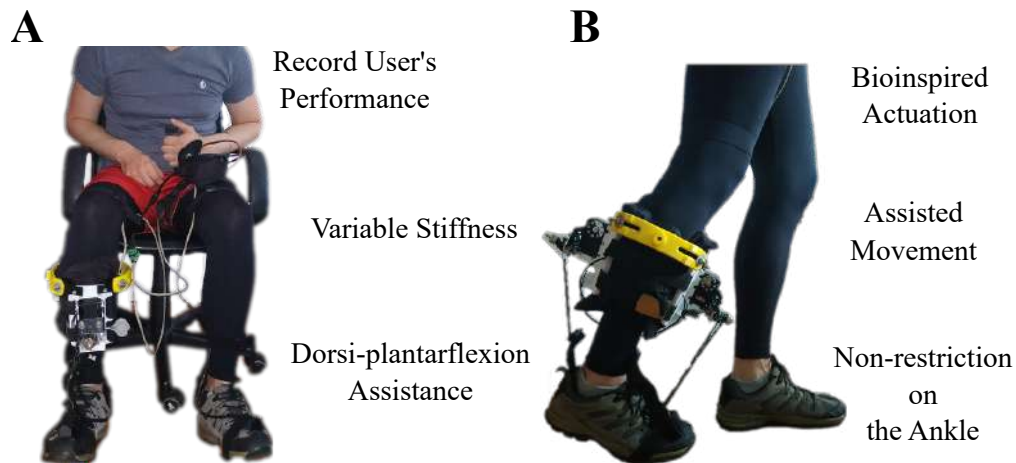


Figure 3.5: T-FLEX's goal applications and their principal characteristics. The left part (**A**) shows the T-FLEX supporting a rehabilitation scenario, and the right figure **B** illustrates the device in an assistive gait application.

#### 3.3.1 Therapy Mode

In this mode, T-FLEX provides the dorsi-plantarflexion movements repetitively according to the values recorded in the calibration stage detailed in the visual interface section. Rehabilitation programs apply this exercise, specifically in patients who present spasticity [101].

Likewise, the device can modify the therapy's intensity, varying the actuation velocity, repetitions frequency, and session duration (see Figure 3.4). T-FLEX can record the patient's performance and user-device interaction during the session. Moreover, the controllers integrate an emergency system to stop the device during any adverse event.

The principal T-FLEX's advantages in this application are monitoring and supervising the therapy (i.e., recording and displaying the user's data in real-time) and assisting the user's movements (i.e., moving the actuators). Furthermore, taking into account the device's soft structure and the ankle movement's freedom, unexpected conditions, such as muscle spasms or spasticity events, can be easily handled by T-FLEX without generating damage or pain to the patient.

On the other hand, as T-FLEX is developed under the ROS framework, additional sensors and actuators can be added easily. Thus, the system can adapt different feedback and interactive strategies to improve the user-device interaction, which is to face discouragement in long-term therapies, and contribute to the neuroplasticity induction [21, 102].

### **3.3.1.1 Control Strategy for Stationary Rehabilitation**

From the T-FLEX's application in rehabilitation scenarios presented above, the actuators receive the position commands to assist the dorsi-plantarflexion (i.e.,  $\theta_1$  for the anterior actuator and  $\theta_2$  for the posterior servomotor). Therefore, the set-points values in each servomotor must be opposite to replicate the movements, and their magnitude depends on the calibration stage (i.e., the process to record the user's ROM) presented in visual interface section.

Furthermore, parameters such as repetitions, frequency between movement, and actuators velocity control the therapy, influencing the user's effort and session's intensity. This way, according to the pathology and the patient's health condition, the exercises can be modified to improve the motor recovery's results [103].

Figure 3.6 shows the control scheme for a passive and assisted stationary rehabilitation sce-

nario using the T-FLEX exoskeleton. The safety restriction stage refers to the physical and software actions (i.e., stopping the actuation commands, turning off the servomotors, and limiting the actuators' ROM) to respond to unexpected events (e.g., spasticity events, joint pain, and skin injuries).

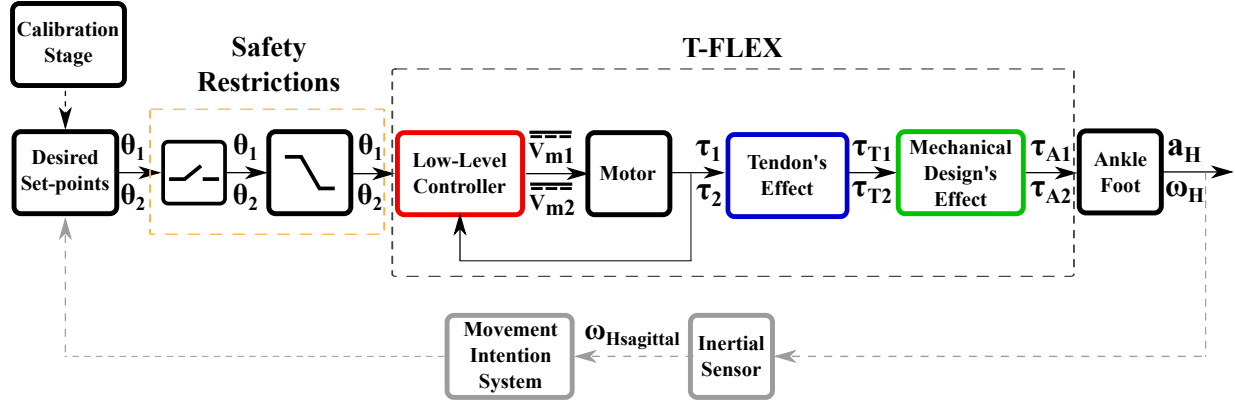


Figure 3.6: Control scheme for stationary rehabilitation using T-FLEX. The orange box represents the protective actions to respond to unexpected events. The red, blue, and green boxes are detailed in T-FLEX's control architecture section. The grey boxes refer to the movement intention's stage including an inertial sensor. The calibration stage denotes the process to record the user's ROM.

**User's Movement Intention:** On the other hand, the user's movement intention included in a control strategy has evidenced promising outcomes in therapy [104,105]. Thus, the active patient's participation can result in improving gait and physical function after a rehabilitation process [104,105]. Therefore, the inertial sensor integrated into T-FLEX can estimate the user movement intention on the paretic foot, replacing the automatic movement in the control scheme (see Figure 3.6).

Thus, initially, a 4th-order Butterworth low-pass filter with a cutoff of 6 Hz removes the noise from the angular velocity along the sagittal plane. Subsequently, the filtered data is compared in real-time with the threshold value calculated in the calibration stage, where the user executes several movements to define the threshold value. This way, T-FLEX assists the dorsi-plantarflexion when the angular velocity exceeds the threshold (see Figure 3.6).

Considering the control strategy and the movement intention system presented in Figure

3.6, Figure 3.7 shows the control signals for a stationary therapy using T-FLEX. Figure 3.7 A and B represent the user's intention module through and statistical algorithm to trigger the device. This way, T-FLEX accomplishes a dorsi-plantarflexion repetition when the user exceeds the threshold (see Figure 3.7C). Moreover, the current and velocity registered by the actuators is shown in Figure 3.7 D and E.

### **3.3.2 Assistance Mode**

For this modality, T-FLEX supports the human gait in assistive and rehabilitation scenarios. This way, the device can be applied in gait rehabilitation processes and during ADL's execution. The principal motivation consists of improving the patient's gait pattern. Thus, bearing in mind the compensatory movements related to the ankle dysfunctions [27], T-FLEX intends to correct the ankle kinematic looking for positive changes on the other joints [37].

In general terms, the device aims at providing stability during the stance phase and transmitting torque to the ankle to assist the propulsion stage. Moreover, the device also intends to avoid foot-slap and toe-drag, guaranteeing the foot-clear during the swing and improving the heel strike's shock contact.

#### **3.3.2.1 Gait Phase Detector**

For assistive applications, T-FLEX requires determining the user's gait cycle in real-time. Thus, the device integrates an algorithm based on a Hidden Markov Model (HMM), and the acceleration and angular velocity in the sagittal plane to estimate the gait phases: heel strike (HS), foot-flat (FF), heel-off (HO), and swing (SW) [99].

In general terms, the gait phase detector models the gait pattern using a left-right model, whose main feature is to limit transitions to consecutive states of the Markov chain [99]. Therefore, the phase change's probabilities are lower than remaining in the same event's probability [99].

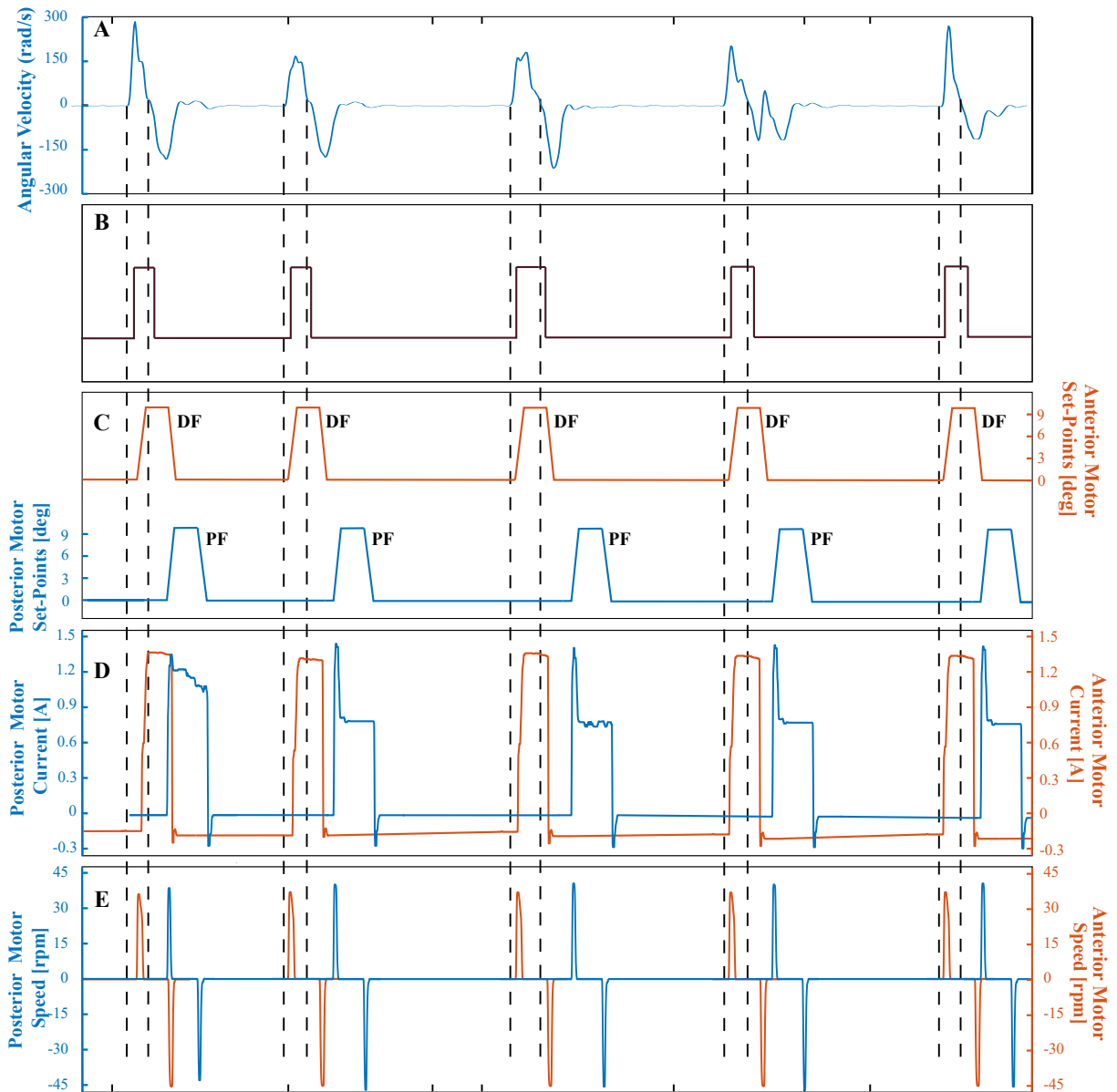


Figure 3.7: T-FLEX's control signals during a stationary therapy. The upper figure (A) shows the user's movement intention acquired from the angular velocity in the sagittal plane (i.e.,  $\omega_{H_{sagittal}}$ ). The B part illustrates the threshold algorithm's results and C the movement programmed to assist the therapy. The lower figures (D and E) show the actuators' current and speed to respond to the set-point commands.

The transition matrix needs a calibration stage for each user, where the device records the patient data during walking and calculates the statistical weights employing a Baum-Welch algorithm [99]. Subsequently, the gait phase detector uses a Viterbi algorithm to compare the model with live data and hence estimate the current gait phase.

### 3.3.2.2 Control Strategy for Gait Assistance

From the assistive application's goals and the gait phase detector presented previously, T-FLEX's control strategy for walking applications mainly includes (1) dorsi-plantarflexion assistance, (2) high stiffness level for stability in the stance phase, and (3) zero torque on the ankle also for the stance phase.

The set-points (i.e.,  $\theta_1$  for the anterior actuator and  $\theta_2$  for the posterior servomotor) are the equivalent as the stationary rehabilitation, although a new state is included, i.e., stiffness movement. This movement produces the maximum tendon's stretching, turning the actuators in the same direction. Moreover, considering the T-FLEX design, the torques' sum on the ankle tends to 0 Nm. The stiffness movement also integrates a calibration stage where the user can modulate the stretching level concerning the ankle's weakness.

In this context, Figure 3.8 shows the T-FLEX's control scheme, which includes a user's gait phases detector based on angular and acceleration measures on the paretic foot (i.e.,  $\omega_{Hsagittal}$ , and  $a_{Hsagittal}$ ). The system incorporates a state machine controller to determine the proper movement in a specific phase (i.e., dorsiflexion for heel strike and swing, plantarflexion for heel off, and stiffness for flat foot). Moreover, as in the stationary rehabilitation scheme, a safety restriction stage is included to ensure the user's security.

From the control strategy illustrated above, Figure 3.9 shows the principal signals measured on the actuators and sensors coupled in T-FLEX during a gait assistance application. Specifically, the user's acceleration and angular velocity (see Figure 3.9A) and the gait phase detector explained previously (see Figure 3.9B). Likewise, Figure 3.9C illustrates the actuators' angles to achieve the T-FLEX's movements (i.e., dorsi-plantarflexion and stiffness). On the other hand, the negative values (see Figure 3.9 D and E) for the current and speed indicate the movement direction related to the assisted movement (see Figure 3.9C)

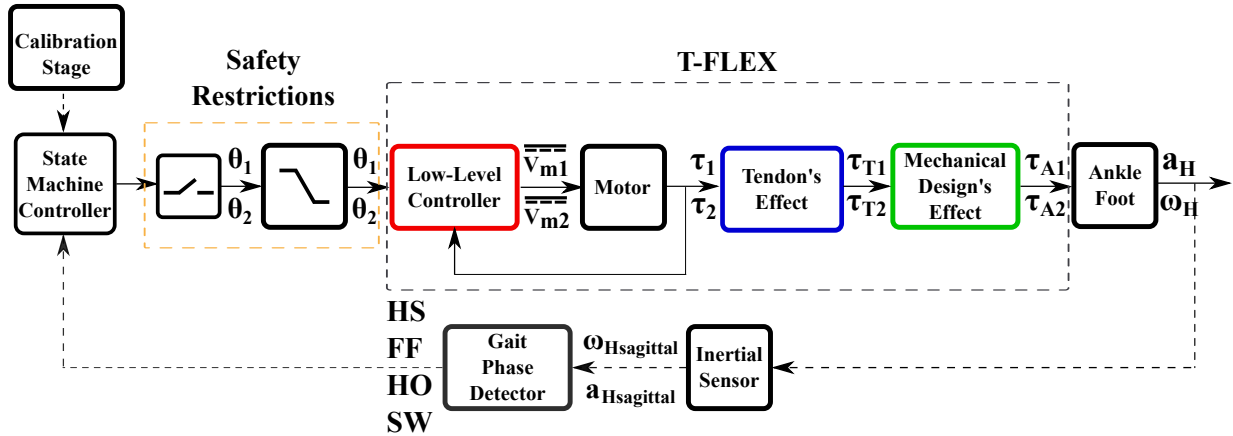


Figure 3.8: T-FLEX's control scheme for gait applications. The orange box refers to the control actions to counteract unexpected events. The red, blue, and green boxes represent the elements detailed in the T-FLEX's control architecture section. The gait phases detector describes the algorithm to detect HS: heel strike, FF: foot flat, HO: heel-off, and SW: swing phase, whose input depends on both the angular velocity and acceleration in the user's sagittal plane. The state machine controller outputs ( $\theta_1$  and  $\theta_2$ ) represent the angles in the actuators to accomplish the device movements (i.e., dorsi-plantarflexion and stiffness).

### 3.3.2.3 T-FLEX's Mechanical Operation

Considering the detection algorithm (see Figure 3.9) and the control strategy in gait (see Figure 3.8), Figure 3.10 shows the gait phases used by the T-FLEX exoskeleton in gait assistance: (A) foot flat (FF), (B) heel off (HO), (C) swing phase (SW), and (4) heel strike (HS). For each phase, the elements involved to assist the user's ankle are different (see involvement in Figure 3.10).

For the foot flat, illustrated in Figure 3.10A, both actuators turn in the same direction stressing the tendons. Thus, the system increases the stiffness for partially restricting the rotational movements on the ankle and stabilizing the foot during this phase. The stiff elements do not work in this configuration.

In the heel off phase, the posterior motor stresses the composite tendon to transmit torque and generate movement on the ankle. Additionally, the anterior motor turns in the opposite direction to aid in the torque transference using the stiff filaments. This way, the device

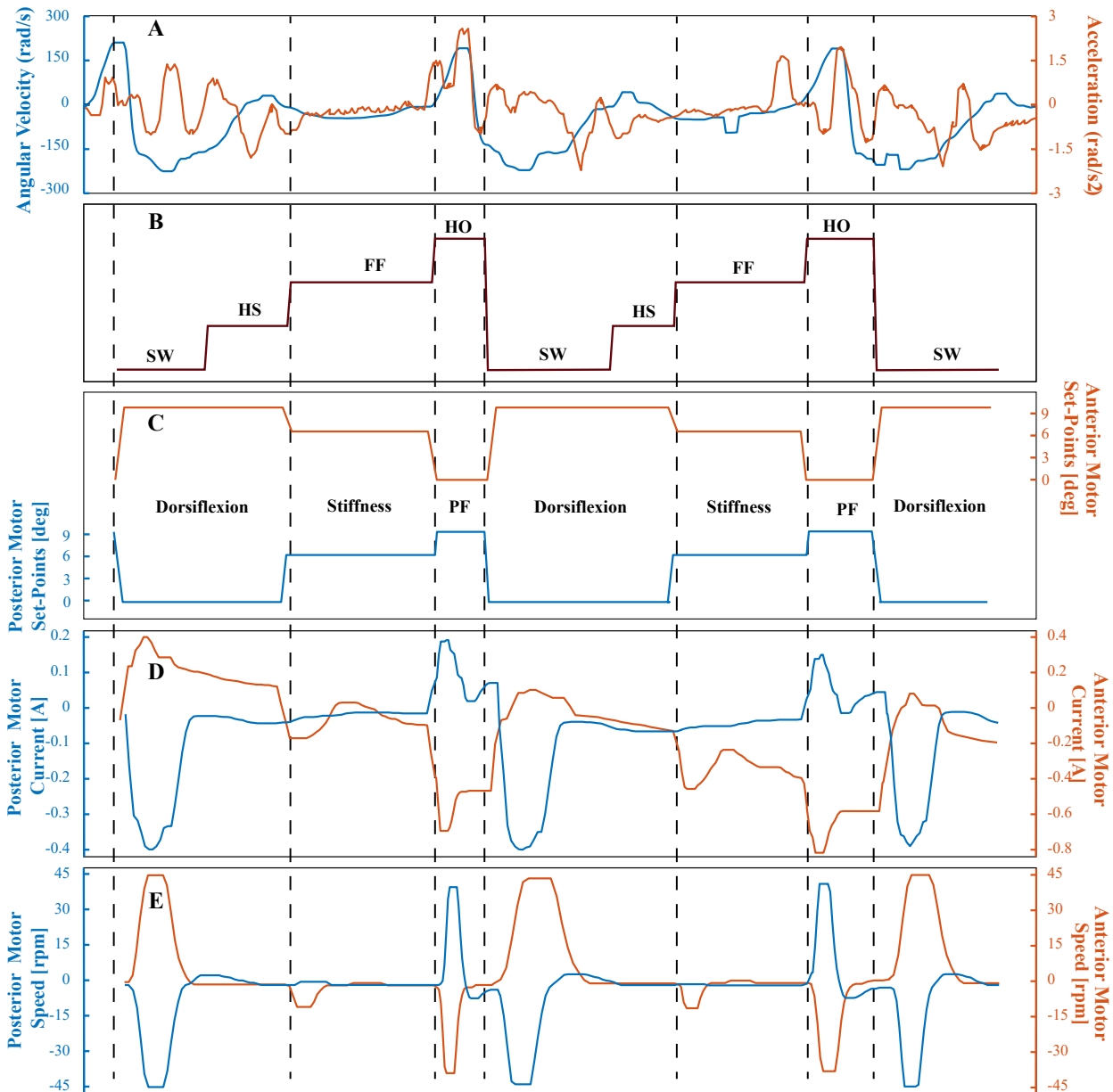


Figure 3.9: T-FLEX's control signals during an assistive application. The upper figure (**A**) shows the user's acceleration and angular velocity in the sagittal plane (i.e.,  $a_{Hsagittal}$ , and  $\omega_{Hsagittal}$ ). The **B** part illustrates the detection algorithm's results and **C** the movement programmed to assist walking. The lower figures (**D** and **E**) show the actuators' current and speed to respond to the set-point commands.

provides torque to propel the foot and initiate the leg swing (see Figure 3.10B).

Finally, in the heel strike and swing phase, the operation of the actuators is inverse, thereby the anterior motor stresses the tendon, and the posterior actuator pulls the stiff elements



(see Figure 3.10 C and D). This configuration aims to guarantee a clean contact of the foot to the ground and avoid toe-drag for improving the foot clearance.

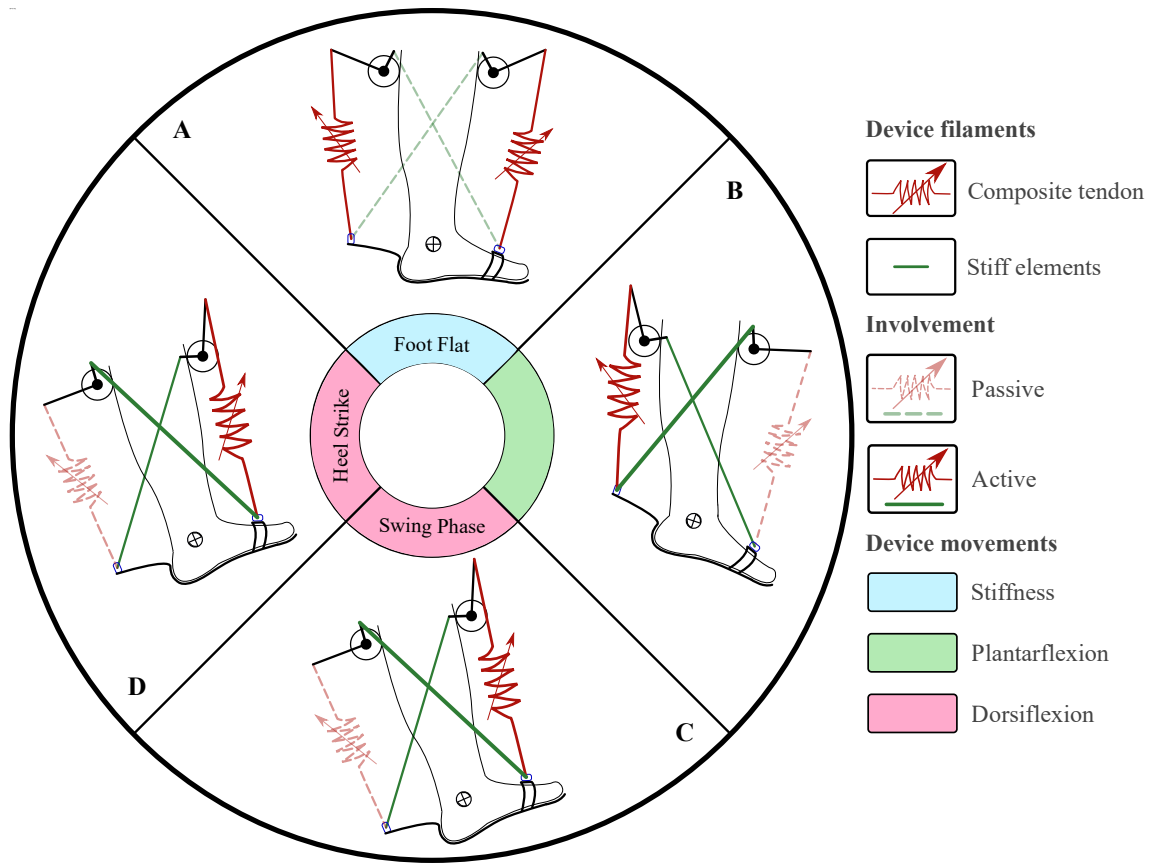


Figure 3.10: Mechanical configurations and elements involved in the T-FLEX exoskeleton during a gait cycle. The gait phases used are: (A) foot flat, (B) heel off, (C) swing phase and (D) heel strike. The elements highlighted have a role during the movement showed. In contrast, the elements with faded colors and segmented lines are not part of the movement. The remarked boxes indicate the configured movement in the device to assist the corresponding gait phase (i.e., blue for stiffness movement, green for plantarflexion, and red for dorsiflexion).

## 3.4 Conclusions

This chapter presented the development of the T-FLEX variable stiffness ankle exoskeleton for rehabilitation and assistive scenarios. The device's design integrated the basic premises for passive orthotic structures and current PAFOs (i.e., stability during stance phase, dorsiplantarflexion assistance, and ankle posture correction). However, T-FLEX also incorporated two fundamental pillars in its design: (1) bio-inspired actuation using composite tendons and (2) the non-restriction of the ankle's movement along the other planes of motion, through a soft structure. This way, T-FLEX can be considered as part of a small exoskeleton's group defined in the literature as fully compliant exoskeletons.

T-FLEX was developed under a modular framework allowing easy replicability and adding of external systems and sensors. The electronic system architecture was defined according to the device's goals. Specifically, T-FLEX included two smart servomotors, an inertial sensor, and a processing unit integrated into ROS. Moreover, a user-friendly visual interface was designed to control and configure T-FLEX in its two operational modes: (1) therapy and (2) assistance. In this context, two control strategies were proposed to allow the proper T-FLEX's use in these scenarios under the actuation premises. The algorithms, the visual interface, the mechanical structure, and the required T-FLEX's configurations were stored in a public repository available at [https://github.com/GummiExo/t\\_flex](https://github.com/GummiExo/t_flex).

## Chapter 4

# Experimental Characterization of T-FLEX

The experimental study of a wearable device, whose goal consists of interacting with people, is a currently under-explored area but of greater importance. Specifically, PAFOs' analysis in an experimental scenario is essential to measure the device's capabilities and determine the suitable configuration. Thus, this analysis allows knowing the applicability to accomplish complex tasks such as gait assistance.

This chapter presents the T-FLEX ankle exoskeleton's experimental characterization, carried out in a test bench structure. The principal goals were focused on (1) determining the appropriate configuration of the device for assisting the human gait with the best performance and (2) measuring the device's capabilities. Therefore, this study assessed the two mechanical principles presented in chapter 3 for three initial force levels on the tendons.

## 4.1 Test Bench's Mechatronic Design

Considering the mechanical structure of the T-FLEX exoskeleton presented in chapter 3, two main dimensions of the human leg affect the device performance, i.e., the length of the user's shank and foot size (see Figure 4.1B). The first measure refers to the distance between the ankle joint and 4cm below the knee joint, where is placed the system support. The second dimension consists of two parts: (1) the length between the 3D-printed anterior piece for attaching the tendon and the ankle and (2) the distance from the posterior tendon fixing piece to the ankle.

Following these technical specifications, Figure 4.1 shows the mechanical structure designed for this study. The test bench consists of an aluminum frame capable of adjusting distances according to T-FLEX operational ranges (i.e., people with a height between 1.50 and 1.85 m). Moreover, 3D-printed pieces, fixed in the structure, supports the actuation system. For the foot, an aluminum piece, similar to the human foot, allows replicating different anthropometric measurements and fixing both the composite tendons and the stiff filaments. Finally, the structure uses rigid couplers on the ankle to restrict the dorsi-plantarflexion movements.

The test bench incorporates a rotary torque sensor FY01 (Forsentek, China) coupled on the ankle joint, with a maximum torque of 50 Nm and a resolution of 0.001 Nm. Moreover, the structure includes 120 ohms strain gauges (RS PRO, UK) placed on the filaments' fixing system (see Figure 4.1A). The strain gauges integrate a complete Wheatstone bridge to estimate the force on the composite tendon. For the system actuation, the test bench includes the same T-FLEX's servomotors (i.e., the Dynamixel servomotor MX106T) running together with the sensors' acquisition system in ROS.

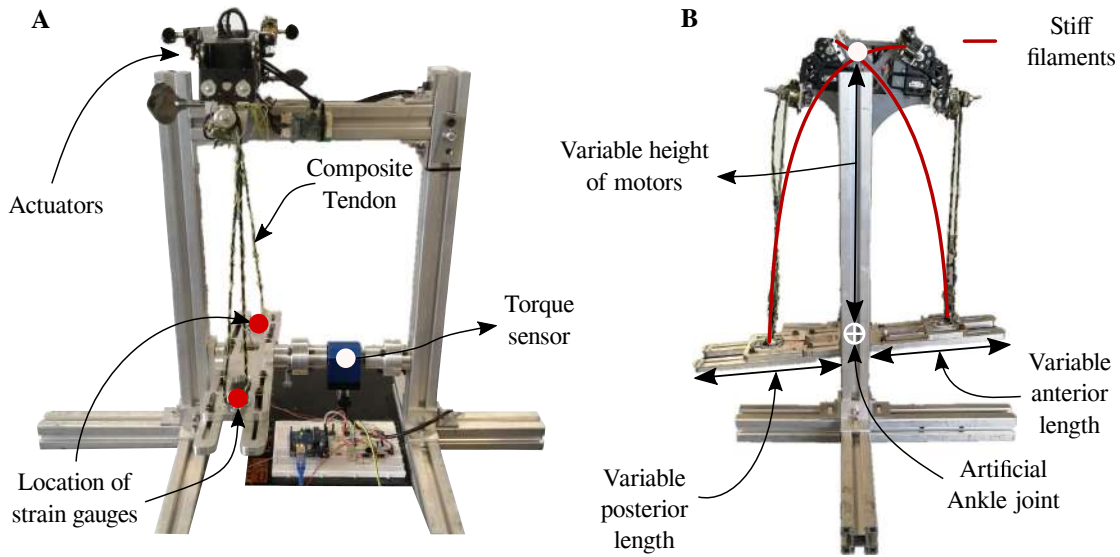


Figure 4.1: Mechanical structure and electronic system of the test bench based on the T-FLEX exoskeleton. The left part (A) shows the main elements of the test bench, and the right part (B) illustrates the dimensions that affect the device performance.

## 4.2 Experimental Design

The experimental design of this study aimed to assess the systems and configurations of the T-FLEX exoskeleton and measure the device's capabilities. Hence, the two setups involved in the study were: (1) the composite tendons working alone (i.e., tendons-alone) and (2) together with the stiff filaments (i.e., stiff-tendons). Moreover, considering the tendon's variable stiffness, this protocol included three initial force levels (i.e., 20 N for a high level, 10 N for medium, and 5 N for low) equals for both sides. Thus, chirp signals and step functions excited the test bench for all cases (i.e., combining the force levels with the two configurations) to measure both the system's response and the ankle joint interaction.

The step function consisted of a vector of two set-points sent repetitively every second, where the first value was the initial position for each motor (i.e., resting position). The second value was a position of 30 degrees concerning the initial state. This position represented the actuators' average value during a real application and assured the no overload condition

during the different trials proposed. The chirp signal performed a frequency sweep from 0 Hz to 10 Hz. Preliminary tests estimated the frequency range, considering the maximum value wherein the device could still respond to the signal. The maximum and minimum values were the same as the step function.

Considering the multiples inputs of T-FLEX, both functions (i.e., chirp and step) replicated the movements performed by the actuators during the system operation in gait showed in chapter 3: (1) dorsi-plantarflexion and (2) stiffness movement, as Figure 3.10 shows.

For the first movements, the actuators move in opposite directions (see Figure 3.10 B, C, and D). Thus, if the anterior motor was to 30 degrees, the posterior actuator performed the resting position. In the second state, the commands were opposite to replicate the dorsi-plantarflexion movements. On the other hand, for the stiffness movement (see Figure 3.10A), the actuators received the same command simultaneity, i.e., both motors in the resting position for the first state and both actuators to 30 degrees in the second state.

### **4.2.1 Experimental Procedure**

In the experimental procedure, both composite tendons were tightened until obtaining one of the three force levels (i.e., 5 N, 10 N, and 20 N). For the configuration that integrates the stiff and flexible elements, a previous installation stage was necessary. In this stage, the bidirectional filaments were tightened until assuring the dorsi-plantarflexion through the motor motion, and then the tendon was stressed.

Once the test bench integrated the configuration and reached the force level, the internal PID controller, detailed in chapter 3 (see Figure 3.3), was adjusted to guarantee the actuator's best performance concerning the torque because of the tendon's initial force level.

Subsequently, the actuators executed the step function's set-points (3 sets of 10 repetitions

each) and the chirp signal (3 times). In total, 27 trials were conducted, including the configurations described and the different levels of force.

## 4.2.2 Data Acquisition and Processing Equipment

For the data acquisition and processing, this protocol used an HP Pavilion Gaming Laptop (IntelCore i5-8300H, CPU@2.30 GHz, USA) running Linux 18.04.4 Bionic Beaver and Windows 10 Home. Likewise, ROS Melodic Morelia was the framework used to control the orthosis and read the sensors.

An analog-to-digital converter of 10 bits, integrated into an ATmega328P microcontroller, read the complete Wheatstone bridge's output in the gauges acquisition. The experimental data were acquired using the ROS package *rosvag*. MATLAB (MathWorks, 2018b, USA) extracted and processed the experimental data in terms of software.

## 4.2.3 Statistical Analysis

This study analyzes two configurations for the T-FLEX exoskeleton for four main movements used in gait (i.e., dorsi-plantarflexion, stiffness, and zero position) to three force levels. Firstly, a Shapiro-Wilk test verified the normality of data (54 tests). For that, the test used individually the variables extracted of each repetition executed (i.e., delay, stabilization, and rise times) for a total sample of 19 per parameter. The parameters with p-values larger than 0.05 followed a normal distribution.

Consequently, considering the data normality, three statistical analysis, using the Mann Whitney Wilcoxon test for non-normal data and t-test for normal distributions, were executed: (1) differences between the movements (i.e., dorsi-plantarflexion and stiffness-zero position) for each configuration in the same force level (27 tests), (2) differences between the same

configuration but different force levels (18 tests), (3) and differences between configurations in the same force level (18 tests).

After the second analysis, the post hoc test using the Bonferroni method determined which groups exhibited significant differences. For the tests performed, the statistical changes were guaranteed by p-values of less than 0.05. The software used for the statistical analyses was RStudio [106].

## 4.3 Results

### 4.3.1 Step Response

The step function measured both the T-FLEX's actuation system's responses and the composite tendons' behavior under tension. Figure 4.2A shows the curve obtained for the tendons-alone configuration with an initial force of 10 N during the dorsi-plantarflexion movements. The first set-point (i.e., segmented black line) describes the dorsiflexion command.

In this movement, the anterior motor turns to pull the foot, and the posterior actuator works reversely (see Figure 3.10 C and D). This way, the system transmits positive torque to assist the ankle. For the second set-point, the actuators operate opposite directions concerning the movement mentioned above (see Figure 3.10B), providing negative torque to assist the plantarflexion. Figure 4.2B shows the stiffness movement (see Figure 3.10A) and the resting position state values. Likewise, positive values of torque refer to assistance in dorsiflexion and negative in plantarflexion.

From the system responses to different configurations and movements, Table 4.1 resumes the temporal parameters obtained in the torque curve for the step function (see Figure 4.2). The central measured values were (1) the delay time, (2) the stabilization time, and (3) the



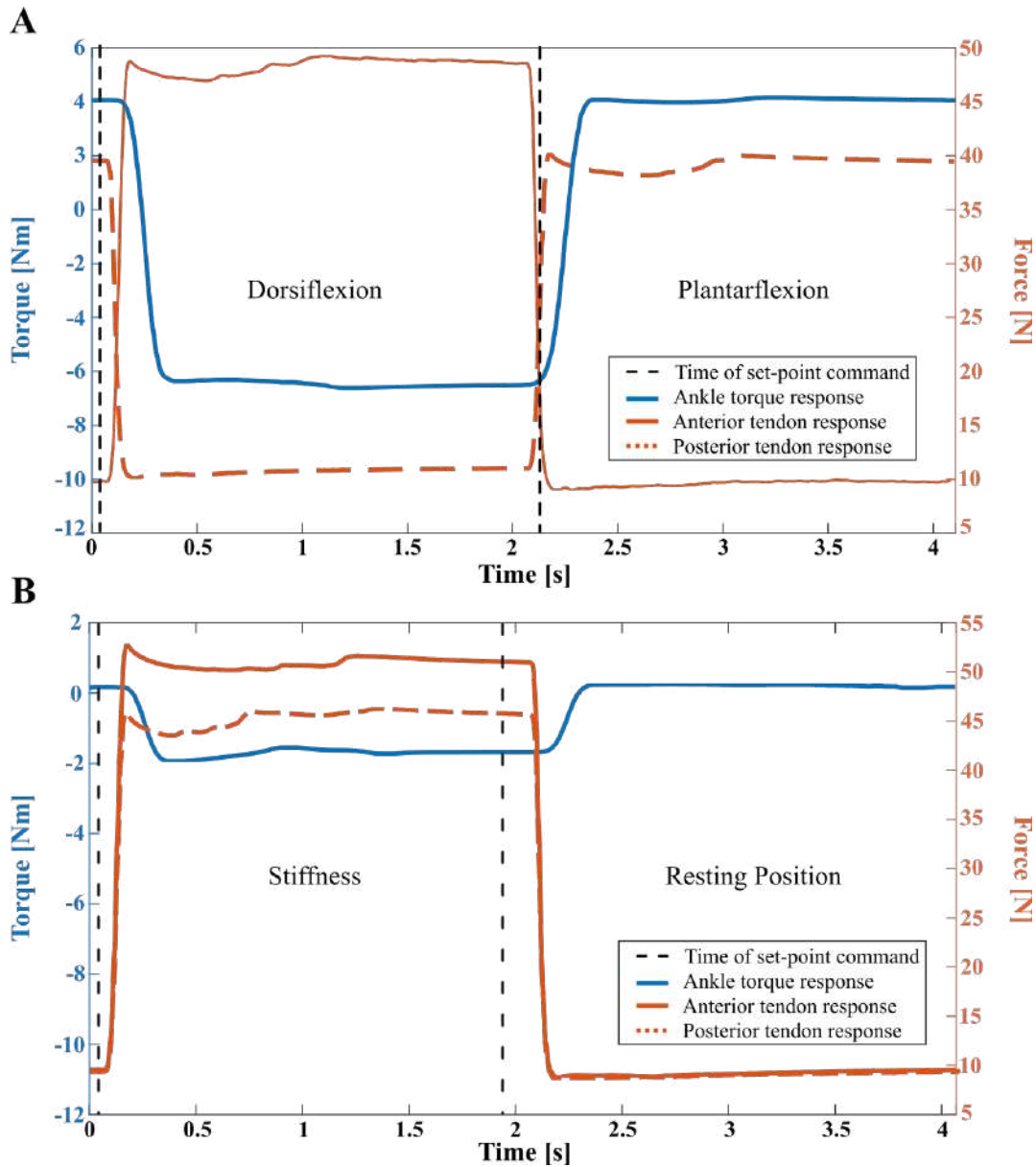


Figure 4.2: Step response of the system for the movements assessed: (A) dorsi-plantarflexion and (B) stiffness movement, in the tendons-alone configuration under an initial tension of 10 N. The segmented black lines refer to the time when the set-point was sent to the actuators. The blue line (left axis) represents the torque response measured on the artificial ankle. The orange lines (right axis) indicate the tendons' force response (i.e., continuous for anterior and segmented for posterior).

rise time, which are detailed in the following sections. In terms of normality, the values marked with an asterisk (\*) followed a normal distribution ( $p > 0.05$ ) estimated using the Shapiro-Wilk test.

Parameter	Movement	Force Level (N)	Configuration	
			Tendons	Stiff and Tendons
Delay Time (ms)	<i>Dorsiflexion</i>	5	43±2*	43±3*
		10	44±2*	42±4
		20	48±2*	53±4*
	<i>Plantarflexion</i>	5	47±1*	45±5
		10	43±6*	49±6
		20	51±5*	50±5*
	<i>Stiffness</i>	5	50±5	-
		10	38±4*	-
		20	39±9*	-
	<i>Zero position</i>	5	46±3*	-
		10	46±2*	-
		20	33±36	-
Stabilization Time (ms)	<i>Dorsiflexion</i>	5	282±8	297±12*
		10	296±10	311±10*
		20	400±22	694±25*
	<i>Plantarflexion</i>	5	285±13	289±6*
		10	289±6	336±20*
		20	558±24*	805±20*
	<i>Stiffness</i>	5	321±6*	-
		10	284±11	-
		20	343±70	-
	<i>Zero position</i>	5	235±4*	-
		10	233±7	-
		20	139±7*	-
Rise Time (ms)	<i>Dorsiflexion</i>	5	209±6*	214±5*
		10	210±7*	210±5*
		20	221±4	218±8*
	<i>Plantarflexion</i>	5	216±3	219±5*
		10	220±5	227±5
		20	240±8	234±7
	<i>Stiffness</i>	5	242±7*	-
		10	210±4*	-
		20	202±17*	-
	<i>Zero position</i>	5	215±4*	-
		10	209±7*	-
		20	134±4*	-

Table 4.1: Temporal parameters of the T-FLEX exoskeleton for the step response in the assessed configurations. Variables with an asterisk followed a normal distribution. Trials without numerical value, i.e., stiffness movement and zero position in stiff and tendons, were not assessed due to the involved elements are the same as tendons-alone (see Figure 3.10A). The orange points refer to the specific configuration with statistical differences compared to the complementary movement (i.e., dorsiflexion with plantarflexion and stiffness movement with zero position.) The blue points represent the parameters that evidenced no statistical difference in the same comparison.

#### 4.3.1.1 Delay Time

The delay time refers to the period between the set-point command and the instant torque changes larger than 1% concerning the initial value. The maximum delay value obtained in the trials was 53 ms that occurred for the dorsiflexion movement in the stiff-tendons configuration with a force level of 20 N.

In contrast, the minimum value was 33 ms in the zero-position movement in the tendons-alone for 20 N. Although, in this case, the standard deviation registered a magnitude above the mean value. Overall, the average of the system delay had a value close to 45 ms for all configurations.

#### 4.3.1.2 Stabilization Time

In the stabilization context (i.e., when the system achieves 97% of the final value), the maximum time registered was 805 ms. This event was carried out in the same configuration where the maximum delay (i.e., Stiff and Tendons to 20 N), although, in this case, for the plantarflexion movement. Moreover, the stiffness movement configuration also presented the minimum stabilization value (i.e., 800 ms) in 20 N.

This response time exhibited significant variation concerning the total trials, tending towards the highest time values for high force levels in the tendon. Likewise, between configurations, the inclusion of stiff elements in the system also increased this parameter compared to the tendons-alone.

#### 4.3.1.3 Rise Time

The rise time represents the moment where the system accomplishes 60% of the final value. This parameter showed a homogeneous behavior, as in the delay time, despite the different

setup variations during the experiment.

The maximum rise time was 240 ms and occurred for the plantarflexion movement in the tendons-alone configuration to 20 N. However, during the zero position movement, this same configuration also presented the minimum value (i.e., 134 ms). In general terms, the rise time evidenced by the system was around 210 ms.

#### **4.3.1.4 Variation Analysis**

Initially, the acquired data's consistency for each test was assessed, calculating the repeatability. This way, a coefficient of multiple determination, adapted from the methodology described in previous studies [107,108], calculated each trial's waveform similarity. For that, the data encompassed the load values measured on the ankle for the different configurations, whose behavior and response are detailed in Figure 4.2 and Table 4.1. In general terms, the trials exhibited high repeatability reaching coefficients from 96.9 % for tendons-alone in the stiffness and zero position movements with a force level of 20 N to 99.3 % also for the tendons-alone in 5N performing dorsi-plantarflexion.

Subsequently, once the data consistency was verified, the variation analysis covered two cases: (1) alterations in the same configuration related to the force levels (i.e., low: 5N, medium: 10N, and high: 20N), and (2) the effect of including stiff filaments in the system. In the first case, to compare the changes because of the force levels, the percentages of variations, using the mean value in Table 4.1, were calculated. Table 4.2 summarizes the values founded in this experiment, where the positive values indicate an increase in the parameter concerning the comparison variable. In contrast, the negative values denote a decrease. Moreover, the highlighted values represent variations above 10% for increase (red) and decrease (green), respectively.

The change in the force level introduced on the tendons for the same configuration led to

		Variation [%]				
		Comparison of Force Levels			Comparison of Configurations	
Parameter	Movement	Force Levels [N]	Tendons	Stiff and Tendons	Force Level [N]	Tendons vs Stiff and Tendons
Delay Time [ms]	<i>Dorsiflexion</i>	5 - 10	2.33 ●	-2.33 ●	5	0.00 ●
		5 - 20	11.63 ●	23.26 ●	10	-4.55 ●
		10 - 20	9.09 ●	26.19 ●	20	10.42 ●
	<i>Plantarflexion</i>	5 - 10	-8.51 ●	8.89 ●	5	-4.26 ●
		5 - 20	8.51 ●	11.11 ●	10	13.95 ●
		10 - 20	18.60 ●	2.04 ●	20	-1.96 ●
	<i>Stiffness</i>	5 - 10	-24.00 ●	-	5	-
		5 - 20	-22.00 ●	-	10	-
		10 - 20	2.63 ●	-	20	-
	<i>Zero position</i>	5 - 10	0.00 ●	-	5	-
		5 - 20	-28.26 ●	-	10	-
		10 - 20	-28.26 ●	-	20	-
Stabilization Time [ms]	<i>Dorsiflexion</i>	5 - 10	4.96 ●	4.71 ●	5	5.32 ●
		5 - 20	41.84 ●	133.67 ●	10	5.07 ●
		10 - 20	35.14 ●	123.15 ●	20	73.50 ●
	<i>Plantarflexion</i>	5 - 10	0.35 ●	16.26 ●	5	1.40 ●
		5 - 20	95.79 ●	178.55 ●	10	17.48 ●
		10 - 20	95.10 ●	139.58 ●	20	44.27 ●
	<i>Stiffness</i>	5 - 10	-11.53 ●	-	5	-
		5 - 20	6.85 ●	-	10	-
		10 - 20	20.77 ●	-	20	-
	<i>Zero position</i>	5 - 10	-0.85 ●	-	5	-
		5 - 20	-40.85 ●	-	10	-
		10 - 20	-40.34 ●	-	20	-
Rise Time [ms]	<i>Dorsiflexion</i>	5 - 10	0.48 ●	-1.87 ●	5	2.39 ●
		5 - 20	5.74 ●	1.87 ●	10	0.00 ●
		10 - 20	5.24 ●	3.81 ●	20	-1.36 ●
	<i>Plantarflexion</i>	5 - 10	1.85 ●	3.65 ●	5	1.39 ●
		5 - 20	11.11 ●	6.85 ●	10	3.18 ●
		10 - 20	9.09 ●	3.08 ●	20	-2.50 ●
	<i>Stiffness</i>	5 - 10	-13.22 ●	-	5	-
		5 - 20	-16.53 ●	-	10	-
		10 - 20	-3.81 ●	-	20	-
	<i>Zero position</i>	5 - 10	-2.79 ●	-	5	-
		5 - 20	-37.67 ●	-	10	-
		10 - 20	-35.89 ●	-	20	-

Table 4.2: Variation percentages for comparing force levels (i.e., 5, 10, and 20 N) and configurations (i.e., tendons-alone and stiff-tendons). The green values indicate significant decreases in the parameter (i.e., greater than 10%) concerning the compared group. Likewise, the highlighted values with red refer to relevant increases. On the other hand, the orange points denote groups with statistical changes, and instead, blue points indicate groups without differences.

alterations in the system response (see the left part in Table 4.2). Thus, 50% of the measured variables evidenced changes greater than 10%. The maximum variation values occurred in the stabilization time for the dorsi-plantarflexion movements in both tendons-alone and stiff-tendons, involving the high force level (i.e., 20 N) always. Wherein, the trend was a longer stabilization time when the system had high force levels on the tendon. In the delay time, the changes followed the same tendency (i.e., high variations when the comparison was with 20 N), although, in this parameter, the values exhibited differences between 11% and 27%. The rise time did not evidence relevant increases, except for reductions close to 40% in the zero position movement when the tendons were in 20 N. Overall, the tendon's highest force level negatively affected the response times for the dorsi-plantarflexion gesture, slowing the system down. However, in the stiffness and zero-position movements, the decreases were positive, leading to accelerated system responses.

On the other hand, the inclusion of stiff elements in the system caused relevant variations for 28% of the trials' parameters (see the right part in Table 4.2). All variations values indicated increases in the system response times when the stiff filaments participated in the movement. Likewise, this effect mainly occurred in higher force levels (i.e., 10 N and 20 N) for the delay and stabilization time. The rise time did not exhibit relevant changes between both configurations.

#### **4.3.1.5 Statistical Analysis**

From the variation results previously presented and to study the influence of including stiff elements and changing the force on the tendons, the t-test and Mann-Whitney-Wilcoxon test determined whether there were statistically differences in the temporal parameters. This way, the 27 assessed trials (see Table 4.1) could be compared in three cases: (1) movements in gait applications (see Figure 3.10), (2) force levels on the tendon (i.e., 5 N, 10 N, and 20 N), and (3) configurations of the device (i.e., tendons-alone and stiff-tendons). The statistical

tests were carried out according to the data normality (see Table 4.1).

The first trial determined the statistical differences ( $p < 0.05$ ) between dorsi and plantar flexion movements for the first case and the maximum stiffness and zero position for the other. In the comparison groups, the same force level was considered. The tests showed significant changes in 21 parameters (see groups with orange points in Table 4.1) and no relevant differences in 6 groups (see groups with blue points in Table 4.1): (1) rise time in tendons-alone for 10 N in stiffness movement, (2) stabilization time in tendons-alone for 5 N in dorsi-plantarflexion, and finally, the delay time in stiff-tendons for (3) 5 N and (4) 10 N, and Tendons in 10 N for (5) dorsi-plantarflexion and (6) 20 N for stiffness movement.

The second trial assessed statistical differences ( $p < 0.05$ ) between the three parameters' force levels in each configuration. The parameters exhibited significant changes in all cases except the delay time in Tendons for the zero position movement ( $p = 0.14$ ). Therefore, considering the number of force levels (3), a post hoc test determined which levels present differences in each configuration and movement.

The analysis exhibited no statistical changes ( $p > 0.05$ ) in 4 cases: (1) stabilization time for tendons-alone in dorsiflexion between the force levels 5 N and 20 N, (2 and 3) the rise time in dorsiflexion for stiff-tendons (force levels: 5 N - 10 N and 5 N - 20 N), and (4) the delay time between the force levels 5 N and 10 N in dorsiflexion for stiff-tendons. Table 4.2 in the left part shows the compared force levels groups with statistical differences (orange point) and no significant changes (blue point).

The third trial analyzed statistical differences between both configurations (i.e., Tendons and Stiff-Tendons) for the same force level (see the right part in Table 4.2). Table 4.3 shows the  $p$  values calculated for each trial, where the highlighted values with blue indicate no significant changes between the configurations, and values in orange represent statistical differences.

The delay and rise times registered no statistical changes in 33% of total movements and

force levels assessed (i.e., 6 of 18 parameters). The stabilization time showed a single value with no significant difference for the plantarflexion movement in a force level of 5 N. The other 11 values evidenced statistical differences between the configurations.

Dorsiflexion movement			
Parameter	Force level [N]		
	5	10	20
Delay Time	$5.09 \cdot 10^{-1}$	$1.68 \cdot 10^{-1}$	$1.20 \cdot 10^{-5}$
Stabilization Time	$1.25 \cdot 10^{-4}$	$3.33 \cdot 10^{-4}$	$3.81 \cdot 10^{-6}$
Rise Time	$2.59 \cdot 10^{-2}$	$7.43 \cdot 10^{-1}$	$1.44 \cdot 10^{-1}$
Plantarflexion movement			
Parameter	Force level [N]		
	5	10	20
Delay Time	$1.08 \cdot 10^{-2}$	$3.34 \cdot 10^{-3}$	$9.52 \cdot 10^{-1}$
Stabilization Time	$2.57 \cdot 10^{-1}$	$3.81 \cdot 10^{-6}$	$3.26 \cdot 10^{-18}$
Rise Time	$5.45 \cdot 10^{-2}$	$4.19 \cdot 10^{-4}$	$3.34 \cdot 10^{-3}$

Table 4.3: P-values for comparing both configurations (i.e., tendons-alone and stiff-tendons) in each analyzed movement. The orange values indicate statistical changes, and the blue values denote no differences.

### 4.3.2 Chirp Response

The chirp signal measured the system response to frequency changes and the maximum torque values on the ankle for the different amplitude values. Figure 4.3 shows the system behavior in terms of torque on the ankle, the tendons force, and T-FLEX's actuators. The responses illustrated in Figure 4.3 occurred in the tendons-alone configuration for the dorsiflexion movements with a force level of 10 N.

The other executed trials followed the same waveform with variations in the signals' amplitude (i.e., initial and throughout the test). However, for tests with a force level of 20 N, both configurations exhibited overload conditions when the signal had the maximum set-point value (i.e., 12 degrees). Consequently, this study did not take into account these trials.



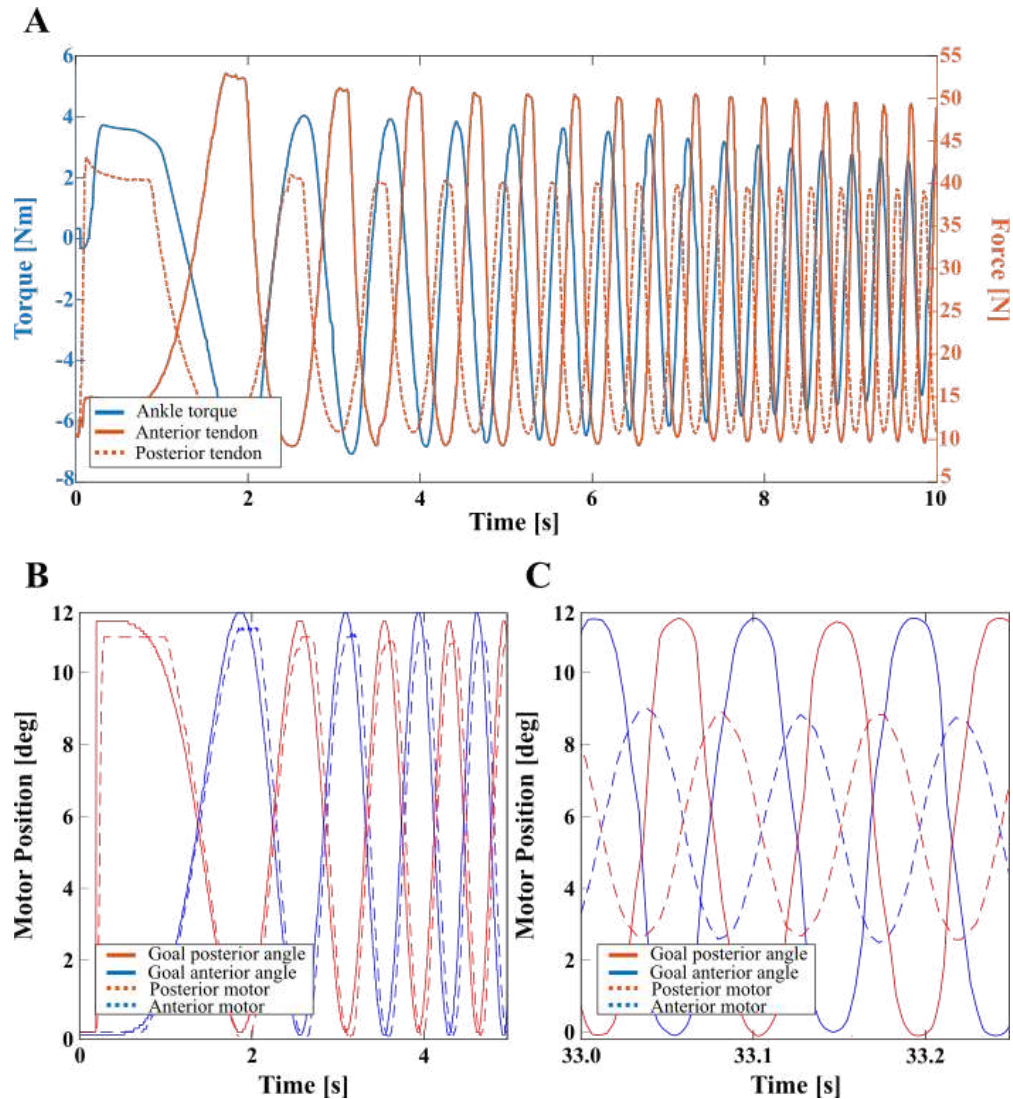


Figure 4.3: System responses for the chirp signal in the tendons-alone configuration executing dorsi-plantarflexion movements under a force level of 10 N. The upper figure (A) illustrates the reaction in terms of torque and force. The blue curve refers to the torque (left axis) registered on the ankle, and the orange curves represent the force (right axis) measured on the posterior (segmented line) and anterior (continuous line) tendons. The lower figures show the position response during the initial (B) and final (C) trial time, which were registered by both T-FLEX's actuators: anterior (blue curve) and posterior (red color).

From the actuators data (see Figure 4.3 B and C), the system bandwidth was estimated using the System Identification Toolbox of MATLAB. For that, the input and output in the toolbox incorporated the desired and achieved angle trajectories measured on the T-FLEX's actuators.

In most cases, the estimated models exhibited fit rates with values greater than 85%. Nevertheless, the tests with high effort for the actuators presented this rate greater than 75% (i.e., goal angle signal with the maximum amplitude in a force level of 10 N, and the trials where the tendons had 20 N). Figure 4.4 resumes the bandwidth values calculated for each motor subjected to the configurations analyzed in this study.

The bandwidth did not evidence relevant changes between the two assessed movements (i.e., dorsi-plantarflexion and stiffness-zero position). Nonetheless, the stiff elements' inclusion in the system caused decreases in this parameter. However, in the posterior actuator under a force level of 20 N, the bandwidth value exhibited increases (see Figure 4.4B).

In general terms, the maximum registered value was 8.0 Hz, which occurred in the posterior motor for both configurations (i.e., tendons-alone and tendons-stiff) under a force level of 10 N and an amplitude of 6 degrees. In the anterior actuator, the tendons-alone registered the highest bandwidth (i.e., 6.9 Hz) when the system had a force level of 5 N. Moreover, the signal amplitude was also 6 degrees (see Figure 4.4A).

On the other hand, the chirp signal also found the maximum torque values measured on the ankle. Figure 4.5 summarizes the highest torque values for the different setups included in this study. For the dorsiflexion movement (see Figure 4.5A), the highest values, close to 20 Nm, occurred when the tendon had force levels of 20 N (stiff-tendons) and 10 N (tendons-alone).

In the plantarflexion movement (see Figure 4.5B), the maximum torque registered was 10 Nm for the tendons-alone configuration with a force level of 10 N. This way, the inclusion of stiff elements did not increase the ankle's torque for either movement. Lastly, the stiffness movement exhibited magnitudes lower than 8 Nm, demonstrating this value for the maximum force levels. The other force levels (i.e., 5N and 10 N) showed torque magnitudes lower than 0.3 Nm in the plantarflexion and 7 Nm in the dorsiflexion movement.

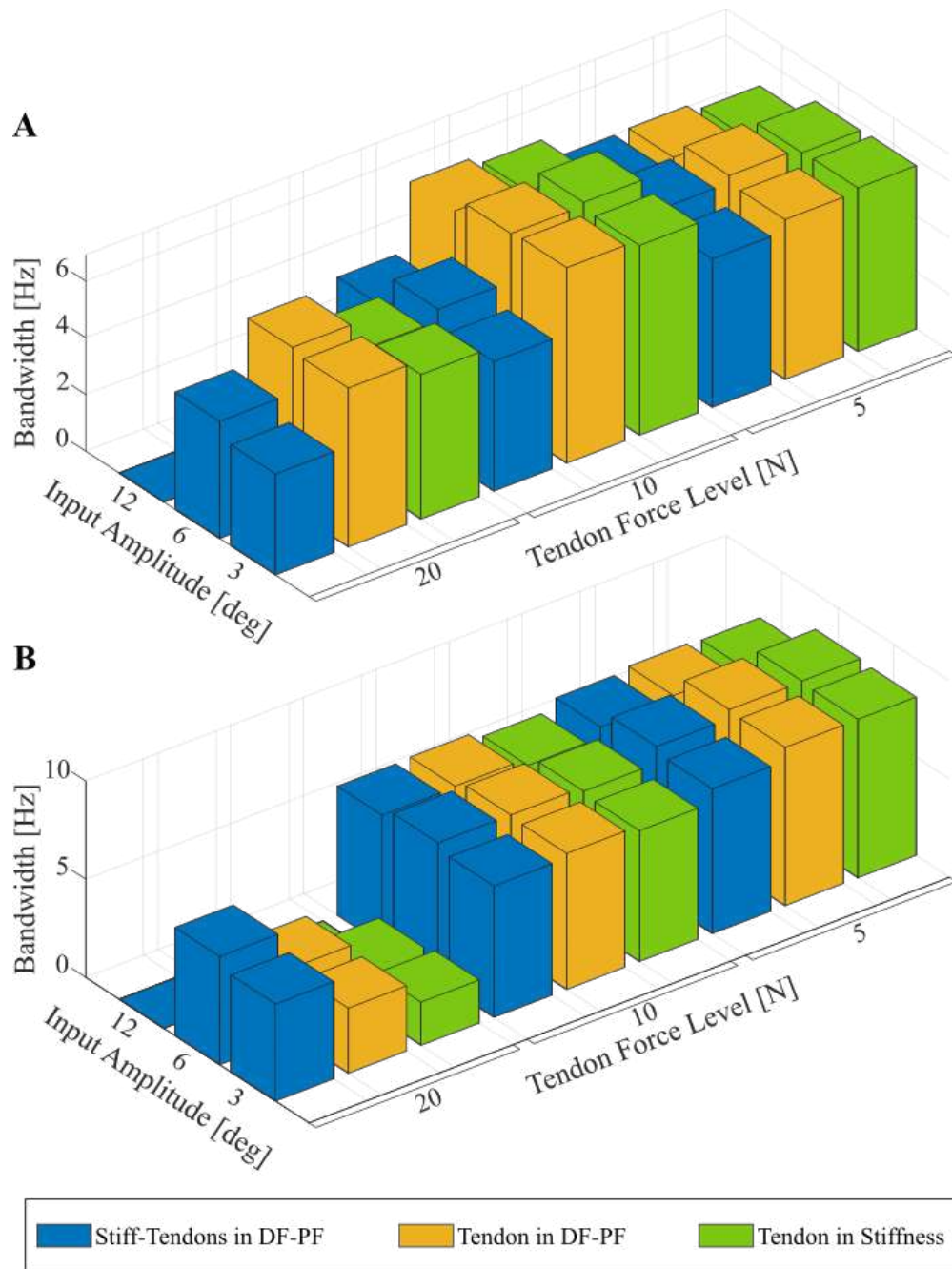


Figure 4.4: Bandwidth values of the T-FLEX’s actuators for different configurations, amplitudes, movements, and force levels on the tendons. The upper figure (**A**) summarizes the bandwidth for the anterior actuator, and the lower part (**B**) shows the values for the posterior actuator. Trials with a bandwidth of 0 Hz (i.e., both actuators under a force level of 20 N and an amplitude of 12 degrees in the chirp signal) were not considered because of the actuators registered an overload condition and a saturation state.

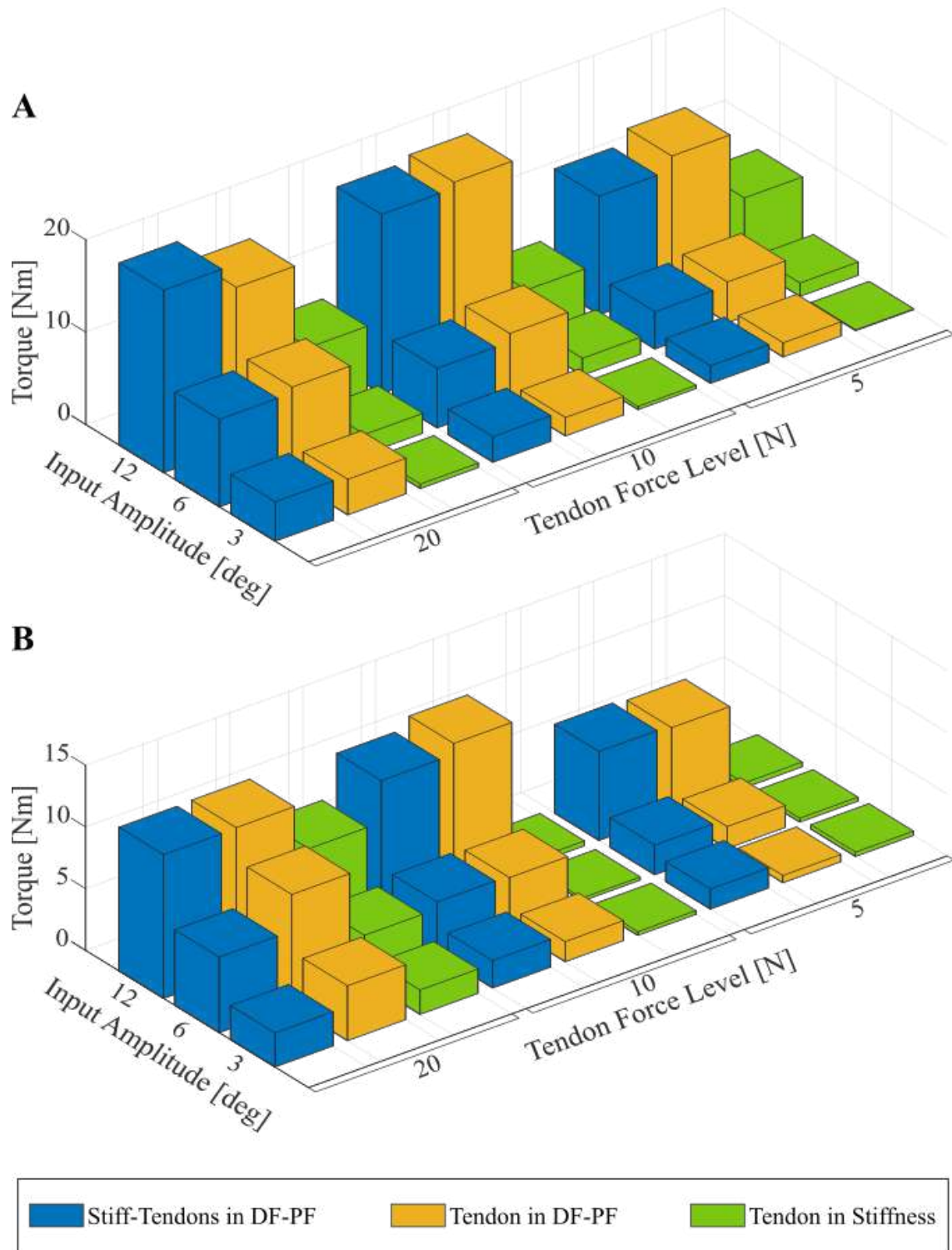


Figure 4.5: Maximum torque values on the ankle for the different analyzed setups. The upper figure (A) shows the torque generated by T-FLEX to assist the dorsiflexion movement, and the lower figure (B) summarizes the torque in the plantarflexion movement.

### 4.3.3 T-FLEX in gait applications

Table 4.4 summarizes the T-FLEX’s capabilities measured in this study from the results presented in previous sections. The device bandwidth was the minimum bandwidth value estimated in the chirp signals, including actuators and the analyzed movements. This because the system response to accomplish the slowest movement will limit the operation described in Figure 3.10. In most cases, the zero position and stiffness movement provided this value, although, in general terms, the estimated bandwidths reflected similar values between them.

Configuration	Force level (N)	Set-point (deg)	T-FLEX bandwidth (Hz)	Minimum gait cycle assisted (sec)	Maximum provided torque (Nm)	
					Propulsion	Dorsiflexion
Tendons	5	3	5.6	0.89	0.59	1.53
		6	5.7	0.88	1.77	4.41
		12	4.9	1.02	7.00	14.32
	10	3	6.5	0.77	1.62	1.99
		6	6.8	0.74	4.03	7.37
		12	6	0.83	12.12	20.04
	20	3	2.1	2.38	4.44	3.82
		6	2.0	2.50	9.06	10.12
		12	-	-	11.70	17.21
Stiff and Tendons	5	3	5.2	0.96	1.62	1.89
		6	5.6	0.89	2.40	4.02
		12	4.9	1.02	7.20	12.82
	10	3	4.5	1.11	2.20	2.76
		6	5.1	0.98	4.19	6.46
		12	3.9	1.28	11.24	19.4
	20	3	2.1	2.38	2.75	4.25
		6	2.0	2.50	6.12	9.47
		12	-	-	11.64	19.75

Table 4.4: T-FLEX’s capabilities for gait applications. The highlighted values indicate times that exceed the mean gait cycle duration in healthy people.

Through the system bandwidth and the gait phases segmentation [109], the minimum gait cycle duration where T-FLEX can assist was calculated (see Table 4.4). The lowest estimated value was 0.74 seconds for the tendons-alone with a force level of 10 N. In contrast, the highest time determined in this study was 2.50 seconds when the tendons had a force level of 20 N in both configurations (i.e., tendons-alone and stiff-tendons). In this time, the values tended to increase the gait cycle duration for the larger set-points.

Likewise, considering the mean gait cycle in healthy people (i.e.,  $1.09 \pm 0.07$  seconds), the trials with a force level of 20 N evidenced to be unsuitable for assistive applications (see highlighted values in Table 4.4). Lastly, the provided torque values were the maximum values exhibited in Figure 4.5 for both movements: (1) plantarflexion for the propulsion task, and (2) dorsiflexion for clean foot contact with the ground and foot clearance (see Table 4.4).

## 4.4 Discussion

This paper shows each element's influence that composes the T-FLEX ankle exoskeleton and analyzes the system response changes concerning the different configurations and movements. Likewise, this study aims to determine the device's feasibility for assistive application in human gait. Thus, the step response results allowed determining a first approximation of the most appropriate T-FLEX configuration to provide its maximum capabilities in a real scenario. The parameters assessed in this signal were the delay, stabilization, and rise time.

For the first parameter, related to the composite tendon's elastic behavior (see Figure 4.2), the mean value for the different trials was close to 45 ms. It should be noted that although statistical tests determined significant differences between the configurations and movements (see Table 4.1), the delay time evidenced variations percentages below 30% (see Table 4.2). Moreover, as the delay time showed small values (i.e., between 33 and 53 ms), the found variations are no relevant. Likewise, the measured delay included the processing time asso-

ciated with the communication between the computer and the actuators. Consequently, the tendon's real effect would probably be around 30 ms.

On the other hand, it was expected to reduce the delay time for higher force levels and when the system included the stiff filaments. Nevertheless, the only evidence of this behavior, in a forceful way, occurred for the stiffness and zero position movements. Therefore, the tendons force levels analyzed in this study were in the same elastic region [97], requiring that time (i.e., 30 ms) to transmit torque to the ankle.

In the stabilization time, the system registered significant variations concerning both the force levels and the inclusion of stiff filaments (see Table 4.2), corroborated by statistical trials (see Table 4.1). For the dorsi-plantarflexion movements, a force level of 20 N led to increases in the time of up to 178%, reaching values of 805 ms. This result responds to the actuators' high effort, because of the tendon force, during the actuation process. Furthermore, in comparing configurations for the same force level, the stiff-tendons reported higher times than the tendons-alone. In this context, the inclusion of stiff elements caused a destabilization in the system reflected in an increased time.

According to the device's real application in walking, this parameter is particularly relevant because it indicates when the system provides the total torque. Consequently, both the highest force level (i.e., 20 N) and the inclusion of stiff elements do not appear to be proper configurations for gait assistive tasks. In contrast, the lower force levels (i.e., 5 and 10 N) in the tendons-alone registered similar times close to 290 ms, which could be manageable values with a control algorithm.

Summarizing the system times, on the one hand, as the tendons' force levels were in the same elastic region, the initial system response (i.e., the delay and rise times) exhibited similar range values. Therefore, the higher force levels did not reduce the tendon elongation delay and accelerated the system. However, the trials whether showed alterations in the stabilization time. This because of the actuators' saturation caused for the tendons force,

where the highest force level led to larger times. On the other hand, the stiff elements' inclusion did not improve the system performance but slowed the response.

The chirp signal results determined both the system bandwidth and the maximum torque assisted on the ankle (see Figure 4.3). In general terms, the estimated bandwidth values followed the results obtained in the step response. Thus, the increase in the tendon force level and the stiff filaments' inclusion reduced the system response in frequency (see Figure 4.4). This behavior resulted from the tendon's highest force level (i.e., 20 N), which caused a actuators' saturation. Likewise, considering the high stabilization times in this level, low bandwidth values were expected no matter the set-point amplitude.

Regarding the other VSAs used in exoskeletons, T-FLEX exhibited a frequency behavior contrary to those devices, where higher stiffness levels increase the bandwidth [31,33]. This aspect is because higher stiffness resembles the actuator bandwidth, avoiding the spring element's frequency losses. However, for T-FLEX, the highest stiffness level resulted in saturation conditions, limiting the actuators' capabilities. Likewise, the low and medium stiffness levels exhibited the frequency behavior prevalent in VSAs, although the changes between them were minimal.

Moreover, according to the fit percentages found during the trials' modeling, the T-FLEX exoskeleton can be approximated as a linear system, as long as it operates under the actuators' saturation limits. Because the highest force level, i.e., 20 N, introduced nonlinear distortions related to saturations for high load coupled to the actuators, similar as was presented in another study [33].

For the torque measured on the ankle, the trials registered magnitudes up to 20 Nm for the dorsiflexion and 12 Nm for the plantarflexion (see Figure 4.5). However, the maximum values occurred in trials with the highest force level (i.e., 20 N). Therefore, considering the analysis mentioned above, this configuration would not be suitable for assistive applications in human walking. On the other part, the inclusion of stiff elements did not evidence relevant increases



in the provided torque. Hence, considering the increases in some system times (see Table 4.2) and the bandwidth decreases (see Figure 4.4), the tendons-alone configuration exhibited the best performance.

Lastly, from the data acquired in the chirp and step signals was estimated the T-FLEX capabilities in gait applications (see Table 4.4). Thus, the highest force level (i.e., 20 N) was confirmed as not applicable for assistive tasks on account of the slow response. The minimum gait cycle time to assist the user reached values greater than 2.3 seconds for this force level.

Hence, considering the healthy people's duration (i.e., close to 1 second), the device would not be synchronized with the user gait. The other levels registered similar values, although the medium force level (i.e., 10 N) exhibited shorter times than the low level (i.e., 5 N), indicating better performance in high velocities.

Therefore, the medium force level (i.e., 10 N) in tendons-alone proved to be the best configuration for the T-FLEX exoskeleton for assistive applications in human gait. This way, T-FLEX can respond to gait cycles from 0.77 sec and assist partially walking, providing torque on the ankle of up to 12 Nm in propulsion and 20 Nm in dorsiflexion.

However, according to the stabilization time for this configuration, the control algorithm described in Figure 3.8 should include an adaptable stage concerning the user velocity, where the commands for each actuator (see Figure 3.10) can be sent at the right time to transmit the torque on the ankle, properly.

Concerning the exoskeletons in the literature, it is essential to clarify that there is still misinformation about actuators' performance aimed at assistive applications [31]. However, T-FLEX achieves the response ranges for soft actuators reported in previous studies, which registered bandwidth values from 2 Hz to 38 Hz [31, 33, 110]. Likewise, in terms of provided torque, T-FLEX also operates under the reported ranges, including values from 3 Nm to 140 Nm for low-weight exoskeletons [31].

## 4.5 Conclusions

This chapter presented T-FLEX's experimental characterization in a static scenario using a test-bench structure. The T-FLEX's actuators were excited to two signals (i.e., step and chirp) under three tendons' force levels (i.e., 5, 10, and 20 N) and two configurations (i.e., tendons-alone and stiff-tendons). The test-bench integrated a torque sensor coupled on the ankle and strain gauges to measure the tendons' force.

The trials assessed the elements that comprehend T-FLEX, establishing the most appropriate configuration and force level to ensure the maximum device's performance in assistive applications (i.e., tendons-alone configuration stressed to 10 N). Therefore, T-FLEX in this configuration can provide 12 Nm in propulsion and 20 Nm to assist the dorsiflexion.

Likewise, this study measured the tendons' effect on the proposed control strategies. Thus, it found a delay time, because of the tendon's elongation, close to 45 ms for all configurations and force levels. In contrast, other system responses (i.e., rise and stabilization times) were affected by the assessed configuration, showing poor performance in the highest force level (i.e., 20 N) related to the actuators saturation. Moreover, the inclusion of stiff elements did not improve the device's capabilities, but on the contrary, the system was slower, and the provided torque did not increase considerably.

In general terms, this study corroborated T-FLEX's applicability in assistive scenarios during human walking. The data acquired from trials determined the maximum gait cycle duration where the device can respond (i.e., 0.74 seconds). Therefore, T-FLEX can be adapted to healthy gait pattern values (i.e., 1.09 seconds approximately).

## Chapter 5

# Experimental Validation of T-FLEX in Paretic Gait Assistance

Robotic-assisted gait is a great challenge because of aspects such as user's adaptability, device's response to continuous changes, and non-cyclic walking's synchronization. Considering the results obtained by the experimental characterization presented in chapter 4, T-FLEX can assist human gait, providing torque in propulsion, and avoiding foot-slap in the swing phase.

This way, this chapter presents the experimental validation of T-FLEX for assistive applications in stroke survivors with ankle dysfunctions. Thus, this study assessed the first-use condition wearing the T-FLEX's actuation system to analyze the effect on lower limbs' during overground walking. Likewise, this chapter shows the user's perception, obtained by a survey obtained at the end of the experiment.

## 5.1 Experimental Design

The experimental validation presented in this chapter aimed to measure the changes in kinematic and Spatio-temporal parameters between the two conditions proposed (i.e., unassisted and assisted gait). Additionally, it also intended to determine the user satisfaction level with the device in aspects such as dimensions, weight, safety, and comfort. This study was executed in the rehabilitation center "*Club de Leones Cruz del Sur*" in Punta Arenas - Chile and had a total duration of three months since the patients' recruitment.

### 5.1.1 Participants

This study enrolled ten participants ( $58 \pm 4.5$  years old) diagnosed with hemiparesis due to a cerebrovascular accident (i.e., eight males and two females). They were active patients who performed therapy processes in a rehabilitation center. Table 5.1 summarizes the clinical information of the patients who accomplished this study. On the other hand, the volunteers were selected according to the inclusion and exclusion criteria described below:

1. **Inclusion criteria:** People who suffered a stroke before six months of being executed this protocol are eligible. The volunteers must present hemiparesis in one side of the body with some ankle dysfunction. Moreover, they must have partial independence for walking without external devices and the ability to follow instructions.
2. **Exclusion criteria:** Candidates with skin alterations in the lower limbs, high level of spasticity (i.e., level 4 of Ashworth scale), and pain of the musculoskeletal system impeding the device's use was not taken into account in this study. Likewise, patients who suffer from weakening diseases, for instance, cancer. Moreover, people with a previous history or suspected of seizures were also not selected.

Subject	1	2	3	4	5	6	7	8	9	10	$\bar{x} \pm sd$
<b>Gender</b>	M	F	F	M	M	M	M	M	M	M	-
<b>Age (years)</b>	54	52	59	54	61	61	66	60	60	53	$58 \pm 4$
<b>Weight (Kg)</b>	80	91	95	87	96	62	67	73	69	84	$80 \pm 12$
<b>Height (cm)</b>	170	165	167	175	168	160	170	166	165	176	$168 \pm 5$
<b>Left leg length (cm)</b>	90	87	88	91	88	83	88	88	85	92	$88 \pm 3$
<b>Right leg length (cm)</b>	90	87	88	91	88	83	88	88	85	93	$88 \pm 3$
<b>Time from injury (years)</b>	2	7	5	1	7	2	4	4	4	5	-
<b>Paretic side</b>	R	R	R	L	L	R	R	L	L	L	-
<b>Ashworth scale</b>	1	1	2	1	3	1	2	2	1	3	-

Table 5.1: Subjects anthropometric measurements and clinical information.

### 5.1.2 Experimental Setup

The participants used the T-FLEX’s actuation system (i.e., actuators, an inertial sensor and the control strategy in gait presented in chapter 3 adapted to the mechanical orthotic structure in their paretic side, as Figure 5.1 shows. Likewise, the gait phase detection employed an inertial sensor placed on the same limb’s foot tip. The actuators operated to the maximum velocity (55 rpm for no-load state) to assist the ankle movements (i.e., dorsiflexion and plantarflexion) along with a 6-meter test (6MT). The volunteers also used a similar insole to balance the effect due to the device’s height for the other foot.

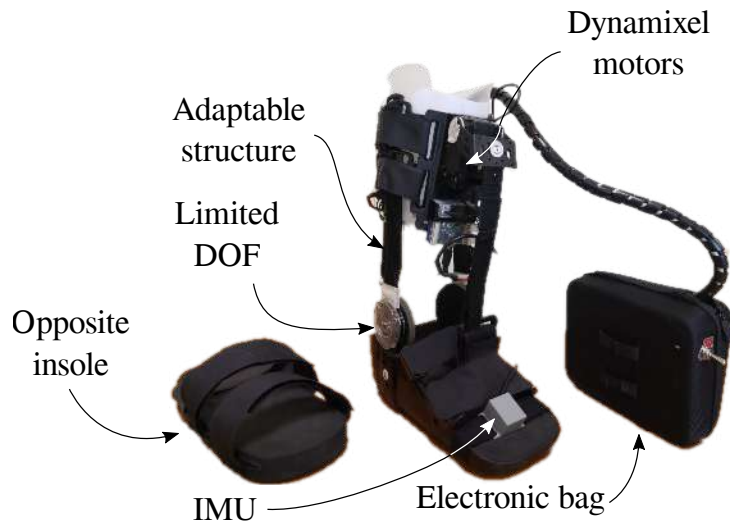


Figure 5.1: T-FLEX exoskeleton's actuation system implemented on the passive orthotic structure. The left part shows the insole added in the non-paretic limb to compensate for the effect due to the device's use.

On the other hand, each participant was instrumented with 25 markers to perform a lower limb kinematic analysis using an optoelectronic motion caption system. Figure 5.2 shows the distribution of the markers over a volunteer in this study.

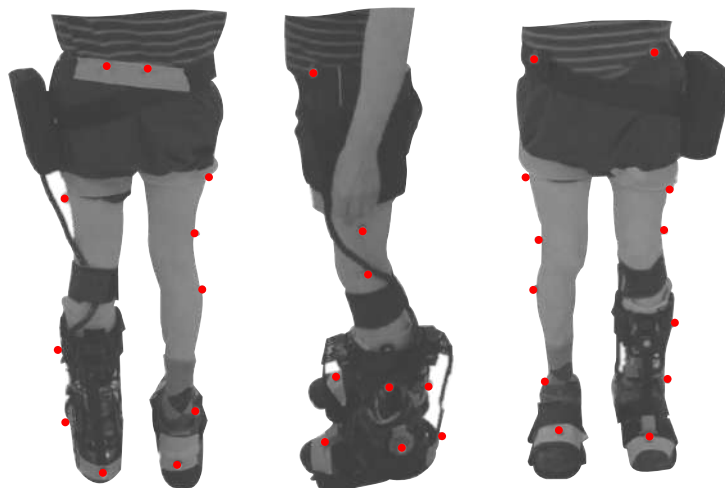


Figure 5.2: Biomechanical setup model used in the study for each participant. The red points on the patient represent the markers for the VICON acquisition system.

### 5.1.3 Biomechanical Analysis

The user kinematic was acquired using ten-cameras VICON (Oxford Metrics, Oxford, UK). Nexus software (Oxford Metrics, Oxford, UK) performed data tracking. Besides, Polygon software (Oxford Metrics, Oxford, UK) carried out each user's kinematic analysis. For this purpose, a biomechanical model *Plug-in Gait* [111] was used, estimating the Spatio-temporal parameters and participants' range of motion (ROM).

On the other hand, the Gait Deviation Index (GDI), which synthesizes all the kinematic examination variables in a single general result, was estimated for each participant's leg [112]. The obtained value represents a global normality's percentage concerning a kinematic reference of people without pathology or mobility alterations. Therefore, values greater than 90% indicates a no pathological gait pattern in the limb. This index allows for identifying joint kinematic changes (i.e., variations above 10%) for several scenarios [113].

Other measures used to detail the kinematic performance were the Movement Analysis Profile (MAP) and the Gait Profile Score (GPS) [114]. The MAP describes the magnitude of the deviation on the lower limb joints across the gait cycle. The GPS compiles and averages the scores of those joints. This evaluation was executed by members from the Movement Analysis Laboratory of the Rehabilitation Corporation Club de Leones Cruz del Sur (Punta Arenas, Chile).

### 5.1.4 Experimental Procedure

To validate the system actuation effect, each participant accomplished two modalities: (1) unassisted and (2) assisted gait. Both scenarios were composed of multiples 6MT tests overground performed in the same session. The first modality consisted of walking without wearing the device. This way, the kinematic analysis used the trial data as a baseline. In

the second modality, the device assisted the volunteer gait according to the control strategy presented in chapter 3. Each scenario was composed of ten trials executed continuously, where the trajectories were analyzed and compared to identify the curves with the highest intra-test consistency. Thus, the biomechanical analysis used the data of those selected curves.

### **5.1.5 Usability Assessment**

Ergonomics and comfort are some of the most relevant aspects of user-machine interaction [75]. For this study, the user perception assessed this interaction employing a Quebec User Evaluation of Satisfaction with assistive Technology QUEST test. The original survey comprises 27 questions related to participants' satisfaction concerning the robotic device [115]. This study included 13 of those questions adapted to a Spanish version selected for their suitability in this protocol.

### **5.1.6 Statistical Analysis**

This study analyzes the device's effect on the biomechanical and Spatio-temporal parameters during stroke patients' first-use. For this purpose, initially, a Shapiro-Wilk test verified the normal data distribution. This way, for each subject, the data segmented by gait phases (i.e., stance phase and swing phase) were averaged. Subsequently, the Student's t-test assessed the statistical significance of changes ( $p < 0.05$ ) between the baseline and assisted gait with the T-FLEX system actuation, for both gait phases.

To analyze the first-use effects, this part included both inter-subject and intra-subject analyses. Thus, it allowed measuring aspects such as the user's performance, device's adaptability, and the influence of actuating the ankle joint. On the other hand, the Spatio-temporal parameters' analysis was also performed by the Student's t-test between the two conditions



for an intra-subject analysis. The software used for the tests was MS Excel with statistical analysis tools.

## 5.2 Results

### 5.2.1 Kinematics

In this study, the users' kinematic results were divided into two main groups: (1) ankle kinematics behavior and (2) lower limb joints' ROM. As an initial approach, ankle kinematics showed no significant changes ( $p > 0.05$ ) for the two assessed groups (i.e., unassisted and assisted), including the complete participants' sample through a Student's t-test. Nevertheless, diverse aspects stated in the following section could explain those results. Therefore, this part presented the results individually for each participant.

For the first group, Figure 5.3 shows the ankle kinematics during a gait cycle for both the healthy pattern and the results for each volunteer, where letters from A to J represent the participant from 1 to 10, respectively. This cycle comprises phases between each heel-strike event for both assessed modalities (i.e., baseline and assisted) and the healthy ankle pattern. Moreover, the vertical line included in the figure highlights the toe-off phase for each case.

Concerning the toe-off phase (TO), 40% of the participants showed differences of more than 5% in this event's occurrence time during the gait cycle (see Figure 5.3), when they used the T-FLEX's actuation system. Likewise, 30% of the subjects brought this event to the estimated percentage in a healthy pattern. The other volunteers did not show changes in this aspect. On the other hand, the ankle angle shape had variations because of using the device. Specifically, subject 5 registered an increase of 15 degrees in the dorsiflexion movement during the swing phase. However, participants 1 and 9 reduced this movement at 10 degrees, although this reduction was within the healthy range.

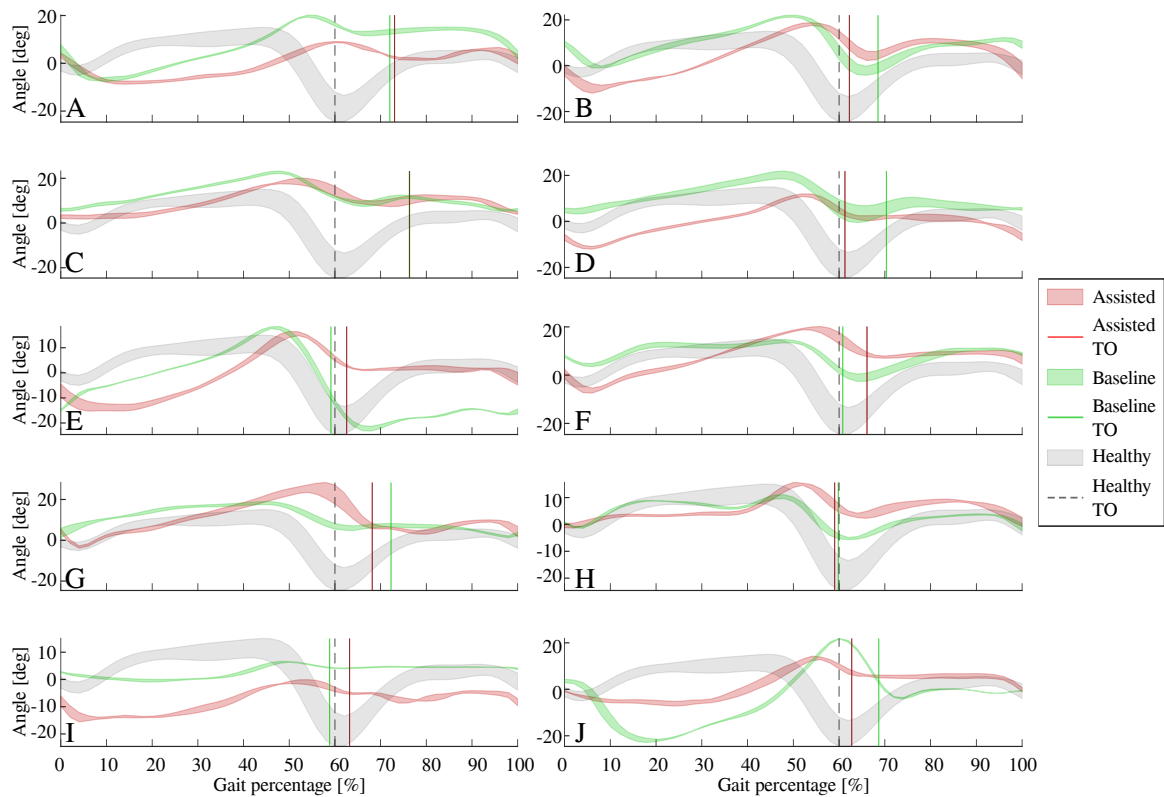


Figure 5.3: Volunteers’ ankle kinematic during the gait cycle. Letters from **A** to **J** represent the participant number in ascending order. The red curve indicates the assisted gait condition. On the other hand, the green curve refers to the natural gait pattern (baseline condition). The gray curve shows a healthy ankle’s gait pattern. Finally, the vertical lines describe the toe-off event for each of these conditions.

For the other group, Table 5.2 summarizes the ROM for the ankle dorsi-plantarflexion, knee flexo-extension, hip flexo-extension, and hip ab-adduction in both modalities. The second part of the table shows the joints’ percental variation when the participant used T-FLEX. Positive values in this variation indicate an increase in the joint’s ROM, and by contrast, negative values represent a decrease in this parameter. For this part, the highlighted values represent increases greater than 10% on the joint concerning the baseline state.

From the variation table, 70% of the volunteers exhibited significant changes in the paretic ankle’s ROM using the device, increasing or decreasing. Likewise, the changes in the paretic ankle’s ROM also varied for the non-paretic joint. On the other hand, the altered joints’

Subjects		1	2	3	4	5	6	7	8	9	10	
<i>Baseline</i>	Paretic	Ankle D-P	27.4	26.1	17.9	22.1	40.5	15.5	17.0	16.2	7.2	44.4
		Knee F-E	62.4	51.7	29.6	70.9	46.6	64.2	18.4	49.4	31.1	40.1
		Hip F-E	39.5	44.4	26.8	42.2	27.1	53.7	16.2	41.8	31.0	35.9
	Non-Paretic	Hip Ab-Ad	7.5	13.9	12.1	11.8	8.1	10.2	10.1	8.4	8.6	11.2
		Ankle D-P	16.2	35.0	21.3	20.5	23.3	18.1	19.6	16.8	20.2	38.7
		Knee F-E	60.1	67.1	33.7	71.5	62.0	62.5	51.9	65.0	71.4	68.1
<i>T-FLEX</i>	Paretic	Hip F-E	39.3	48.2	38.7	46.1	39.3	48.7	39.4	54.9	49.5	52.1
		Hip Ab-Ad	9.9	15.3	12.7	12.1	10.1	10.3	4.9	8.3	19.5	14.8
		Ankle D-P	17.2	29.7	17.0	23.4	29.9	26.3	30.6	17.3	14.3	20.8
	Non-Paretic	Knee F-E	50.6	61.2	31.7	65.1	41.3	53.1	20.3	51.2	29.3	39.4
		Hip F-E	38.4	47.5	26.9	41.1	30.5	53.1	31.9	37.6	25.2	31.7
		Hip Ab-Ad	7.7	14.8	11.7	8.7	14.1	6.5	8.9	7.2	9.8	8.8
<i>Variation</i>	Paretic	Ankle D-P	-37.2	13.8	-5.4	5.9	-26.2	69.6	79.6	7.0	97.6	-53.1
		Knee F-E	-19.1	18.4	7.2	-8.2	-11.3	-17.4	10.5	3.1	-5.8	-1.6
		Hip F-E	-2.8	-4.4	0.5	-2.8	1.0	-1.1	96.6	-10.0	-18.8	-11.6
	Non-Paretic	Hip Ab-Ad	2.2	-7.9	-2.9	-26.2	75.1	-35.9	-11.5	-14.3	13.5	-21.3
		Ankle D-P	0.4	-35.8	-13.1	-0.1	-8.7	31.0	38.9	29.7	41.1	-34.2
		Knee F-E	-13.8	13.6	2.9	-26.5	-16.3	0.4	15.6	-14.4	-3.4	-12.5
<i>Variation</i>	Paretic	Hip F-E	2.3	-2.0	-2.2	-7.3	-2.8	0.4	30.4	5.7	-2.5	0.6
		Hip Ab-Ad	-18.7	-1.7	-4.3	-34.5	-7.9	-30.2	107.3	-29.7	-4.7	29.8
		Ankle D-P	-37.2	13.8	-5.4	5.9	-26.2	69.6	79.6	7.0	97.6	-53.1
	Non-Paretic	Knee F-E	-19.1	18.4	7.2	-8.2	-11.3	-17.4	10.5	3.1	-5.8	-1.6
		Hip F-E	-2.8	-4.4	0.5	-2.8	1.0	-1.1	96.6	-10.0	-18.8	-11.6
		Hip Ab-Ad	2.2	-7.9	-2.9	-26.2	75.1	-35.9	-11.5	-14.3	13.5	-21.3
<i>Variation</i>	Paretic	Ankle D-P	0.4	-35.8	-13.1	-0.1	-8.7	31.0	38.9	29.7	41.1	-34.2
		Knee F-E	-13.8	13.6	2.9	-26.5	-16.3	0.4	15.6	-14.4	-3.4	-12.5
		Hip F-E	2.3	-2.0	-2.2	-7.3	-2.8	0.4	30.4	5.7	-2.5	0.6
	Non-Paretic	Hip Ab-Ad	-18.7	-1.7	-4.3	-34.5	-7.9	-30.2	107.3	-29.7	-4.7	29.8
		Ankle D-P	-37.2	13.8	-5.4	5.9	-26.2	69.6	79.6	7.0	97.6	-53.1
		Knee F-E	-19.1	18.4	7.2	-8.2	-11.3	-17.4	10.5	3.1	-5.8	-1.6

Table 5.2: Range of motion on the participants' lower limb joints in the proposed scenarios. Each one divides the limbs in paretic and non-paretic, where the analyzed movements comprise the flexo-extension on the ankle, knee, and hip joints (D-P and F-E), and the add-abduction on the hip (Ab-Ad). The second part shows the variation percentage on the joints using the device concerning the baseline. The positive values refer to increases in this value in contrast to the negative values that indicate decreases. The highlighted values indicate significant joint changes greater than 10% for both increases (green) and decreases (red).

number was directly proportional to the change presented on the ankle, where paretic ankle's ROM values with variation above 50% registered changes in at least half of the analyzed joints. In general, the changes did not show a common tendency in terms of increases or decreases. Furthermore, the larger values corresponded to the D-P alterations, although subjects 4, 5, and 7 showed the Ab-Ad value as the maximum variation.

According to the lower limb joints' ROM variations(see Table 5.2), it is essential to determine whether this change represents a positive or negative effect in the participant' joint (see Fig. 5.4). The obtained ROM was compared with the mean value in a healthy gait [116]. In this context, 60% of the volunteers showed improvement in the D-P using the device. Among this, subjects 2, 5, and 7 achieved values whose errors, regarding the healthy people's ROM, were less than 2%. This way, positive changes in the paretic ankle joint improved the non-paretic joints' ranges, especially in the ankle joint. For 30% of the participants, the variations in the D-P did not represent significant improvements. Additionally, one volunteer exhibited a negative effect in this ROM related to a reduction of 33%.

Thus, Figure 5.4 summarizes the consequences of using T-FLEX's system actuation on each participant's analyzed joints. The positive effects indicate improvement in the corresponding joint's ROM, approaching this value to healthy ranges. Negative impacts indicate a pattern disruption, and hence a distancing of the movement with a healthy pattern. Undetermined conditions grouped changes where, although the variation is significant (i.e., above 10%), this value does not improve or impair the ROM. Lastly, the no-changes group integrates the differences between both scenarios of less than 10%.

Bearing in mind the variations' classification for each subject (see Figure 5.4), 70% of the volunteers showed a positive effect on at least one joint, where the paretic ankle was the more prevalent. The exhibited negative impacts were mainly related to the ROM's reduction, although they did not represent a participant's risk.

On the other part, Table 5.3 contains the GDI values for each participant. The GDI showed

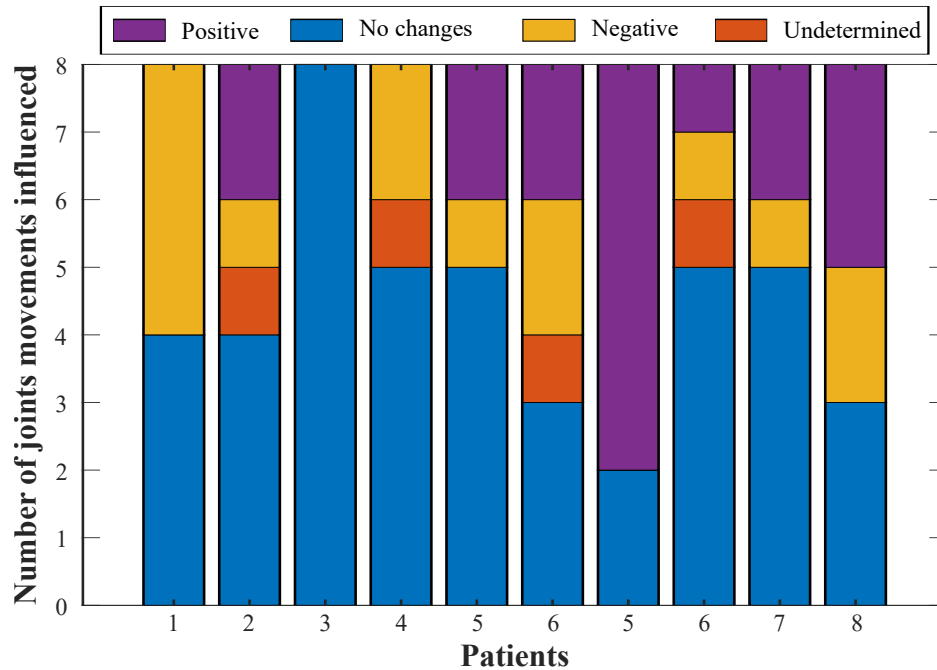


Figure 5.4: T-FLEX’s effect on the joints range of motion. Positive changes (purple bar) refer to variations that approach the value to a healthy pattern. Negative changes (orange bar) comprehend joints where the ROM departs from the normal gait. Undetermined conditions (red bar) integrate magnitudes that exhibit variation, but they do not generate an improvement or an impairment. Lastly, no changes state (blue bar) include percentages of less than 10%.

a significant difference for 30% of the participants’ paretic limbs, wherein 20% manifested a reduction below 14%, and one volunteer registered an increase of 14%. For the non-paretic, 40% of the participants exhibited decreases by less than 30% for this index. Reduction in GDI is related to a higher difference between the participant kinematics and a healthy pattern. In contrast, an improvement in the gait kinematics depends on an increase in this index. The GDI mean value for the participants (see Table 5.5) did not present a significant difference between the scenarios. Both limbs remained the no healthy condition as the GDI percentage was less than 90%.

Lastly, Figure 5.5 illustrates the MAP for the paretic (Fig. 5.5a) and non-paretic (Fig. 5.5b) limbs between baseline and assisted gait. The most affected joints in the scenarios were the ankle, the knee, and the hip (i.e., ankle rotation, hip rotation, and knee flexo-extension).

Subjects		1	2	3	4	5	6	7	8	9	10
<i>Baseline</i>	<b>P</b>	72.0	75.9	69.1	80.2	78.5	80.5	73.3	76.4	67.7	53.8
	<b>N-P</b>	73.0	74.0	57.4	85.3	84.0	101.4	80.8	91.0	64.7	73.2
<i>T-FLEX</i>	<b>P</b>	64.6	61.9	67.2	84.5	67.2	83.0	68.6	78.4	62.6	68.1
	<b>N-P</b>	65.6	60.7	64.7	83.2	85.7	74.3	68.3	60.7	57.9	71.5
<i>Variation</i>	<b>P</b>	-7.3	-14.0	-1.8	2.2	-11.3	2.5	-4.7	2.0	-5.2	14.3
	<b>N-P</b>	-7.4	-13.3	7.3	-2.1	1.7	-27.1	-12.5	-30.3	-6.7	-1.7

Table 5.3: Gait Deviation Index for each subject in Baseline and T-FLEX scenarios. The first part has the index for the paretic (P) and non-paretic (N-P) limbs. The highlighted values denote variation above 10% for both increases (green) and decreases (red).

The ankle dorsi-plantarflexion did not show significant changes in both the paretic and non-paretic. The GPS significantly increased between unassisted and assisted conditions for the non-paretic limb, although this change moved away from the healthy people' value. Nevertheless, this value did not exhibit significant changes for the paretic side.

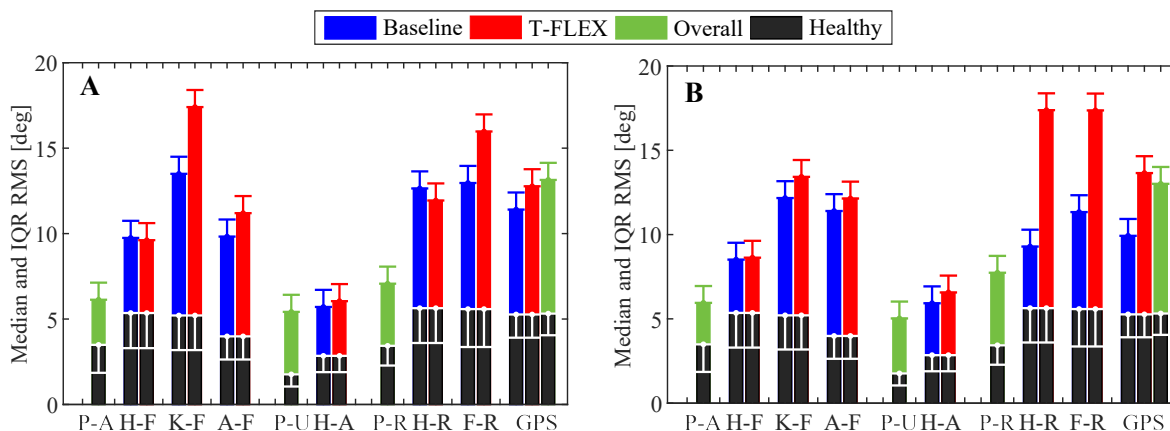


Figure 5.5: Movement Analysis Profile. The upper part of the figure refers to the paretic limb. The lower illustrates the part non-paretic side. Each column represents one of the kinematic variables such as P-A (Pelvis Anterior-Posterior), H-F (Hip Flexion-Extension), K-F (Knee Flexion-Extension), A-F (Ankle Dorsi-Plantarflexion), P-U (Pelvic Up-Down), H-A (Hip Abd-Adduction), P-R (Pelvic Rotation), F-R (Foot Rotation), and GPS (Gait Profile Score). The height of the bar indicates the median and IQR RMS value during the trial. Black columns at the bottom denote the mean value for healthy gait pattern. Unassisted and assisted scenarios correspond to red and blue columns, respectively.

## 5.2.2 Spatio-temporal Parameters

Considering the variation in ROM presented above, the second part of this study analyzes the changes in Spatio-temporal values. For this purpose, Table 5.4 shows the variation percentages for the parameters in each participant. The parameters include mean values for the paretic (P) and non-paretic limbs (N-P) in aspects such as the duration's percentage for the stance phase (SP) on the gait cycle, as well as the step length (SL) and the step width (SW). Likewise, walking speed (S), stride length (ST), and cadence (C) also are part of this table.

Subject		1	2	3	4	5	6	7	8	9	10
<b>P</b>	<b>SP</b>	7.8	-1.9	1.4	-1.1	3.5	1.1	2.3	-0.8	4.1	-5.9
	<b>SW</b>	0.0	0.0	0.0	0.1	0.0	0.0	0.0	0.0	-0.0	0.0
	<b>SL</b>	0.1	-0.1	0.0	-0.1	-0.1	-0.1	0.1	-0.1	0.1	0.0
<b>N-P</b>	<b>SP</b>	1.6	-5.3	0.0	2.6	-2.1	5.3	-4.1	0.6	-1.4	-1.7
	<b>SW</b>	0.0	0.0	0.0	0.0	0.0	0.0	0.0	0.0	0.0	0.0
	<b>SL</b>	0.0	-0.1	0.0	0.0	0.0	-0.1	0.2	-0.1	0.0	-0.1
<b>S</b>		0.0	-0.1	0.0	-0.3	-0.2	0.0	0.2	-0.3	-0.1	-0.1
<b>ST</b>		0.0	-0.1	0.0	-0.2	0.0	-0.1	0.4	-0.2	0.0	0.0
<b>C</b>		-11.0	2.0	-6.1	-15.0	-21.1	-24.0	-11.60	20.0	-17.8	-14.7

Table 5.4: Percentage of variation of spatial-temporal parameters. The first part includes values for the paretic (P) and non-paretic (N-P), which are the percentage of the stance phase (SP), the step width (SW), and step length (SL). The second part shows general parameters such as walking speed (S), stride length (ST), and cadence (C). The highlighted values indicate a change above 10% for both increases (green) and decreases (red).

In general terms, the Spatio-temporal parameters did not show significant changes using the T-FLEX actuation system to either of the participants' limbs. Nevertheless, the cadence exhibited a reduction in 70% of the volunteers. This parameter registered decreases below 24% of the baseline state, although subject 8 presented an increase in 20% of the assisted gait cadence.

On the other hand, Table 5.5 contains the mean values for the participants' parameters. This table summarizes the results aforementioned, showing a decrease in the cadence of 14% (i.e., from 99 to 85 steps per minute). Additionally, this table also exhibits other Spatio-temporal

values without significant changes.

	Baseline			T-FLEX		
	<i>P</i>	<i>Mean</i>	<i>N-P</i>	<i>P</i>	<i>Mean</i>	<i>N-P</i>
<b>GDI</b>	72.9	-	78.5	70.6	-	69.3
<b>SL</b>	-	0.9	-	-	0.9	-
<b>C</b>	-	99.0	-	-	85.1	-
<b>S</b>	-	0.8	-	-	0.7	-
<b>SP</b>	62.9	-	70.0	63.6	-	69.5
<b>ST</b>	0.5	-	0.5	0.5	-	0.4
<b>SW</b>	0.2	-	0.2	0.2	-	0.2

Table 5.5: Spatial-temporal parameters and Gait Deviation Index for the baseline and assisted gait with T-FLEX’s actuation system. It is also divided into paretic (P) and non-paretic (N-P) side. GDI is defined in percentage, as well as the stance phase (SP). Following the step width [m] (SW), and step length [m] (SL). The second part shows general parameters such as walking speed [m/s] (S), stride length [m] (ST), and cadence [step/min] (C). The highlighted values are parameters with significant changes.

### 5.2.3 Usability Assessment

This part describes the device performance in terms of user-machine interaction and the participants’ perception of assistive technology. Firstly, no patient exhibited issues (i.e., affectations in the locomotor system, pressure points, skin injuries or falls) during and after wearing the device.

Figure 5.6 shows the participant’s relevant aspects through the QUEST survey to measure the users’ perception. The most selected parameter was the device’s comfort with 70% of recurrence. Other important aspects for the users were safety, weight, and dimensions. Finally, the user satisfaction’s level was between satisfied and very satisfied in 60% and 40% of the users, respectively.

### 5.2.4 Statistical Analysis

To understand the participants’ effects on the gait cycle, statistical analysis aimed to identify differences between assisted and baseline conditions. In terms of the ankle kinematics, the



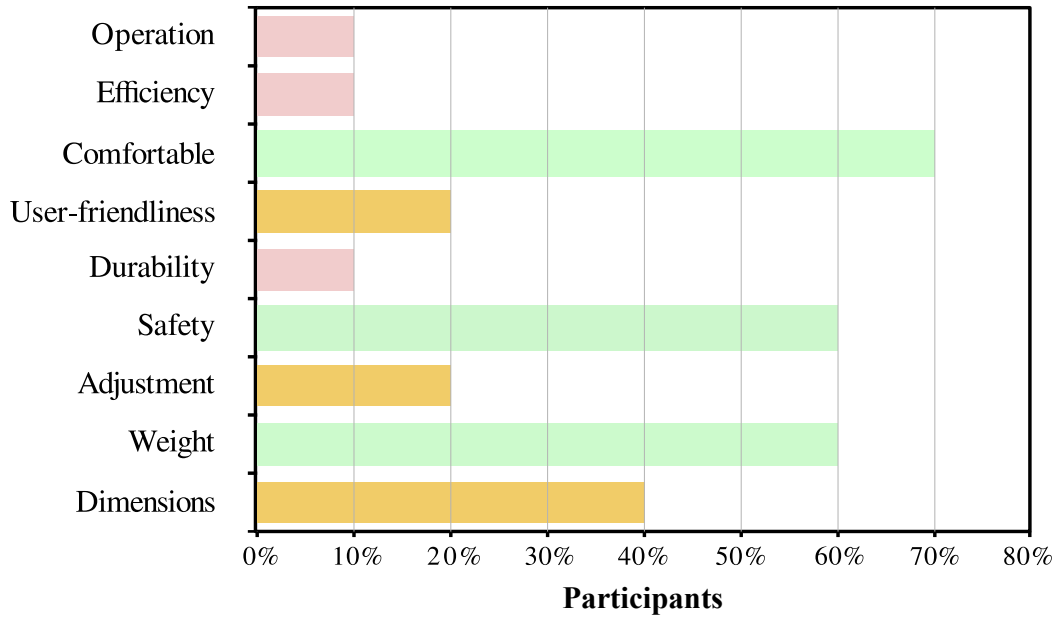


Figure 5.6: Results of the usability assessment through the QUEST test. The percentage of each topic refers to the number of participants who considered that characteristic as relevant.

results revealed statistically significant changes for 70% of the subjects in at least one gait phase for the angle. Specifically, this joint showed statistical differences in the stance and swing phase for 60% and 70% of the participants, respectively (see Table 5.6). Moreover, 40% of them exhibited variations in the entire gait cycle.

Subject	Stance phase	Swing phase
1	1.41e-4	4.38e-11
2	3.10e-3	8.54e-1
3	1.40e-3	2.85e-1
4	1.03e-9	1.18e-10
5	5.27e-2	1.67e-23
6	8.12e-3	3.21e-2
7	8.89e-1	8.26e-2
8	7.47e-1	1.65e-8
9	3.90e-15	1.08e-33
10	8.10e-2	1.14e-12

Table 5.6: Probability value (p-value) of each subject for stance and swing phases. The highlighted cells indicate a statistical difference.

In the Spatio-temporal context, the parameters showed a statistically significant decrease in the cadence ( $p=0.0002$ ) and speed ( $p=0.03$ ) concerning the assisted gait. The parameters that did not show statistically significant changes were: (1) long stride, (2) step length, (3)

step width, and (4) stance phase .

### 5.3 Discussion

The results showed in the previous section intend to find the effects on the lower limb joints for the assisted gait with the T-FLEX's actuation system. For that, the kinematics presented the results for the participants individually. This analysis allowed determining aspects such as the participant performance during the trial, adaptability to the device, improvement in the ankle kinematics, and the consequences on the other planes of motion. On the other hand, an inter-subject analysis did not evidence significant changes comparing unassisted and assisted gait. However, those results could be affected by the poor-performance exhibited in some participants. Thus, an experimental setup's modification that includes the training stage could improve the user's performance and adaptability to the device.

In this context, the ankle kinematics described the device's influence in this joint for each user (see Figure 5.3). The T-FLEX's actuation system positively impacted the dorsiflexion movement from the significant changes found in both phases, improving the joint's angle and hence the foot clearance during the swing phase. Therefore, the device reduced the risk of falls and injuries in the participants [117]. For the stance phase, subjects experimented with a reduction in the ankle's angle due to the actuators, providing stability to the user during this phase. Other changes related to the dorsi-plantarflexion movements can be associated with both the user-device synchronization and the calibration stage carried out manually. However, those changes did not represent a risk for the users' stability. On the other hand, considering the first 10% of the gait cycle, 60% of the volunteers exhibited a kinematic behavior similar to the healthy pattern's shape. Likewise, assisted gait also showed a smoother transition between phases, ensuring a suitable control of the joint to provide stability and safety.

In general terms, the kinematic results during the first use of the T-FLEX actuation system showed improvements in some participants (i.e., increase foot clearance, and early push-off), which are similar to a robust PAFO based on pneumatic actuation [118]. Additionally, these results are comparable to devices controlled by Force Sensitive Resistor (FSR) for gait detection [79, 119] that is the most common detection strategy used in ankle exoskeletons. Nevertheless, those previous studies enrolled a smaller subjects' sample reducing the probability of poor-performance in the participants. Lastly, the ankle kinematics results also tended to another study's outcomes that included a training stage [82], unlike this protocol.

Gait performance can also be analyzed through the other joints of both paretic and non-paretic sides [120]. Usually, this assessment includes at least the knee and ankle joints, where the results commonly exhibit kinematics improvement [119]. This study showed proper adjustment of ankle's ROM to avoid foot drop, compared to the mechanical structures limiting the sagittal plane. In the hip context, the Ab-Ad movement decreased by 70% of the non-paretic limb participants. This reduction is a result of the restriction and actuation on the paretic ankle. In contrast to the non-paretic, the other side presented disruptions in 40% of the subjects related to reductions in the ROM value.

In particular, subject 7 showed high performance in the estimated ROM for both sides. The positive effects were in 75% of the analyzed joints with the best improvement in the D-P for the non-paretic limb. This outcome could not be associated with the user's spasticity level because subjects 2 and 8 have clinical conditions comparable to this participant, but they did not exhibit similar performance. Hence, it could relate to external variables such as the device's correct synchronism and the appropriated actuation performance.

Spatial-temporal parameters allow measuring the device's effects on the user [29, 120]. Mainly, orthotic devices should improve the subjects' parameters to enhance their mobility in the ADL's execution [121]. The first use of T-FLEX showed a decrease in cadence. This reduction is related to both the training stage (not included in this study) and the ankle's restricted

structure. Therefore, the inclusion of training stages is imperative to improve the obtained results.

On the other hand, Table 5.3 shows the GDI and the variation according to each scenario. Regarding the baseline, most of the participants decreased the GDI, although only 30% of the limbs registered a reduction above 10%. Several factors can explain the decrease in this index. The first factor is related to the MAP information (see Figure 5.3), where the foot rotation represents one of the most significant movements with affectations. This alteration is due to the mechanical structure coupled to the T-FLEX actuation system. The ankle's restriction triggers a disruption in the other joints pattern, which induces a decline in this index. The second factor comprehends the actuation system's performance in aspects such as response time to position set-points, processor speed for running the detection algorithm, and the manual calibration stage that recorded the maximum flexo-extension angles of the user. On the other part, multiple studies have presented GDI analysis for children with cerebral palsy using a passive orthotic device [122–124]. However, in studies that involve patients with stroke using PAFO, this index was not shown.

Finally, in the MAP context (see Figure 5.5a), assisted gait with T-FLEX affected several paretic joints' movements (e.g., K-F, A-F, and F-R). Nevertheless, as mentioned previously, the changes could lead to a mechanical restriction on the ankle. This block alters the natural gait pattern and induces compensatory motions on the other joints, although the training stage' lack could also cause this wrong pattern. For the non-paretic side (see Figure 5.5b), the main affectations were the H-R and F-R movements related to the device's weight compensation. As GDI, different studies used GPS to analyze the effects on people with cerebral palsy [125,126]. Although, in protocols that include patients with stroke in assisted gait with PAFOs, the score was not reported.

## 5.4 Conclusions

This chapter presented an assessment of the T-FLEX's actuation system during its first use. A passive orthotic structure was modified, in such a way that the T-FLEX's actuators and inertial sensor were attached to it. Ten patients who suffered a stroke used the modified passive orthotic structure and performed overground walking test. Regarding inter-subject analysis, the biomechanical outcomes showed improvements for some patients in the dor-siflexion phase, avoiding foot slapping and controlling the ankle in the phases transition. Moreover, the other joints exhibited positive and negative changes related to the actuation on the paretic ankle with T-FLEX. For the intra-subject analysis, the results showed no significant differences between baseline and assisted gait. This result could be related to the poor-performance evidenced by several participants.

The Spatio-temporal parameters did not present significant changes, although the cadence decreased for the assisted gait trials. Lastly, the GPS and GDI measured the kinematic behavior for each participant in both modalities. Those parameters did not evidence significant improvements between subjects and the healthy pattern. These indicators also determined the main joints that were altered by the device.

## Chapter 6

# Experimental Validation of T-FLEX in Therapy Mode

Robotics' inclusion in rehabilitation processes has evidenced a higher user's recovery level, as chapter 2 previously presented. Thus, the devices apply neuroplasticity's concepts and the central nervous system's adaptability in their actuation control designs, which are induced by repetitive and task-oriented therapies. T-FLEX is an ankle exoskeleton able to work in rehabilitation scenarios through the therapy modality that is detailed in chapter 3.

In this context, this chapter presents the initial results in a stroke survivor for the therapy mode using T-FLEX. This study's first goal was related to determining the appropriate exercises for this modality. The second goal consisted of assessing the T-FLEX's effects on the patient's kinematic and Spatio-temporal parameters. Finally, the last goal is intended to analyze the effects of the patient's spasticity after the therapy sessions.

## 6.1 Experimental Design

The experimental design intended to analyze and determine the T-FLEX's effects and impact on a stroke survivor. Thus, the device was tested in a rehabilitation scenario using the therapy mode, consisting of repetitive flexion and extension movements on the ankle. To this end, four phases were defined: pre and post functional assessment, the experimental procedure, and a usability assessment.

### 6.1.1 Participant

This study involved a 32-year-old female volunteer who suffered a hemorrhagic stroke. The participant's diagnosis was chronic hemiplegia on the body's right side and ankle spasticity (i.e., 1+ in the Ashworth scale). The participant was selected using the inclusion and exclusion criteria shown below.

1. **Inclusion Criteria** A patient with chronic stroke who suffers some ankle dysfunction. The participant must have a low spasticity level on the ankle (i.e., up to level 3 in the Ashworth scale) and partial independence during walking.
2. **Exclusion Criteria** According to the experimental setup and the system features, participants under 150 cm and over 190 cm were not considered. Likewise, subjects with any visual, auditory, or cognitive impairments that prevent the correct understanding of the activity will not be part of this study. On the other hand, the subject must not present injuries, ulcers, and pain in the affected lower limb or the spinal cord.

### 6.1.2 Pre and Post Functional Assessment

This study aims to evaluate T-FLEX's effect on Spatio-temporal and kinematic parameters. For this purpose, two functional evaluation assessed those parameters before and after the

rehabilitation sessions. Within the assessment, a 10-meter test determined the subject's overground speed, which was used to set a rehabilitation treadmill (NIZA RX K153D-A-3, SportFitness, Colombia).

Thus, the participant walked on the treadmill at a zero-degree inclination wearing a G-WALK (BTS Bioengineering, Italy) located on L2 and an inertial sensor (Shimmer3, Shimmer, Ireland) placed on the foot tip. The trial lasted 6 min, where data acquisition only started once the self-selected speed was reached.

On the other hand, this stage also included a physical assessment executed by a physiotherapist. Therefore, spasticity (through the Ashworth scale) and lower limb joints' ROM (e.g., knee, ankle, hallux, among others) were measured. Table 6.1 summarizes the measured parameters, where the initial evaluation was used as a baseline to compare the results before the rehabilitation sessions.

### 6.1.3 Experimental Procedure

The rehabilitation program proposed in this study included 18 sessions (i.e., 3 per week for a total of 6 weeks) under a standard therapy procedure. Likewise, considering the motivation of increasing the patient's muscular activity, each session integrated two modalities:

1. **First modality (20 minutes):** Sitting on a chair with 90-degree knee flexion, the volunteer's lower limb was slightly raised to avoid floor contact (See Figure 6.1A).
2. **Second modality (20 minutes):** Sitting on a chair with a full knee extension, the volunteer's lower limb was horizontally raised to avoid floor contact (See Figure 6.1B).

Between modalities, there was a five minute rest period. Each session carried out the same experimental conditions. First, the participant was equipped with electrodes located on the



tibialis anterior and gastrocnemius muscles of the paretic side. An electromyogram (EMG) sensor (Shimmer3 EMG unit, Shimmer, Ireland) running at 500 Hz acquired the muscles' electrical activity.

After this, T-FLEX was installed on the participant's paretic side (See Figure 6.1). It is important to emphasize that after the instrumentation, the device recorded the volunteer's maximum range of motion during the calibration stage explained in chapter 3. This calibration was executed for each session, obtaining different values throughout the experiment.

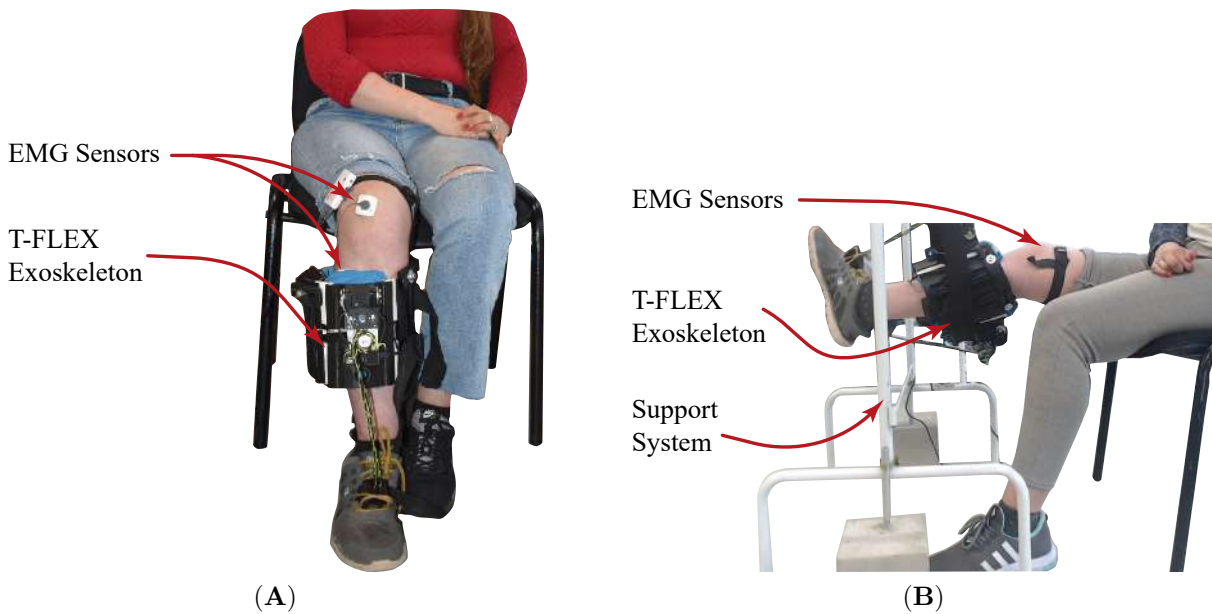


Figure 6.1: Experimental setup postures proposed for this study. The first posture (A) consists of a 90-degree knee flexion. The second posture (B) refers to a complete knee extension.

#### 6.1.4 T-FLEX's Parameters

T-FLEX was configured to work in the therapy mode detailed in chapter 3. Specifically, the device had a repetition rate of 0.6 Hz. Moreover, the actuators worked with a velocity of 50% of the maximum motor speed (i.e., 10 rpm approximately). To complete the modality time (i.e., 20 minutes), T-FLEX performed 370 movements for a total amount of 740 repetitions per session. These parameters were the same during the experiment.

### **6.1.5 Data processing and acquisition**

Data processing was performed offline using MATLAB software (MathWorks, 2018b, USA) and an Asus VivoBook S15 S510UA (IntelCore i5-8250U, CPU@1.80 GHz, Taiwan) running Windows 10 Home. The output EMG signals were processed with a band-pass filter to eliminate the atypical values and remove the noise. Then, these signals were rectified with absolute values. Subsequently, a data smoothing was performed using a 100 ms moving average window. Finally, RMS values were calculated to provide as much information as possible about the EMG signal's amplitude, since it gives a measure of the signal power.

### **6.1.6 Usability Assessment**

To evaluate the patient's satisfaction during this study, a QUEST survey was carried out at the end of the experiment. This survey consisted of 8 questions, with a maximum score of 5 (i.e., completely satisfied), focused on aspects such as dimensions, ease of use, and comfort using T-FLEX. The assessed aspects are detailed in Table 6.2.

### **6.1.7 Statistical Analysis**

The software SPSS (IBM-SPSS Inc, Armonk, NY, USA) was used for the statistical analysis. First, data's normal distribution was verified employing the Shapiro–Wilks test. Subsequently, the ANOVA test was carried out to find statistically significant differences among each muscle's electrical activity in two cases: (1) comparison between two modalities and (2) comparison of the muscular activity during each session.

## 6.2 Results

### 6.2.1 Pre and Post functional Assessment

This study measured the kinematic and Spatio-temporal parameters obtained from the functional assessment presented above. Table 6.1 illustrates the values corresponding to the pre and post evaluations in terms of passive ROM. These values show changes in 20 of 22 measured motions on the lower limb joints. Extension on the hallux metatarsophalangeal and proximal extension on the fifth toe interphalangeal remained the same. However, the most significant changes were related to increases in the joint range for the movements on the hip, dorsi-plantarflexion on the ankle, flexo-extension on the hallux interphalangeal joint, and flexion on the fifth toe interphalangeal joint. The other measures exhibited changes of less than 15% concerning the initial assessment.

Moreover, for the kinematic results, the ankle angular motion during the walking over treadmill followed a normal distribution. Thus, the gait cycles were averaged to obtain a unique curve. This curve allowed estimating the parameters shown in Figure 6.2. The maximum kinematic change presented during the walking analysis reduced 25% of the extension movement on the swing phase. Additionally, the Spatio-temporal parameters showed improvement inherently related to an increase in the subject's natural walking speed.

In terms of spasticity, the patient exhibited a reduction in the Ashworth scale from 1+ to 1 after the therapy sessions. A physiotherapist estimated this scale during the functional assessment detailed previously

Initial Functional Evaluation			Final Functional Evaluation		
Body Part	Paretic Side (deg)	Healthy Side (deg)	Body Part	Paretic Side (deg)	Healthy Side (deg)
Hip Abduction	30	45	Hip Abduction	45	45
Hip Adduction	20	35	Hip Adduction	30	35
Hip Flexion	116	125	Hip Flexion	122	125
Hip Extension	18	25	Hip Extension	20	25
Knee Flexion	140	136	Knee Flexion	140	136
Knee Extension	10	4	Knee Extension	10	4

(A)

Initial Functional Evaluation		Final Functional Evaluation	
Body Part	Paretic Side (deg)	Body Part	Paretic Side (deg)
Ankle Plantarflexion	15	Ankle Plantarflexion	45
Ankle Dorsiflexion	15	Ankle Dorsiflexion	24
Ankle Inversion	33	Ankle Inversion	35
Ankle Eversion	22	Ankle Eversion	25
Hallux Metatarsophalangeal Flexion	43	Hallux Metatarsophalangeal Flexion	45
Hallux Metatarsophalangeal Extension	47	Hallux Metatarsophalangeal Extension	47
Fifth Finger Metatarsophalangeal Flexion	64	Fifth Finger Metatarsophalangeal Flexion	68
Fifth Finger Metatarsophalangeal Extension	60	Fifth Finger Metatarsophalangeal Extension	65
Hallux Interphalangeal Flexion	37	Hallux Interphalangeal Flexion	44
Hallux Interphalangeal Extension	0	Hallux Interphalangeal Extension	5
Fifth Toe Interphalangeal Proximal Flexion	34	Fifth Toe Interphalangeal Proximal Flexion	40
Fifth Toe Interphalangeal Proximal Extension	0	Fifth Toe Interphalangeal Proximal Extension	0
Fifth Toe Interphalangeal Distal Flexion	36	Fifth Toe Interphalangeal Distal Flexion	39
Fifth Toe Interphalangeal Distal Extension	30	Fifth Toe Interphalangeal Distal Extension	34

(B)

Table 6.1: Subject's Range of Motion (ROM) on the hip and knee joints (A) and the ankle-foot joints (A) for the pre and post functional assessments. The highlight values indicate the most relevant changes after the therapy sessions.

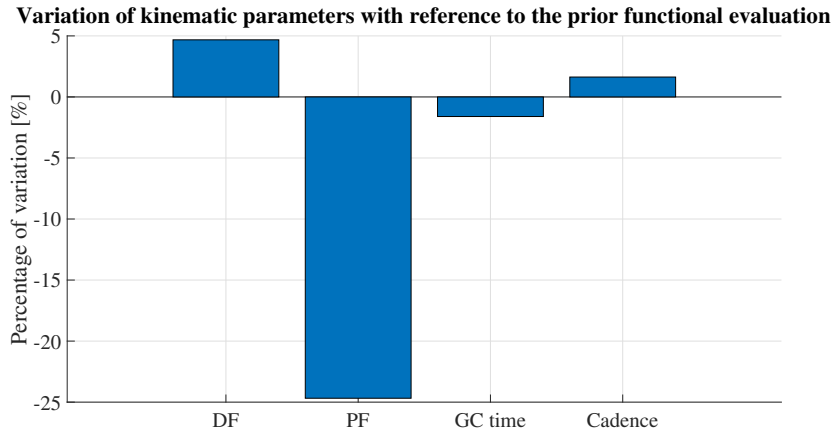


Figure 6.2: Percentage of variation for the kinematic and Spatio-temporal parameters in walking over the treadmill (DF: Average values of the maximum dorsiflexion angles during gait cycles, PF: Average values of the maximum plantarflexion angles during gait cycles, GC: gait cycle). The positive values refer to increases concerning the initial functional evaluation. In contrast, negative values represent a reduction in the parameter.

## 6.2.2 Muscular Activity

The second part constitutes the muscular activity measured on the tibialis anterior and gastrocnemius muscles during the session. Figure 6.3 shows the mean RMS values per session in each modality. On the one hand, the tibialis anterior registered a significant muscular activity increase up to the third session (See Figure 6.3A). For the following sessions, this value reduced and maintained its magnitude between 0.004 mV and 0.015 mV. Moreover, both modalities showed similar electrical amplitudes throughout the experiment.

On the other hand, the gastrocnemius' muscular activity increased to the fourth session (See Figure 6.3B). The mean RMS values after this session had a reduction as also occurred in the tibialis anterior. In general terms, the gastrocnemius reached a greater activation of electrical activity concerning the tibialis anterior during the first sessions. Nevertheless, this activity showed lower mean RMS values than the other muscle from the ninth session.

Additionally, the muscular activity's behavior during the therapy session was analyzed. To this end, it was calculated the mean of the electrical activity on time windows with a size of

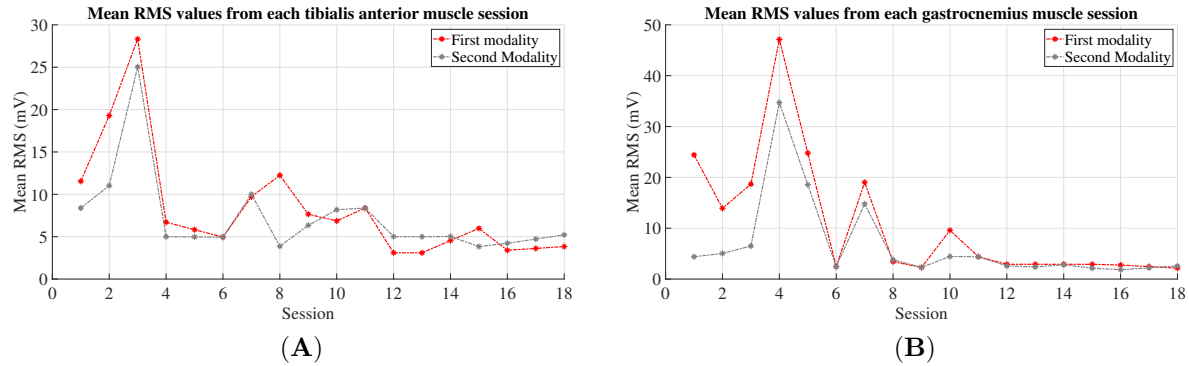


Figure 6.3: Mean RMS values per session during the study for the (A) tibialis anterior and (B) gastrocnemius. The red line represents the values for the modality with 90-degree knee flexion. The gray line refers to obtained values with a posture of complete extension of the knee.

10 seconds. The first window was used as a reference to calculate the change in the other moments. Figure 6.3 illustrates this behavior throughout the session.

The anterior tibialis muscle presented variability at the first modality's half time. However, this muscle tended to increase its electrical activity at the end-stage of the sessions (See Figure 6.3A). The gastrocnemius muscle showed high variability for the complete knee extension posture taking values up to 130 % concerning the first minutes. Conversely, the 90-degree knee flexion posture had similar variation all the time, although with a slight increase in the final part.

### 6.2.2.1 Statistical values

ANOVA tests were performed to find statistically significant differences among the muscular activity between modalities during the study and the electrical activity progression during the session. The results are presented below.

- **Muscular activity between modalities:** The tibialis anterior's electrical activity did not show statistically significant differences ( $p > 0.05$ ) during the study. In the same way, the gastrocnemius muscle also did show statistical differences between modalities.

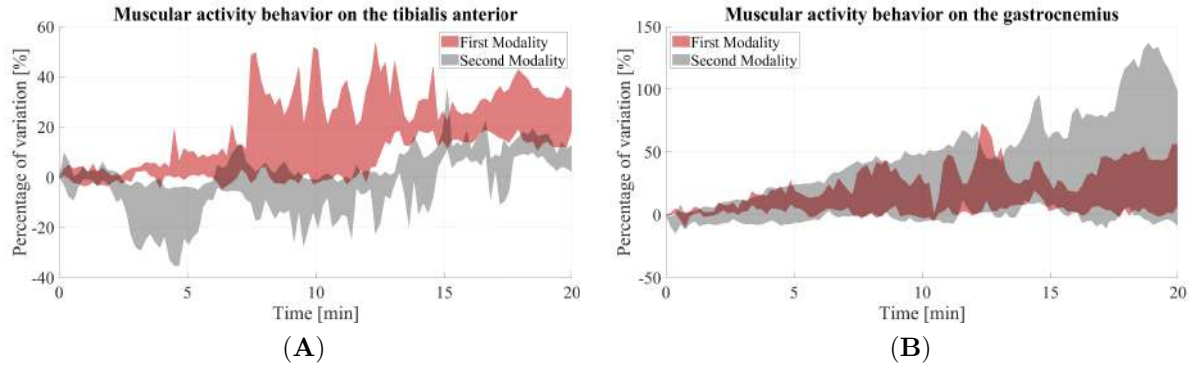


Figure 6.4: Muscular activity behavior throughout the session in terms of mean and standard deviation between sessions. The left part (A) shows the tibialis anterior and the right part (B) for the gastrocnemius. The red curve describes the behavior of the muscle in the modality with 90-degree knee flexion. The gray curve shows the behavior in the complete knee extension modality.

- **Muscular activity progression during the session:** Results related to the electrical activity progression of the anterior tibialis muscle showed statistically significant differences ( $p < 0.05$ ). Likewise, gastrocnemius muscular activity also showed statistical differences.

### 6.2.3 Usability Assessment

Finally, this part presents the QUEST test results to the patient after therapy sessions (see Table 6.2). In general terms, the user's perception of the device was acceptable, emphasizing aspects such as safety and comfort. However, other topics (i.e., adjustments, and ease of use) presented the lowest score.

## 6.3 Discussion

According to the pre and post functional evaluation, the preliminary results reported significant changes in different passive joint ROM, such as the ankle, hip, and the hallux interphalangeal joints. However, regarding the other measures, there is only a slight increase of

Table 6.2: QUEST survey responses for the T-FLEX after the therapy sessions. The values are assessed on a scale of 0 to 5

QUEST's item	Satisfaction's Level
Dimensions (size, height, length,width)	4
Weight	3
Adjustments (fixing,fastening)	3
Safety (secure)	4
Ease of use	3
Comfort	4
Effectiveness	4
<b>Device's satisfaction</b>	<b>3.57</b>

less than 15 %. On the other hand, the greatest increase in terms of ROM occurred in the ankle joint, specifically in the dorsi-plantarflexion movement. These changes are related to the foot spasticity's reduction reflected in the Ashworth scale measured in both assessments.

This study evidenced an inherent improvement in Spatio-temporal parameters due to an increase in the patient's speed from the kinematic results. Also, it showed a 25 % reduction in the plantarflexion movement. This value is related to an increase in ankle dorsiflexion during the swing phase, which indicates an enhancement in the foot clearance for the patient in walking. This improvement is associated with decreases in fall risks and ankle injuries [117]. The above suggests that effectively a rehabilitation program with the T-FLEX helps to improve the Spatio-temporal and kinematic parameters at the end of the entire therapy sessions.

Regarding Ashworth scale results, the participant exhibited a reduction in one from 1+ to 1 at the end of the entire therapy sessions. This way, this preliminary study suggests that the T-FLEX has potential in rehabilitation and could reduce the patient's spasticity level.

These results coincide with the changes presented in previous studies, where the Spatio-temporal parameters had an increase, and the spasticity level decreased after the sessions [127]. However, in contrast to this protocol, they used electrical stimulation after the repetition exercises. Likewise, another study also presented similar results asserting that if it is included electromyography as a control signal, the results will be more effective in terms of



spasticity and ROM [128]. Therefore, to engage the patient with the therapy and improve the outcomes reported in this study, the following protocols could include active control and feedback strategies.

In the second place, for the muscular activity context, this study evidenced an increase in electrical activity during the experiment's first stage. Nevertheless, this activity presented a decrease from the third and fourth sessions for both assessed muscles. These results suggest that during the first sessions, given that the muscle comes from a period of inactivity, any exercise performed over it induces high electrical values. However, as early as the muscle overcame the adaptation period, the same training did not produce enough effort to generate high electrical activity values [129, 130]. Hence, a variable rehabilitation program with T-FLEX, where the requirement and the effort increase over time, could provide better results.

Concerning the muscular activity in the session, the results showed an increase in the electrical values at the end-stage for both muscles. This also can be seen in the statistical outcomes, since the trials reported statistically significant differences. Nevertheless, it should be emphasized of high variability between sessions illustrated in Figure 6.4. This variability can be related to the muscular activity's decrease after the adaptation period, where the electrical activity showed minimum increases.

Another aspect analyzed was the difference between the modalities proposed in this study. Nevertheless, the statistical results suggest that the modalities do not affect the measured muscles' electrical activity.

Finally, the patient perception about T-FLEX in A rehabilitation program was positive. The most important aspects highlighted by the user were safety, comfort, and effectiveness. Although other characteristics such as weight, ease of use, and adjustments, should be considered in subsequent studies.

## 6.4 Conclusions

This chapter presented the outcomes of a single case study for the therapy mode with the T-FLEX exoskeleton during a rehabilitation program of 18 sessions. A chronic stroke patient with ankle dysfunctions performed repetitions using T-FLEX under two modalities: (1) 90-degree knee flexion and (2) full knee extension. Each session had a duration of 50 minutes divided into 20 minutes per modality and 10 minutes for installation and instrumentation. Moreover, two functional assessments measured the patient's health condition before and after the study.

In general terms, this study showed improvement in the patient's kinematic and Spatio-temporal parameters. Specifically, the ankle dorsiflexion decreased on the swing phase, resulting in motor control improvement. Moreover, the cadence and the user's speed increased after the experiment. Likewise, the participant exhibited spasticity reduction according to the Ashworth scale.

On the other hand, muscular activity increased during the first sessions, although this value had a reduction probably related to adaptation issues. Moreover, the measured muscles showed increases in their electrical activity at the end-stage of each session, though they presented high variability between sessions. Finally, the patient's perception in the use of T-FLEX for rehabilitation programs was positive.

# Chapter 7

## Conclusions and Future Works

A wearable and portable ankle exoskeleton has been developed as a rehabilitation and assistive tool in patients who exhibit ankle dysfunctions. T-FLEX ankle exoskeleton, which is part of the robotic platform AGoRA, integrates an actuation system based on VSA and a soft structure. This way, T-FLEX can be considered part of a small exoskeleton's group with compliant mechanisms and soft structures called fully compliant exoskeletons.

In electronic terms, control architecture and a visual interface were implemented in T-FLEX under a modular framework, which presents advantages in aspects as the connection of additional systems or sensors and an easy device's replicability. Likewise, high-level control strategies for assistive and rehabilitation were implemented to ensure the proper T-FLEX's use in these scenarios, as chapter 3 presented. Likewise, a visual interface was developed to allow the user (i.e., patient or therapist) to configure and control the device in a robotic-assisted therapy for motor recovery.

Concerning the experimental characterization of T-FLEX detailed in chapter 4, a test bench structure was developed and sensor-equipped to analyze the system response to different configurations and force levels. This structure was excited to signals (i.e., chirp and step), acquiring the data from sensors and actuators. Thus, the system times (i.e., delay, rise, and

stabilization) and the bandwidth were estimated for each configuration.

Specifically, the trials exhibited similarity in the delay time related to the tendon's elastic behavior for the assessed initial force levels. Likewise, the highest force level did not evidence a faster rise and stabilization times, as expected. By contrast, it caused saturations limiting the actuators' capabilities. On the other hand, the stiff elements' inclusion did not improve the device performance and reduced the frequency response reflected in the bandwidth values. From that, the best setup for the maximum performance in T-FLEX is the tendons-alone configuration with an initial force level on the tendon of 10 N.

In terms of applicability, the study found that the T-FLEX exoskeleton can assist human walking, i.e., when the gait cycle duration is greater than 0.74 seconds, hence the healthy people's walking is included. However, the control architecture should integrate an adaptable stage to modify the moment when the actuators' commands are sent, looking for compensating for the system's stabilization time. This way, T-FLEX could provide a proper torque on the ankle at the right time. Moreover, considering the maximum device's torque capacity (i.e., 12 Nm in propulsion and 20 Nm in dorsiflexion), T-FLEX is within the reported ranges for other low weight exoskeletons.

Regarding the experimental validation in gait described in chapter 5, ten patients who suffered stroke wore the device in overground walking. The participants walked in two conditions: (1) using the T-FLEX's actuation system adapted to a passive orthotic structure in assistance mode and (2) without the device. Moreover, a motion capture system acquired the patients' kinematics in both cases, and a survey registered the users' perceptions.

In the biomechanical context, the inter-subject analysis showed improvements for some patients in dorsiflexion to avoid foot slap and control of the ankle in the phases transition. Moreover, the other joints exhibited positive and negative changes related to the actuation on the paretic ankle with T-FLEX. For the intra-subject analysis, the results showed no significant differences between baseline and assisted gait. This result could be related to the

poor-performance evidenced by several participants.

Likewise, the Spatio-temporal parameters did not present significant changes, although the cadence decreased for the assisted gait. The GPS and GDI measured the kinematic behavior for each participant in both modalities. Those parameters did not evidence significant improvements between subjects and a healthy pattern, and they also determined the main joints altered by the device. On the other hand, users' perceptions were positive. No patients exhibited issues (i.e., affectations in the locomotor system, pressure points, skin injuries, or falls) during and after wearing the device.

Lastly, for the T-FLEX's validation in a rehabilitation scenario, chapter 6 presented the results for a single case study on a chronic stroke patient who used the T-FLEX exoskeleton. The participant accomplished 18 sessions divided into two conditions (i.e., 90-degrees knee flexion and complete knee extension). The active therapy had a duration of 40 minutes (i.e., 20 minutes for posture), where the patient's muscular activity was acquired during the session. Moreover, two functional assessments were carried out by a physiotherapist to assess the lower limb joints and the patient's physical condition.

Thus, this study showed improvement in kinematic and spatiotemporal parameters on a chronic stroke patient. Moreover, the participant exhibited a spasticity reduction according to the Ashworth scale. On the other hand, muscular activity increased its value during the first sessions, although this value had a reduction probably related to adaptation issues. Moreover, the measured muscles showed increases in their electrical activity at the end-stage of each session, though they presented high variability between sessions. Finally, the patient's perception concerning the T-FLEX's use in rehabilitation programs was positive.

Future works should be aimed at improving the visual interface to display in the user's interaction during the implemented modes' execution. This way, T-FLEX could recreate automated therapies to improve the patients' motor recovery. Additionally, future works should also be addressed in incorporating a database to record and subsequently analyze the

user's progress during a rehabilitation program. Thus, the device could manage and design appropriate therapy sessions considering patients' performance. On the other hand, future works could be focused on integrating the T-FLEX's algorithms under the ROS2 framework that exhibits better performance in real-time applications.

Future works should be focused on assessing the system performance in dynamic tests, where the user interaction forces will be considered from the results presented in the T-FLEX's characterization. Likewise, the T-FLEX's setup could incorporate different force levels for each tendon to maximize the device's capabilities during the system operation in gait. Moreover, the signals used to excite the system should include variation in amplitude and frequency simultaneously to analyze the T-FLEX's responses. On the other hand, future studies could include T-FLEX's tendons as the bidirectional system (i.e., instead of the stiff filaments) to counteract the found drawbacks and properly integrate both actuators in the assisted movements.

Future works should also be aimed at designing and integrating an adaptation stage to synchronize the user's gait velocity to the state machine controller. This way, this stage could counteract the delay and stabilization times found in T-FLEX's characterization. Moreover, the set-point commands could be sent at the right time to transmit the appropriate torque profile on the ankle. Thus, the system could assist walking, providing its maximum capabilities.

Future works should focus on the assessment of T-FLEX in a more extensive sample of patients with ankle dysfunctions in terms of experimental validations. Additionally, for gait applications, the device's calibration stage (i.e., the manual procedure to record the user's ROM) should be optimized to guarantee assistive movements during the gait phase detection. Moreover, the actuation's performance should be improved to synchronize the device in walking applications, as mentioned in T-FLEX's experimental characterization. This way, the kinematics results could improve, and the effect on the other lower limb joints could be

more evident.

Future studies should also be addressed in assessing novel strategies to improve the patient's effort and discouragement found in long-term therapies. Thus, considering the system modularity and the ROS framework, feedback based on visual, audio, and haptic strategies could be easily adapted in T-FLEX to design interactive therapies where the user can be participating actively. Likewise, future studies could be focused on assessing these strategies independently and then combine them to propose complete scenarios.

Future developments should include the user's intention modules based on the EMG signals to trigger the device once the user performs the contraction. Thus, patients who exhibit high spasticity levels, and the movement intention cannot be detected through the inertial sensor could use T-FLEX in therapy scenarios. Likewise, future developments should also incorporate wearable sensors (e.g., a force-sensing insole, pressure-sensing, and textile-based goniometers) to improve the user-device interaction and record the user's progress.

Finally, future works will address the total integration of T-FLEX with the AGoRA exoskeleton and the AGoRA smart walker in terms of hardware, software and control to form a robotic tool able to support rehabilitation and assistive scenarios.

# Bibliography

- [1] S. Sierra, L. Arciniegas, F. Ballen-Moreno, D. Gomez-Vargas, M. Munera, and C. A. Cifuentes, “Adaptable robotic platform for gait rehabilitation and assistance: Design concepts and applications,” in *Exoskeleton Robots for Rehabilitation and Healthcare Devices*, pp. 67–93, Springer, 2020.
- [2] C. A. Cifuentes and A. Frizera, *Human-Robot Interaction Strategies for Walker-Assisted Locomotion*, vol. 115 of *Springer Tracts in Advanced Robotics*. Cham: Springer International Publishing, 2016.
- [3] J. Perry and J. M. Burnfield, “Gait analysis: normal and pathological function,” *Developmental Medicine and Child Neurology*, vol. 35, pp. 1122–1122, 1993.
- [4] A. H. Snijders, B. P. van de Warrenburg, N. Giladi, and B. R. Bloem, “Neurological gait disorders in elderly people: clinical approach and classification,” *The Lancet Neurology*, vol. 6, pp. 63–74, jan 2007.
- [5] World Health Organization, “Disability and Health.” <http://www.who.int/mediacentre/factsheets/fs352/en/>, 2018.
- [6] V. L. Feigin, E. Nichols, Alam, *et al.*, “Global, regional, and national burden of neurological disorders, 1990–2016: a systematic analysis for the Global Burden of Disease Study 2016,” *The Lancet Neurology*, vol. 18, pp. 459–480, 5 2019.



- [7] M. Katan and A. Luft, “Global Burden of Stroke,” *Seminars in Neurology*, vol. 38, pp. 208–211, apr 2018.
- [8] The Internet Stroke Center, “Stroke Statistics.” <http://www.strokecenter.org/patients/about-stroke/stroke-statistics/>, 2018.
- [9] J. J. Eng and P.-F. Tang, “Gait training strategies to optimize walking ability in people with stroke: a synthesis of the evidence,” *Expert Review of Neurotherapeutics*, vol. 7, pp. 1417–1436, oct 2007.
- [10] B. Ovbiagele and M. N. Nguyen-Huynh, “Stroke Epidemiology: Advancing Our Understanding of Disease Mechanism and Therapy,” *Neurotherapeutics*, vol. 8, pp. 319–329, jul 2011.
- [11] World Health Organization, “Spinal cord injury: Key facts.” <https://www.who.int/news-room/fact-sheets/detail/spinal-cord-injury>, 2013.
- [12] N. Sezer, “Chronic complications of spinal cord injury,” *World Journal of Orthopedics*, vol. 6, no. 1, p. 24, 2015.
- [13] N. Paneth, T. Hong, and S. Korzeniewski, “The Descriptive Epidemiology of Cerebral Palsy,” *Clinics in Perinatology*, vol. 33, pp. 251–267, jun 2006.
- [14] C. L. Richards and F. Malouin, “Cerebral palsy,” in *Handbook of Clinical Neurology*, vol. 111, pp. 183–195, Elsevier B.V., 2013.
- [15] B. Bártlová, E. Nosavcovová, M. Nováková, L. Drlíková, A. Al Fadhli, and F. Anbais, “Physiotherapy and occupational therapy in patients with stroke,” *Scripta Medica Facultatis Medicae Universitatis Brunensis Masarykianae*, vol. 81.3, 2008.
- [16] G. DeJong, C.-H. Hsieh, K. Putman, R. J. Smout, S. D. Horn, and W. Tian, “Physical Therapy Activities in Stroke, Knee Arthroplasty, and Traumatic Brain Injury Reha-

- bilitation: Their Variation, Similarities, and Association With Functional Outcomes,” *Physical Therapy*, vol. 91, no. 12, pp. 1826–1837, 2011.
- [17] R. P. Van Peppen, G. Kwakkel, S. Wood-Dauphinee, H. J. Hendriks, P. J. Van der Wees, and J. Dekker, “The impact of physical therapy on functional outcomes after stroke: what’s the evidence?,” *Clinical rehabilitation*, vol. 18, no. 8, pp. 833–862, 2004.
- [18] I. Díaz, J. J. Gil, and E. Sánchez, “Lower-Limb Robotic Rehabilitation: Literature Review and Challenges,” *Journal of Robotics*, vol. 2011, no. i, pp. 1–11, 2011.
- [19] D. J. Reinkensmeyer, J. L. Emken, and S. C. Cramer, “Robotics, Motor Learning, and Neurologic Recovery,” *Annual Review of Biomedical Engineering*, vol. 6, no. 1, pp. 497–525, 2004.
- [20] B. H. Dobkin, “Training and exercise to drive poststroke recovery,” *Nature Clinical Practice Neurology*, vol. 4, no. 2, pp. 76–85, 2008.
- [21] M. A. Dimyan and L. G. Cohen, “Neuroplasticity in the context of motor rehabilitation after stroke,” *Nature Reviews Neurology*, vol. 7, no. 2, pp. 76–85, 2011.
- [22] L. R. Sheffler and J. Chae, “Technological Advances in Interventions to Enhance Post-stroke Gait,” *Physical Medicine and Rehabilitation Clinics of North America*, vol. 24, pp. 305–323, may 2013.
- [23] T. Mikolajczyk, I. Ciobanu, D. I. Badea, A. Iliescu, S. Pizzamiglio, T. Schauer, T. Seel, P. L. Seiciu, D. L. Turner, and M. Berteau, “Advanced technology for gait rehabilitation: An overview,” *Advances in Mechanical Engineering*, vol. 10, no. 7, pp. 1–19, 2018.
- [24] M. Zhang, T. C. Davies, and S. Xie, “Effectiveness of robot-assisted therapy on ankle rehabilitation—a systematic review,” *Journal of neuroengineering and rehabilitation*, vol. 10, no. 1, p. 30, 2013.

- [25] J. Graham, "Foot drop: explaining the causes, characteristics and treatment," *British Journal of Neuroscience Nursing*, vol. 6, no. 4, pp. 168–172, 2010.
- [26] B. H. Dobkin, "Rehabilitation after Stroke," *New England Journal of Medicine*, vol. 352, pp. 1677–1684, apr 2005.
- [27] C. J. Wutzke, G. S. Sawicki, and M. D. Lewek, "The influence of a unilateral fixed ankle on metabolic and mechanical demands during walking in unimpaired young adults," *Journal of Biomechanics*, vol. 45, pp. 2405–2410, sep 2012.
- [28] J.-M. Belda-Lois, S. Mena-del Horno, I. Bermejo-Bosch, J. C. Moreno, J. L. Pons, D. Farina, M. Iosa, M. Molinari, F. Tamburella, A. Ramos, *et al.*, "Rehabilitation of gait after stroke: a review towards a top-down approach," *Journal of neuroengineering and rehabilitation*, vol. 8, no. 1, p. 66, 2011.
- [29] M. Moltedo, T. Baček, T. Verstraten, C. Rodriguez-Guerrero, B. Vanderborght, and D. Lefeber, "Powered ankle-foot orthoses: the effects of the assistance on healthy and impaired users while walking," *Journal of NeuroEngineering and Rehabilitation*, vol. 15, p. 86, dec 2018.
- [30] A. Weerasingha, W. Withanage, A. Pragnathilaka, R. Ranaweera, and R. Gopura, "Powered Ankle Exoskeletons: Existent Designs and Control Systems," *Proceedings of International Conference on Artificial Life and Robotics*, vol. 23, pp. 76–83, feb 2018.
- [31] M. D. C. Sanchez-Villamañan, J. Gonzalez-Vargas, D. Torricelli, J. C. Moreno, and J. L. Pons, "Compliant lower limb exoskeletons: A comprehensive review on mechanical design principles," *Journal of NeuroEngineering and Rehabilitation*, vol. 16, no. 1, pp. 1–16, 2019.
- [32] S. Wolf, G. Grioli, O. Eiberger, W. Friedl, M. Grebenstein, H. Hoppner, E. Burdet, D. G. Caldwell, R. Carloni, M. G. Catalano, D. Lefeber, S. Stramigioli, N. Tsagarakis, M. Van Damme, R. Van Ham, B. Vanderborght, L. C. Visser, A. Bicchi, and

- A. Albu-Schaffer, "Variable Stiffness Actuators: Review on Design and Components," *IEEE/ASME Transactions on Mechatronics*, vol. 21, pp. 2418–2430, oct 2015.
- [33] M. Moltedo, G. Cavallo, T. Baček, J. Lataire, B. Vanderborght, D. Lefeber, and C. Rodriguez-Guerrero, "Variable stiffness ankle actuator for use in robotic-assisted walking: Control strategy and experimental characterization," *Mechanism and Machine Theory*, vol. 134, pp. 604–624, 2019.
- [34] P. K. Jamwal, S. Hussain, and S. Q. Xie, "Review on design and control aspects of ankle rehabilitation robots," *Disability and Rehabilitation: Assistive Technology*, vol. 10, pp. 93–101, mar 2013.
- [35] M. Moltedo, T. Baček, B. Serrien, K. Langlois, B. Vanderborght, D. Lefeber, and C. Rodriguez-Guerrero, "Walking with a powered ankle-foot orthosis: the effects of actuation timing and stiffness level on healthy users," *Journal of neuroengineering and rehabilitation*, vol. 17, no. 1, pp. 1–15, 2020.
- [36] S. Angin and İ. Demirbüken, "Ankle and foot complex," in *Comparative Kinesiology of the Human Body*, pp. 411–439, Elsevier, 2020.
- [37] C. L. Brockett and G. J. Chapman, "Biomechanics of the ankle," *Orthopaedics and Trauma*, vol. 30, pp. 232–238, jun 2016.
- [38] R. Burdett, "Forces predicted at the ankle during running.," *Medicine and Science in Sports and Exercise*, vol. 14, no. 4, pp. 308–316, 1982.
- [39] D. A. Winter, "Foot Trajectory in Human Gait: A Precise and Multifactorial Motor Control Task," *Physical Therapy*, vol. 72, pp. 45–53, 1 1992.
- [40] W. Pirker and R. Katzenschlager, "Gait disorders in adults and the elderly," *Wiener klinische Wochenschrift*, vol. 129, pp. 81–95, feb 2017.
- [41] World Health Organization, *World Report on Disability 2011*. WHO Press, 2011.

- [42] The World Bank, “Disability Inclusion.” <https://www.worldbank.org/en/topic/disability>, 2018.
- [43] World Health Organization, “Ageing and health.” <http://www.who.int/en/news-room/fact-sheets/detail/ageing-and-health>, 2018.
- [44] C. O. Johnson and M. Nguyen, “Global, regional, and national burden of stroke, 1990–2016: a systematic analysis for the Global Burden of Disease Study 2016,” *The Lancet Neurology*, vol. 18, pp. 439–458, may 2019.
- [45] NIH: National Institute of Neurological Disorders and Stroke, “Stroke,” 2018.
- [46] B. P. B. Carvalho-Pinto and C. D. C. M. Faria, “Health, function and disability in stroke patients in the community,” *Brazilian Journal of Physical Therapy*, vol. 20, pp. 355–366, aug 2016.
- [47] Mayo Clinic, “Spinal cord injury.” <https://www.mayoclinic.org/diseases-conditions/spinal-cord-injury/symptoms-causes/syc-20377890>, 2019.
- [48] National Institute of Child Health and Human Development, “Spinal Cord Injury (SCI): Condition Information,” 2016.
- [49] P. Mimi Poinsett, “Cerebral Palsy Prevalence and Incidence.” <https://www.cerebralpalsyguidance.com/cerebral-palsy/research/prevalence-and-incidence/>, oct 2019.
- [50] Healthline, “Cerebral Palsy.” <https://www.healthline.com/health/cerebral-palsy#causes>, 2019.
- [51] M. Stavsky, O. Mor, S. A. Mastrolia, S. Greenbaum, N. G. Than, and O. Erez, “Cerebral Palsy—Trends in Epidemiology and Recent Development in Prenatal Mechanisms of Disease, Treatment, and Prevention,” *Frontiers in Pediatrics*, vol. 5, feb 2017.

- [52] Center for Disease Control and Prevention, “What is Cerebral Palsy?.” <https://www.cdc.gov/ncbddd/cp/facts.html>, 2019.
- [53] S. Nadeau, C. Duclos, L. Bouyer, and C. L. Richards, “Guiding task-oriented gait training after stroke or spinal cord injury by means of a biomechanical gait analysis,” *Progress in Brain Research*, vol. 192, pp. 161–180, 2011.
- [54] K. Cahill-Rowley and J. Rose, “Etiology of impaired selective motor control: Emerging evidence and its implications for research and treatment in cerebral palsy,” *Developmental Medicine and Child Neurology*, vol. 56, no. 6, pp. 522–528, 2014.
- [55] American Stroke Association, “Physical Effects of Stroke.” <https://www.stroke.org/en/about-stroke/effects-of-stroke/physical-effects-of-stroke/physical-impact>, 2019.
- [56] J. D. Stewart, “Foot drop: where, why and what to do?,” *Practical neurology*, vol. 8, no. 3, pp. 158–169, 2008.
- [57] B. Freire, L. Abou, and C. P. Dias, “Equinovarus foot in stroke survivors with spasticity: a narrative review of muscle–tendon morphology and force production adaptation,” *International Journal of Therapy And Rehabilitation*, vol. 27, no. 1, pp. 1–8, 2020.
- [58] M. Cioni, A. Esquenazi, and B. Hirai, “Effects of botulinum toxin-a on gait velocity, step length, and base of support of patients with dynamic equinovarus foot,” *American journal of physical medicine & rehabilitation*, vol. 85, no. 7, pp. 600–606, 2006.
- [59] A. Pandyan, M. Gregoric, M. Barnes, D. Wood, F. v. Wijck, J. Burridge, H. Hermens, and G. Johnson, “Spasticity: clinical perceptions, neurological realities and meaningful measurement,” *Disability and rehabilitation*, vol. 27, no. 1-2, pp. 2–6, 2005.
- [60] M. Mazlan, N. Hamzah, and K. Ramakrishnan, “Unilateral ankle dorsiflexor spasticity: an uncommon, disabling complication of transverse myelitis,” *Archives of medical science: AMS*, vol. 8, no. 5, p. 939, 2012.

- [61] J. R. Engsberg, S. A. Ross, K. S. Olree, and T. S. Park, "Ankle spasticity and strength in children with spastic diplegic cerebral palsy," *Developmental Medicine and Child Neurology*, vol. 42, no. 1, pp. 42–47, 2000.
- [62] T.-S. Wei, P.-T. Liu, L.-W. Chang, and S.-Y. Liu, "Gait asymmetry, ankle spasticity, and depression as independent predictors of falls in ambulatory stroke patients," *PLoS One*, vol. 12, no. 5, p. e0177136, 2017.
- [63] N. K. Latham, D. U. Jette, M. Slavin, L. G. Richards, A. Procino, R. J. Smout, and S. D. Horn, "Physical therapy during stroke rehabilitation for people with different walking abilities," *Archives of Physical Medicine and Rehabilitation*, vol. 86, 2005.
- [64] P. Langhorne, J. Bernhardt, and G. Kwakkel, "Stroke rehabilitation," *The Lancet*, vol. 377, pp. 1693–1702, may 2011.
- [65] K. Nair and A. Taly, "Stroke rehabilitation: traditional and modern approaches," *Neurol India*, vol. 50, no. 50, pp. 85–93, 2002.
- [66] J.-C. Chen and F.-Z. Shaw, "Progress in sensorimotor rehabilitative physical therapy programs for stroke patients," *World Journal of Clinical Cases: WJCC*, vol. 2, no. 8, p. 316, 2014.
- [67] G. Pratt and M. Williamson, "Series elastic actuators," in *Proceedings 1995 IEEE/RSJ International Conference on Intelligent Robots and Systems. Human Robot Interaction and Cooperative Robots*, vol. 1, pp. 399–406, IEEE Comput. Soc. Press, 2004.
- [68] F. Daerden and D. Lefeber, "Pneumatic Artificial Muscles actuators for robotics and automation.pdf," *Eur J Mech Environ Eng*, vol. 47, pp. 11–21, 2002.
- [69] S. Davis, N. Tsagarakis, J. Canderle, and D. G. Caldwell, "Enhanced Modelling and Performance in Braided Pneumatic Muscle Actuators," *The International Journal of Robotics Research*, vol. 22, pp. 213–227, mar 2003.

- [70] W. Durfee, Jicheng Xia, and E. Hsiao-Wecksler, "Tiny hydraulics for powered orthotics," in *2011 IEEE International Conference on Rehabilitation Robotics*, pp. 1–6, IEEE, jun 2011.
- [71] A. Petcu, M. Georgescu, and D. Tarniță, "Actuation Systems of Active Orthoses Used for Gait Rehabilitation," *Applied Mechanics and Materials*, vol. 880, pp. 118–123, mar 2018.
- [72] M. Alam, I. A. Choudhury, and A. B. Mamat, "Mechanism and Design Analysis of Articulated Ankle Foot Orthoses for Drop-Foot," *The Scientific World Journal*, vol. 2014, pp. 1–14, 2014.
- [73] J. An and D.-s. Kwon, "Modeling of a Magnetorheological Actuator Including Magnetic Hysteresis," *Journal of Intelligent Material Systems and Structures*, vol. 14, pp. 541–550, sep 2003.
- [74] I. Ebert-Uphoff and P. Voglewede, "On the connections between cable-driven robots, parallel manipulators and grasping," in *IEEE International Conference on Robotics and Automation, 2004. Proceedings. ICRA '04. 2004*, pp. 4521–4526 Vol.5, IEEE, 2004.
- [75] J. L. Pons, *Wearable robots: Biomechatronic Exoskeletons*. John Wiley & Sons, feb 2008.
- [76] L. Marchal-Crespo and D. J. Reinkensmeyer, "Review of control strategies for robotic movement training after neurologic injury," *Journal of NeuroEngineering and Rehabilitation*, vol. 6, p. 20, dec 2009.
- [77] J. Jiang, K.-M. Lee, and J. Ji, "Review of anatomy-based ankle-foot robotics for mind, motor and motion recovery following stroke: design considerations and needs," *International Journal of Intelligent Robotics and Applications*, vol. 2, pp. 267–282, sep 2018.



- [78] Y. M. Khalid, D. Gouwanda, and S. Parasuraman, “A review on the mechanical design elements of ankle rehabilitation robot,” *Proceedings of the Institution of Mechanical Engineers, Part H: Journal of Engineering in Medicine*, vol. 229, no. 6, pp. 452–463, 2015.
- [79] L. F. Yeung, C. Ockenfeld, M. K. Pang, H. W. Wai, O. Y. Soo, S. W. Li, and K. Y. Tong, “Design of an exoskeleton ankle robot for robot-assisted gait training of stroke patients,” *IEEE International Conference on Rehabilitation Robotics*, pp. 211–215, 2017.
- [80] M. R. Haque, H. Zheng, S. Thapa, G. Kogler, and X. Shen, “A Robotic Ankle-Foot Orthosis for Daily-Life Assistance and Rehabilitation,” in *Volume 1: Advances in Control Design Methods; Advances in Nonlinear Control; Advances in Robotics; Assistive and Rehabilitation Robotics; Automotive Dynamics and Emerging Powertrain Technologies; Automotive Systems; Bio Engineering Applications; Bio-Mecha*, vol. 1, pp. 1–7, American Society of Mechanical Engineers, sep 2018.
- [81] Y. Ren, Y. N. Wu, C. Y. Yang, T. Xu, R. L. Harvey, and L. Q. Zhang, “Developing a Wearable Ankle Rehabilitation Robotic Device for in-Bed Acute Stroke Rehabilitation,” *IEEE Transactions on Neural Systems and Rehabilitation Engineering*, vol. 25, pp. 589–596, jun 2017.
- [82] J. Ward, T. Sugar, A. Boehler, J. Standeven, and J. R. Engsborg, “Stroke survivors’ gait adaptations to a powered ankle-foot orthosis,” *Advanced Robotics*, vol. 25, no. 15, pp. 1879–1901, 2011.
- [83] K. A. Witte, J. Zhang, R. W. Jackson, and S. H. Collins, “Design of two lightweight, high-bandwidth torque-controlled ankle exoskeletons,” in *2015 IEEE International Conference on Robotics and Automation (ICRA)*, pp. 1223–1228, IEEE, 2015.
- [84] K. A. Shorter, Y. Li, E. A. Morris, G. F. Kogler, and E. T. Hsiao-Wecksler, “Experimental evaluation of a portable powered ankle-foot orthosis,” in *2011 Annual International*

- Conference of the IEEE Engineering in Medicine and Biology Society*, pp. 624–627, IEEE, aug 2011.
- [85] S. Galle, W. Derave, F. Bossuyt, P. Calders, P. Malcolm, and D. De Clercq, “Exoskeleton plantarflexion assistance for elderly,” *Gait & posture*, vol. 52, pp. 183–188, 2017.
- [86] N. Costa, M. Bezdicek, M. Brown, J. O. Gray, D. G. Caldwell, and S. Hutchins, “Joint motion control of a powered lower limb orthosis for rehabilitation,” *International Journal of Automation and Computing*, vol. 3, no. 3, pp. 271–281, 2006.
- [87] B. C. Neubauer, J. Nath, and W. K. Durfee, “Design of a portable hydraulic ankle-foot orthosis,” in *2014 36th Annual International Conference of the IEEE Engineering in Medicine and Biology Society*, pp. 1182–1185, IEEE, 2014.
- [88] A. Gmerek, N. Meskin, E. S. Tehrani, and R. Kearney, “Design of a hydraulic ankle-foot orthosis,” in *2016 6th IEEE International Conference on Biomedical Robotics and Biomechatronics (BioRob)*, pp. 1041–1048, June 2016.
- [89] Y. Ding, M. Sivak, B. Weinberg, C. Mavroidis, and M. K. Holden, “Nuvabat: northeastern university virtual ankle and balance trainer,” in *2010 IEEE Haptics Symposium*, pp. 509–514, IEEE, 2010.
- [90] M. Manchola, D. Serrano, D. Gómez, F. Ballen, D. Casas, M. Munera, and C. A. Cifuentes, “T-FLEX: Variable Stiffness Ankle-Foot Orthosis for Gait Assistance,” in *Wearable Robotics: Challenges and Trends* (J. González-Vargas, J. Ibáñez, J. L. Contreras-Vidal, H. van der Kooij, and J. L. Pons, eds.), vol. 16 of *Biosystems & Biorobotics*, pp. 160–164, Springer International Publishing, 2017.
- [91] B. Brackx, J. Geeroms, J. Vantilt, V. Grosu, K. Junius, H. Cuyppers, B. Vanderborght, and D. Lefeber, “Design of a modular add-on compliant actuator to convert an orthosis

- into an assistive exoskeleton,” in *5th IEEE RAS/EMBS International Conference on Biomedical Robotics and Biomechatronics*, pp. 485–490, IEEE, 2014.
- [92] C. M. Thalman, J. Hsu, L. Snyder, and P. Polygerinos, “Design of a soft ankle-foot orthosis exosuit for foot drop assistance,” in *2019 International Conference on Robotics and Automation (ICRA)*, pp. 8436–8442, May 2019.
- [93] A. T. Asbeck, S. M. M. De Rossi, K. G. Holt, and C. J. Walsh, “A biologically inspired soft exosuit for walking assistance,” *The International Journal of Robotics Research*, vol. 34, no. 6, pp. 744–762, 2015.
- [94] L. Konradsen, “Sensory-motor control of the uninjured and injured human ankle,” *Journal of Electromyography and Kinesiology*, vol. 12, no. 3, pp. 199–203, 2002.
- [95] J. Olivier, A. Ortlieb, P. Bertusi, T. Vouga, M. Bouri, and H. Bleuler, “Impact of ankle locking on gait implications for the design of hip and knee exoskeletons,” in *2015 IEEE International Conference on Rehabilitation Robotics (ICORR)*, pp. 618–622, IEEE, 2015.
- [96] J. J. Eng and M. R. Pierrynowski, “The effect of soft foot orthotics on three-dimensional lower-limb kinematics during walking and running,” *Physical therapy*, vol. 74, no. 9, pp. 836–844, 1994.
- [97] J. Casas, A. Leal Junior, C. Díaz, A. Frizera, M. Munera, and C. Cifuentes G., “Large-range polymer optical-fiber strain-gauge sensor for elastic tendons in wearable assistive robots,” *Materials*, vol. 12, p. 1443, 05 2019.
- [98] F. Petit, M. Chalon, W. Friedl, M. Grebenstein, A. Albu-Schäffer, and G. Hirzinger, “Bidirectional antagonistic variable stiffness actuation: Analysis, design & implementation,” *Proceedings - IEEE International Conference on Robotics and Automation*, pp. 4189–4196, 2010.

- [99] M. D. Manchola, M. J. Bernal, M. Munera, and C. A. Cifuentes, “Gait phase detection for lower-limb exoskeletons using foot motion data from a single inertial measurement unit in hemiparetic individuals,” *Sensors (Switzerland)*, vol. 19, no. 13, 2019.
- [100] L. Joseph and J. Cacace, *Mastering ROS for Robotics Programming: Design, build, and simulate complex robots using the Robot Operating System*. Packt Publishing Ltd, 2018.
- [101] S. Yamamoto, M. Ebina, M. Iwasaki, S. Kubo, H. Kawai, and T. Hayashi, “Comparative study of mechanical characteristics of plastic afos,” *JPO: Journal of Prosthetics and Orthotics*, vol. 5, no. 2, p. 59, 1993.
- [102] K. Lohse, N. Shirzad, A. Verster, N. Hodges, and H. M. Van der Loos, “Video games and rehabilitation: using design principles to enhance engagement in physical therapy,” *Journal of Neurologic Physical Therapy*, vol. 37, no. 4, pp. 166–175, 2013.
- [103] D. Gomez-Vargas, M. J. Pinto-Bernal, F. Ballen-Moreno, M. Munera, and C. A. Cifuentes, “Therapy with t-flex ankle-exoskeleton for motor recovery: A case study with a stroke survivor,” *8th IEEE RAS & EMBS International Conference on Biomedical Robotics and Biomechatronics (BioRob)*, 2020.
- [104] C. Krishnan, R. Ranganathan, S. S. Kantak, Y. Y. Dhaher, and W. Z. Rymer, “Active robotic training improves locomotor function in a stroke survivor,” *Journal of neuro-engineering and rehabilitation*, vol. 9, no. 1, p. 57, 2012.
- [105] D. J. Reinkensmeyer, O. M. Akoner, D. P. Ferris, and K. E. Gordon, “Slacking by the human motor system: computational models and implications for robotic orthoses,” in *2009 Annual International Conference of the IEEE Engineering in Medicine and Biology Society*, pp. 2129–2132, Ieee, 2009.

- [106] J. Allaire, “Rstudio: Integrated development environment for r,” in *The R User Conference, useR! 2011 August 16-18 2011 University of Warwick, Coventry, UK*, p. 14, 2011.
- [107] O. Lariviere, T. Provot, L. Valdes-Tamayo, M. Bourgain, and D. Chadeaux, “Force pattern and acceleration waveform repeatability of amateur runners,” in *Multidisciplinary Digital Publishing Institute Proceedings*, vol. 49, p. 136, 2020.
- [108] M. Kadaba, H. Ramakrishnan, M. Wootten, J. Gainey, G. Gorton, and G. Cochran, “Repeatability of kinematic, kinetic, and electromyographic data in normal adult gait,” *Journal of orthopaedic research*, vol. 7, no. 6, pp. 849–860, 1989.
- [109] D. A. Neumann, *Kinesiology of the musculoskeletal system-e-book: foundations for rehabilitation*. Elsevier Health Sciences, 2013.
- [110] Y. Zhang, R. J. Kleinmann, K. J. Nolan, and D. Zanotto, “Preliminary Validation of a Cable-Driven Powered Ankle–Foot Orthosis With Dual Actuation Mode,” *IEEE Transactions on Medical Robotics and Bionics*, vol. 1, no. 1, pp. 30–37, 2019.
- [111] S. P. Nair, S. Gibbs, G. Arnold, R. Abboud, and W. Wang, “A method to calculate the centre of the ankle joint: A comparison with the vicon® plug-in-gait model,” *Clinical Biomechanics*, vol. 25, no. 6, pp. 582–587, 2010.
- [112] M. H. Schwartz and A. Rozumalski, “The gait deviation index: a new comprehensive index of gait pathology,” *Gait & posture*, vol. 28, no. 3, pp. 351–357, 2008.
- [113] A. Guzik and M. Druzbicki, “Application of the Gait Deviation Index in the analysis of post-stroke hemiparetic gait,” *Journal of Biomechanics*, vol. 99, 2020.
- [114] R. Baker, J. L. McGinley, M. H. Schwartz, S. Beynon, A. Rozumalski, H. K. Graham, and O. Tirosh, “The Gait Profile Score and Movement Analysis Profile,” *Gait and Posture*, vol. 30, no. 3, pp. 265–269, 2009.

- [115] L. Demers, R. Weiss-Lambrou, and B. Ska, “Development of the Quebec User Evaluation of Satisfaction with assistive Technology (QUEST),” *Assistive Technology*, vol. 8, pp. 3–13, jun 1996.
- [116] J. P. Dormans, “Orthopedic management of children with cerebral palsy,” *Pediatric Clinics of North America*, vol. 40, no. 3, pp. 645–657, 1993.
- [117] J. L. Burpee and M. D. Lewek, “Biomechanical gait characteristics of naturally occurring unsuccessful foot clearance during swing in individuals with chronic stroke,” *Clinical Biomechanics*, vol. 30, pp. 1102–1107, dec 2015.
- [118] K. Z. Takahashi, M. D. Lewek, and G. S. Sawicki, “A neuromechanics-based powered ankle exoskeleton to assist walking post-stroke: A feasibility study,” *Journal of NeuroEngineering and Rehabilitation*, vol. 12, no. 1, pp. 1–13, 2015.
- [119] J. Kim, S. Hwang, R. Sohn, Y. Lee, and Y. Kim, “Development of an active ankle foot orthosis to prevent foot drop and toe drag in hemiplegic patients: A preliminary study,” *Applied Bionics and Biomechanics*, vol. 8, no. 3-4, pp. 377–384, 2011.
- [120] D. Shakti, L. Mathew, N. Kumar, and C. Kataria, “Effectiveness of robo-assisted lower limb rehabilitation for spastic patients: A systematic review,” *Biosensors and Bioelectronics*, vol. 117, no. June, pp. 403–415, 2018.
- [121] A. J. Young and D. P. Ferris, “State of the art and future directions for lower limb robotic exoskeletons,” *IEEE Transactions on Neural Systems and Rehabilitation Engineering*, vol. 25, no. 2, pp. 171–182, 2016.
- [122] A. J. Ries, T. F. Novacheck, and M. H. Schwartz, “The Efficacy of Ankle-Foot Orthoses on Improving the Gait of Children With Diplegic Cerebral Palsy : A Multiple Outcome Analysis,” *PM&R*, pp. 1–8, 2015.

- [123] A. J. Ries, T. F. Novacheck, and M. H. Schwartz, "Gait & Posture A data driven model for optimal orthosis selection in children with cerebral palsy," *Gait & Posture*, vol. 40, no. 4, pp. 539–544, 2014.
- [124] M. Schwarze, J. Block, T. Kunz, M. Alimusaj, D. W. W. Heitzmann, C. Putz, T. Dreher, and S. I. Wolf, "Gait & Posture The added value of orthotic management in the context of multi-level surgery in children with cerebral palsy," *Gait & Posture*, vol. 68, no. June 2018, pp. 525–530, 2019.
- [125] M. Galli, V. Cimolin, C. Rigoldi, and G. Albertini, "Quantitative Evaluation of the Effects of Ankle Foot Orthosis on Gait in Children with Cerebral Palsy Using the Gait Profile Score and Gait Variable Scores," *Journal of Developmental and Physical Disabilities*, vol. 28, no. 3, pp. 367–379, 2016.
- [126] I. Skaaret, H. Steen, A. B. Huse, and I. Holm, "Comparison of gait with and without ankle-foot orthoses after lower limb surgery in children with unilateral cerebral palsy," *Journal of Children's Orthopaedics*, vol. 13, no. 2, pp. 180–189, 2019.
- [127] J.-S. Cheng, Y.-R. Yang, S.-J. Cheng, P.-Y. Lin, and R.-Y. Wang, "Effects of Combining Electric Stimulation With Active Ankle Dorsiflexion While Standing on a Rocker Board: A Pilot Study for Subjects With Spastic Foot After Stroke," *Archives of Physical Medicine and Rehabilitation*, vol. 91, pp. 505–512, 4 2010.
- [128] F. Tamburella, J. C. Moreno, M. Iosa, I. Pisotta, F. Cincotti, D. Mattia, J. L. Pons, and M. Molinari, "Boosting the traditional physiotherapist approach for stroke spasticity using a sensorized ankle foot orthosis: a pilot study," *Topics in Stroke Rehabilitation*, vol. 24, pp. 447–456, 8 2017.
- [129] J. Brumitt and T. Cuddeford, "Current concepts of muscle and tendon adaptation to strength and conditioning.," *International journal of sports physical therapy*, vol. 10, pp. 748–59, 11 2015.

- [130] M. D. Peterson, E. Pistilli, G. G. Haff, E. P. Hoffman, and P. M. Gordon, "Progression of volume load and muscular adaptation during resistance exercise.," *European journal of applied physiology*, vol. 111, pp. 1063–71, 6 2011.